SEEPAGE THROUGH PARTIALLY SATURATED SHALE WASTES

Prepared for

United States Department of the Interior
Bureau of Mines

by

G. L. Bloomsburg
R. D. Wells
Agricultural Engineering Department
University of Idaho
Moscow, Idaho 83843

FINAL REPORT

on

Contract No. H0252065
Seepage Through Partially Saturated Shale Wastes

September 1978

Disclaimer Notice

1. Report No.

2.

3. Recipient Accession No.

4. Title and Subtitle

SEEPAGE THROUGH PARTIALLY SATURATED SHALE WASTES

5. Report Date

September 1978

6.

7. Author(s)

G. L. Bloomsburg and R. D. Wells

8. Performing Organization Report No.

9. Performing Organization Name and Address

Agricultural Engineering Department
University of Idaho
Moscow, Idaho 83843

10. Project/Task/Work Unit No.

11. Contract or Grant No.

HO 252065

12. Sponsoring Organization Name and Address

Office of Assistant Director - Mining
Bureau of Mines
Department of the Interior
Washington, D.C. 20241

13. Type of Report

FINAL

14.

15. Supplementary Notes

16. Abstract

This report describes work which was done to apply an existing finite element computer program UNSAT2 to the unsteady, unsaturated flow of water through waste shale piles. The work was done in three phases:

1. Verification of program through comparison with existing data.

2. Verification of program through simulation of flow from field seepage ponds at Rifle, Colorado. Considerable laboratory work was done in this phase to obtain capillary pressure-saturation-relative permeability data and hydraulic conductivity values for retorted shale.

3. Application of program to flow due to natural rainfall in a section through the Piceance Basin in Colorado, and a typical waste shale pile.

17. Originator's Key Words

Colorado
Computer Modelling
Environmental Impact
Finite Element Metho
Hydrology
Oil Shale
Piceance Creek Basin
Spent Shale
Disposal

18. Availability Statement

19. U.S. Security Classification of the Report

20. U.S. Security Classification of this Page

21. No. of Pages

22. Price

FOREWORD

This report was prepared by G. L. Bloomsburg and R. D. Wells of the Agricultural Engineering Department, University of Idaho, Moscow, Idaho 83843 under USBM Contract Number H0252065. The contract was initiated under the Oil Shale Mining Research Program. It was administered under the technical direction of Spokane Mining Research Center with Mr. R. A. Bloomfield acting as the Technical Project Officer. Ms. Limke was the contract administrator for the Bureau of Mines.

This report is a summary of work recently completed as part of this contract during the period June 11, 1975 to June 11, 1978. The draft report was submitted on June 27, 1978.

The University of Idaho certifies that no patents or inventions have resulted from this study.

TABLE OF CONTENTS

	Page
Report Documentation Page	1
Foreword	2
Table of Contents	3
List of Tables	5
List of Figures	6
Units and Definitions of Terms	10
Summary	12
Introduction	13
Phase I	16
I-1 Verification of Computer Program	16
I-2 Modification of Program for Air Flow	20
I-3 Summary	24
Phase II	25
II-1 Shale Hydraulic Properties	25
II-2 Simulation of Seepage Ponds with UNSAT2	25
II-3 Summary	38
Phase III	39
III-1 Simulation of Natural Profile - Piceance Basin	39
III-2 Comparison of UNSAT2 with CFLOW	45
III-3 Analysis of Waste Shale Piles	49
III-4 Summary	87
References	90

TABLE OF CONTENTS (Cont.)

Page

Appendix A. UNSAT2 Program Documentation and User Instructions. 92

Appendix B. Laboratory Data 118

Appendix C. Sinclair Program Documentation and User Instructions 143

Appendix D. Input Data - Test Programs Phase I 147

LIST OF TABLES

Table		Page
II-1	Boundary Conditions and Values of Parameters for Simulation of Pond 2	32
II-2	Drainage Outflow Pond 2	37
II-3	Cumulative Leaching After Sprinkling	37
III-1	Hydraulic Properties used for Simulation of Piceance Basin	44
III-2	Evaporation Potential and Data	51
III-3	Climatological Data - Grand Junction, Colorado	55
B-1	Saturated Hydraulic Conductivity for Waste Shale	130
B-2	Permeability-Capillary Pressure-Saturation Data 75 pcf Density	132
B-3	Permeability-Capillary Pressure-Saturation Data 85 pcf Density	133
B-4	Permeability-Capillary Pressure-Saturation Data 95 pcf Density	134
B-5	Permeability-Capillary Pressure-Saturation Data Poudre Sand	135

LIST OF FIGURES

Figure		Page
I-1	One-Dimensional Drainage	17
I-2	Steady Downward Flow - Initially Saturated	18
I-3	Downward Flow - Initially Hydrostatic	19
I-4	Capillary Pressure Distribution - Evaporation from Poudre Sand	21
I-5	Infiltration into Dry Soil	22
I-6	Two-Dimensional Drainage	23
II-1	Finite Element Mesh for Pond 1	27
II-2	Simulation of Pond 1 - December 1975 - January 1976	28
II-3	Simulation of Pond 1 - February - April, 1976	29
II-4	Finite Element Mesh for Pond 2	31
II-5	Simulation of Pond 2 - December, 1975	33
II-6	Simulation of Pond 2 - May, 1976	35
II-7	Simulation of Pond 2 - June - July, 1976	36
III-1	Location of Piceance Creek Basin and Study Sites	40
III-2	Geohydrologic Section through the Piceance Basin	41
III-3	Finite Element Mesh - Piceance Basin	42
III-4	Geohydrology Model of Site 1	43
III-5	Tailings Pond	47
III-6	Finite Element Mesh - Tailings Pond	48
III-7	Finite Element Mesh - General Design	50
III-8	Profile Construction	53
III-9	Moisture Distribution in Processed Oil Shale 0 Hour Infiltration - Uniform Profiles	57
III-10	Moisture Distribution in Processed Oil Shale 5 Minute Infiltration - Uniform Profiles	58

LIST OF FIGURES (Cont.)

Figure		Page
III-11	Moisture Distribution in Processed Oil Shale 5 Minute-Evaporation-Uniform Profiles	59
III-12	Moisture Distribution in Processed Oil Shale 6 Hour-Infiltration-Uniform Profiles	60
III-13	Moisture Distribution in Processed Oil Shale 6 Hour-Infiltration-Uniform Profiles	61
III-14	Moisture Distribution in Processed Oil Shale 6 Hour-Evaporation-Uniform Profiles	62
III-15	Moisture Distribution in Processed Oil Shale 24 Hour-Infiltration-Uniform Profiles	63
III-16	Moisture Distribution in Processed Oil Shale 24 Hour-Infiltration-Uniform Profiles	64
III-17	Moisture Distribution in Processed Oil Shale 24 Hour-Evaporation-Uniform Profiles	65
III-18	Moisture Distribution in Processed Oil Shale 0 Hour-Infiltration-Composite Profiles	67
III-19	Moisture Distribution in Processed Oil Shale 1 Hour-Infiltration-Composite Profiles	68
III-20	Moisture Distribution in Processed Oil Shale 1 Hour-Evaporation-Composite Profiles	69
III-21	Moisture Distribution in Processed Oil Shale 1 Hour-Infiltration-Composite Profiles	70
III-22	Moisture Distribution in Processed Oil Shale 1 Hour-Evaporation-Composite Profiles	71
III-23	Moisture Distribution in Processed Oil Shale 5 Minute-Evaporation-Uniform Profiles	72
III-24	Moisture Distribution in Processed Oil Shale 5 Minute-Evaporation-Uniform Profiles	73
III-25	Moisture Distribution in Processed Oil Shale 24 Hour-Infiltration-Uniform Profiles	74
III-26	Moisture Distribution in Processed Oil Shale 24 Hour-Evaporation-Uniform Profiles	75
III-27	Moisture Distribution in Processed Oil Shale 24 Hour-Infiltration-Uniform Profiles	76

LIST OF FIGURES (Cont.)

Figure		Page
III-28	Moisture Distribution in Processed Oil Shale 24 Hour-Evaporation-Uniform Profiles	77
III-29	Moisture Distribution in Processed Oil Shale 1 Hour-Infiltration-Composite Profiles	79
III-30	Moisture Distrubution in Processed Oil Shale 1 Hour-Evaporation-Composite Profiles	80
III-31	Moisture Distribution in Processed Oil Shale 1 Hour-Infiltration-Composite Profiles	81
III-32	Moisture Distribution in Processed Oil Shale 1 Hour-Evaporation-Composite Profiles	82
III-33	Moisture Distribution in Processed Oil Shale 1 Hour-Infiltration-Composite Profiles	83
III-34	Moisture Distribution in Processed Oil Shale 1 Hour-Evaporation-Composite Profiles	84
III-35	Finite Element Mesh - 2-D Waste Shale Pile	86
III-36	Saturated Zones After One Year of Ponding	88
A-1	Scheme for Numbering Modes and Elements in Finite Element Mesh	95
A-2	Definition of Principal Conductivities	110
A-3	Numbering Convention for Element Corner Modes	113
B-1	Permeameters Used in Disturbed Sample Tests	120
B-2	Schematic of Capillary Pressure-Saturation Apparatus	120
B-3	Two Sets of Vacuum Saturation Apparatus	122
B-4	Capillary Pressure-Saturation Curve for 85 pcf Density	123
B-5	Capillary Pressure-Saturation Data	124
B-6	Schematic of Permeability Measuring Apparatus	126
B-7	Components of Undisturbed Permeameter Apparatus	126
B-8	Undisturbed Permeameter Mounted on the Wall	127

LIST OF FIGURES (Cont.)

Figure		Page
B-9	Two Sets of Gravity Type Permeability Apparatus	127
B-10	Conductivity vs Porosity for Retorted Shale	131
B-11	Capillary Pressure-Saturation Data	136
B-12	Relative Permeability - 75 pcf Density	138
B-13	Relative Permeability - 85 pcf Density	139
B-14	Relative Permeability - 95 pcf Density	140
B-15	Undisturbed Sample Permeability Values	141

UNITS AND DEFINITION OF TERMS

The primary system of units used is S.I. or the international metric system. In cases where the concern is with field values which are usually given in the British Engineering System these are given in parentheses. An exception to this is in the case of the three densities of shale which are used; 75, 85 and 95 pcf or pounds per cubic foot. In terms of kg per cubic meter it is simply too difficult to recognize the proper density, therefore these densities are written as above throughout the report.

Symbol	Definition
P_c	Capillary pressure - also called tension or suction $P_c = P_a - P_w$ where P_a and P_w are pressures in air and water respectively. In most cases air pressure in the soil is assumed atmospheric so $P_c = -P_w$.
$\frac{P_c}{\rho g}$ or ψ	Capillary pressure head - most convenient unit for capillary pressure is height of a water column.
S	Saturation - given by $S = \frac{V_w}{V_v}$ where V_w is the volume of water in the soil voids and V_v is the volume of voids. S therefore is 1.0 at complete water saturation and 0.0 at a completely dry condition.
ϕ	Porosity - given by $\frac{V_v}{V}$ where V is total soil volume.
θ	Moisture content (volume basis) - given by $\theta = \frac{V_w}{V}$ or by $S\phi$.
k	Permeability (intrinsic permeability) - the Darcy coefficient which is independent of fluid properties and has the units of length squared.

UNITS AND DEFINITION OF TERMS (Cont.)

Symbol	Definition
K	Hydraulic conductivity (formerly coefficient of permeability) - the Darcy coefficient which depends on both fluid or porous material properties given by $K = \frac{k\rho g}{\mu}$ where ρ is fluid mass density, g is acceleration due to gravity and μ is fluid absolute viscosity. Has the units of length per unit time.
k_e	Effective permeability - the permeability at less than complete saturation.
K_e	Effective conductivity - the hydraulic conductivity at less than complete saturation.
k_r or K_r	Relative permeability or relative hydraulic conductivity. Given by $k_r = \frac{k_e}{k} = \frac{K_e}{K} = K_r$.

Final Report

Seepage Through Partially Saturated Shale Wastes
U.S. Bureau of Mines
Contract No. H0252065

This contract was initiated in June 1975 for a period of two years. It was later extended for a period of one year with no change of funds. This report includes all results and data from the entire project.

Summary

The overall goal of this project was to provide the Bureau of Mines with a computer code which could be used for unsteady, unsaturated flow of water through a soil profile. Although the project was directed toward flow of water through retorted oil shale, the computer program has much wider applicability.

The input data necessary to run the program includes saturated hydraulic conductivity, porosity, and capillary pressure-saturation-relative conductivity data for each material in the flow field. Non-homogeneous and anisotropic soil conditions can be considered with a variety of boundary and initial conditions. Infiltration, evaporation, plant use and seepage surfaces may be considered in two dimensional or axial-symmetric flow fields.

The verification of the program for field use was done by comparison with data obtained from infiltration ponds at the Anvil Points site near Rifle, Colorado. The conditions simulated were seepage due to ponding up to 1 m in depth, drainage of the shale after the pond was empty and seepage from the shale after sprinkling the pond with water. Field data and computer simulation agreed very well in most cases. The capillary pressure-saturation-relative conductivity data used were obtained both from small laboratory packed samples and from core samples taken from the pond and tested in the laboratory. The saturated hydraulic conductivities used were field values obtained from the seepage ponds.

After the program was verified with field data a series of computer runs were made in both 1 and 2 dimensions on hypothetical shale profiles to determine the disposition of water from 100 year frequency storms of various intensities and durations. The two dimensional pile was 573 m long by 91 m deep and consisted of shale packed to two different densities to represent different compactive efforts during placement. A 1.5 m layer of sand was under the entire pile. Computer simulation showed that there would not be surface runoff from shale packed to 85 pcf density during either 1 hour or 6 hour storms whereas with shale packed to 95 pcf density there would be surface runoff from both storms. The 2 dimensional pile was also run with ponding of 1.5 m. During a one year period for this condition the saturated zone moved into the shale approximately 12 m.

A hypothetical tailings pond was also investigated to determine the rate of buildup of a water table mound beneath the pond. This mound was approximately 2 m high at the end of 5 years even though the flow region below the pond was unsaturated at all times.

There are many other problems in ground water hydrology that may be analyzed by the use of this computer program.

Introduction

The basic purpose of this project is best described by quoting the background, objectives, and scope of work from the contract document.

> "Sec. 1.1 Background and Discussion The objectives of the Bureau of Mines oil shale program are to develop and demonstrate the technology to mine deep, saline-rich, oil shale deposits of the Green River Formation. Treatment of the environmental problems associated with waste disposal and water management are an important aspect of this program.
>
> Commercial shale oil production could involve a number of mining methods and at least three retort processes (gas combustion, TOSCO, and Union Oil). Before the cost-effectiveness of alternative waste disposal and materials handling schemes can be evaluated, the Bureau must carefully assess the engineering and environmental problems connected with the disposal of spent shale. An important consideration in this assessment is the effects of water infiltration caused by rainfall or discharge from the processing plant. The manner in which this water enters the shale waste and flows downward toward the water table will determine the stability of the waste deposits and the amount of leachate contaminating the groundwater system. The Bureau of Mines, therefore, wishes to obtain a proven computer program which can calculate the variables associated with unsaturated, unsteady flow during infiltration and, thereby, determine their effect on stability and groundwater contamination.
>
> Sec. 1.2 Objectives
>
> 1.2.1 To develop a computer code to analyze unsteady, unsaturated flow during infiltration of water. This must be able to handle anisotropic, nonhomogeneous, two-dimension flow problems with various boundary conditions.
>
> 1.2.2 To demonstrate the program by analyzing flow of water through a typical spent oil shale deposit.
>
> 1.2.3 To determine the feasibility of analyzing flow of water through a natural soil and rock profile with perched water tables.
>
> Sec. 1.3 Scope of Work The scope of work to be performed by the Contractor is divided into three phases according to the three objectives stated above. All work to be performed under

this contract, to include the submission of an approved Final Report, shall be accomplished within two (2) years of the effective date of the contract.

1.3.1 Phase I The Contractor shall obtain the existing computer program developed by Neuman for unsteady, unsaturated flow through an earth dam and from a canal.

1.3.1.1 The program shall be modified for use on the IBM 370-145 computer.

1.3.1.2 An attempt shall be made to further modify the program to account for air flow ahead of water flow.

1.3.2 Phase II The Government shall furnish to the Contractor at least four (4) samples of retorted shale from the gas combustion process (Development Engineering process). The Contractor shall perform laboratory tests to obtain capillary pressure/saturation and capillary pressure/permeability relationships.

1.3.2.1. The samples shall be taken from the four (4) infiltration test ponds constructed by Development Engineering, Inc. at the Anvil Points test site. The Contractor shall be present at the site when samples are selected and shall inform himself as to site conditions existing in the sampling areas.

1.3.2.2 Using a computer program developed by Sinclair or Reisenauer, the Contractor shall attempt to calculate values of unsaturated permeability from capillary pressure/saturation data.

1.3.2.3 Using measured or computed values of unsaturated permeability, the Contractor shall model infiltration of water (pressure and velocity) through the shale wastes used in the construction of the four (4) test ponds in 1.3.2.1.

1.3.2.4 The Contractor shall compare his computed values of infiltration with the actual measured runoff from the impervious membranes underlying the test ponds.

1.3.2.5 The source of water to the infiltration ponds shall be either normal rainfall or water supplied by the sprinkler system installed over the test ponds.

1.3.2.6 Modeling shall incorporate a range of soil moisture conditions varying from the natural moisture content during the dry season to complete saturation.

1.3.2.7 Water shall be assumed to enter the ground surface at a range of pressures including ponding up to two feet in depth.

1.3.2.8 A Phase II report, covering the results of model demonstration on the four infiltration test ponds, shall be prepared and submitted to the Bureau of Mines.

1.3.3 Phase III

1.3.3.1 Frequency of storm intensities will be determined for the Western Colorado area and used as input in tasks 1.3.3.2 and 1.3.3.4.

1.3.3.2 Using soil profile data furnished by the Bureau of Mines and storm intensities from task 1.3.3.1, the Contractor shall analyze at least two situations involving flow through oil shale deposits of the Green River Formation.

1.3.3.3 Based on the flow studies in task 1.3.3.2, the Contractor shall determine the feasibility of using this computer code to analyze infiltration through natural soil profiles with perched water tables. Also benefits of this method over conventional (saturated) methods will be determined.

1.3.3.4 Flow through a hypothetical shale waste pile using precipitation data from task 1.3.3.1 will be analyzed to estimate seepage expected through an actual waste pile.

1.3.3.5 The contractor shall provide the necessary assistance required in adapting the computer code to the CDC 3200 at the Spokane Mining Research Center."

The above listing of Phase III is not the original work listed in this phase but was expanded at the time the contract was extended to three years.

In general, this report is organized in the same order as the above tasks.

PHASE I

The computer program, UNSAT2, was obtained from the report by Neuman et. al. (1974). The program is written in Fortran IV and was originally developed for an IBM 370/165 computer. The total storage required to run the program is highly dependent on the number of nodes in the finite element mesh and requires three scratch tapes or discs. The work reported on here has been done on the University of Idaho IBM 370/145 computer.

The formulation of the program UNSAT2 is based on the Galerkin method in conjunction with a finite element discretization scheme and may be used for a wide variety of unsteady, unsaturated flow problems in porous media. The program may be used in anisotropic, nonhomogenous materials for horizontal plane, vertical plane or axisymmetric problems where the axis of symmetry is vertical. It can be used with a variety of boundary conditions such as constant flux, constant pressure, maximum flux, minimum pressure, and infiltration, evaporation and seepage surfaces. The maximum flux and minimum pressure boundaries are used when maximum or minimum conditions are controlled by exterior factors such as atmospheric conditions, but the actual flow in the porous media is determined by properties of the porous media.

I-1 VERIFICATION OF COMPUTER PROGRAM

Several one-dimensional problems were run because laboratory data were available which could be easily compared with the computer output. The finite element network used for the first two of these problems was a vertical column of eight elements. The lower seven elements were 20 cm by 20 cm and the top one (at the ground surface) was 20 cm by 6.5 cm.

I-1.1 Drainage

In this problem the initial condition was complete saturation. Drainage began from the bottom at time zero and continued for 36 hours. There was no inflow at the top. Figure I-1 shows a comparison of the total outflow as a function of time from the computer program and from laboratory data reported by Corey, et. al. (1965). The computer program input data set for all problems is given in Appendix A.

I-1.2 Steady Downward Flow

The initial condition of the soil was complete saturation. At time zero, drainage from the bottom began and a constant flux of 1 cm per hour at the ground surface was imposed. At 36 hours the flow had reached a steady state. In Figure I-2 pressure distribution from the program is compared with an analytical solution for steady state flow.

Figure I-3 shows the pressure distribution from the computer program if the initial condition is a hydrostatic pressure distribution and a flux of 1 cm per hour at the surface is imposed.

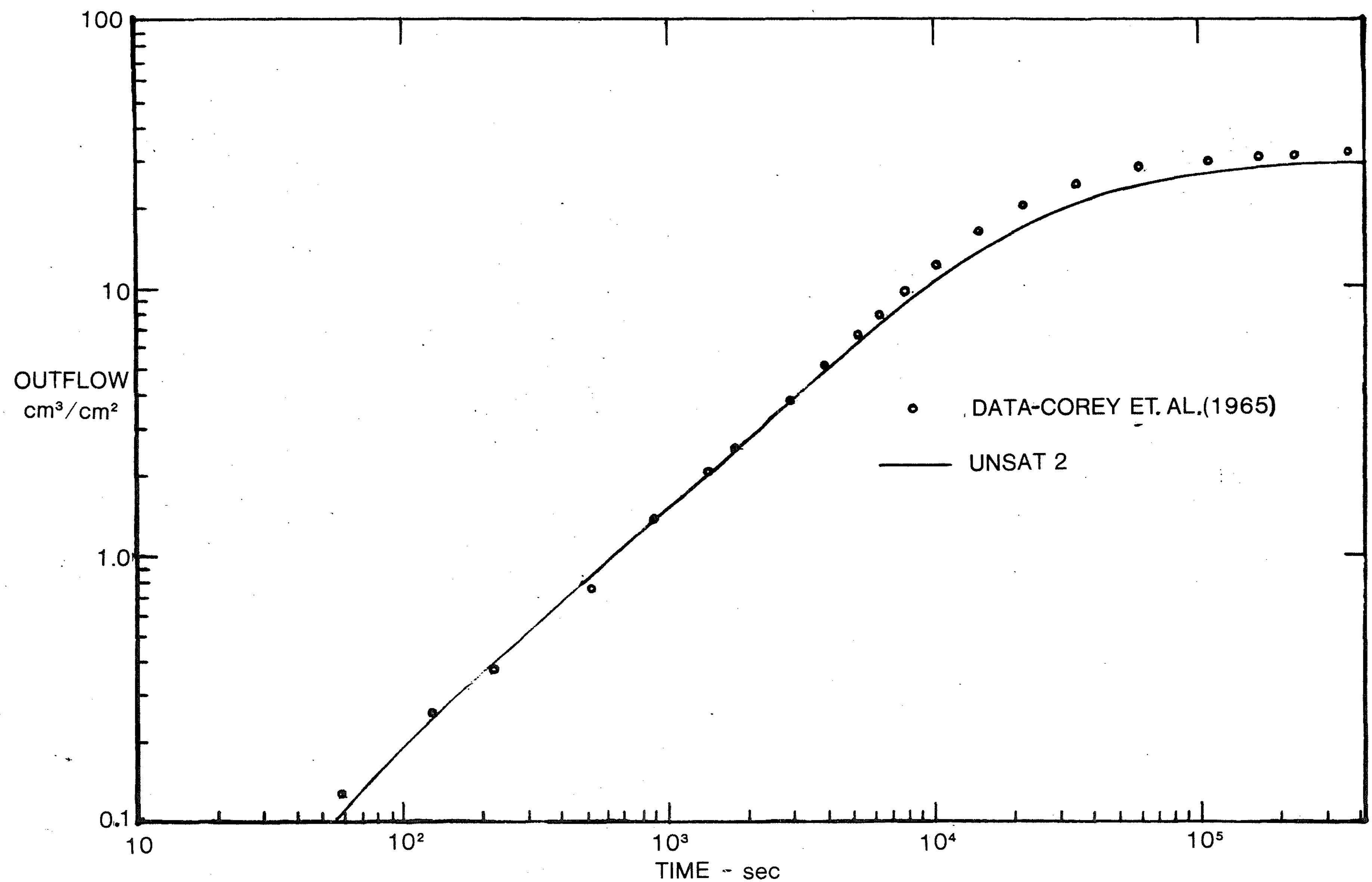

FIGURE I -1 ONE-DIMENSIONAL DRAINAGE

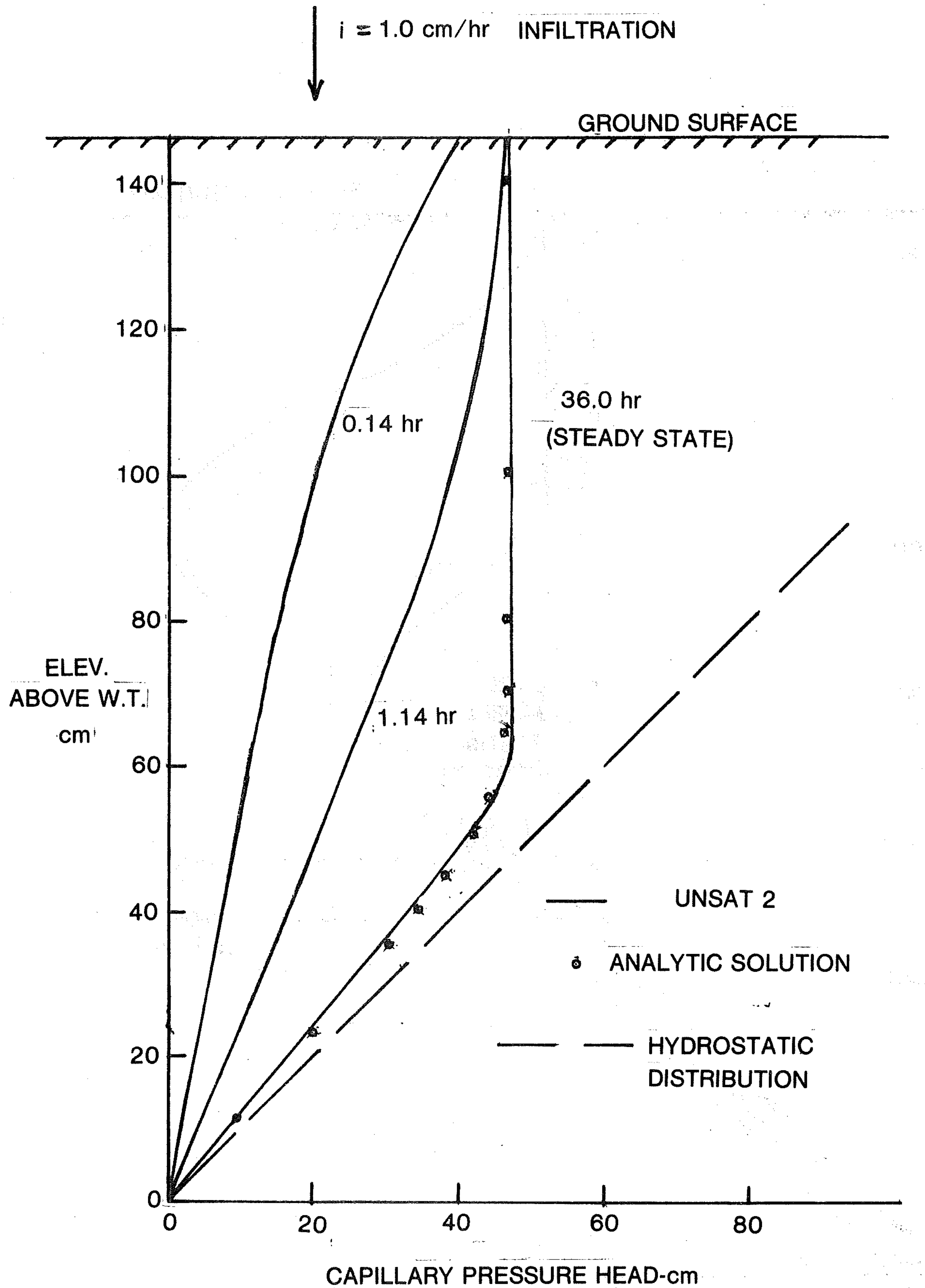

FIGURE I-2 STEADY DOWNWARD FLOW-INITIALLY SATURATED

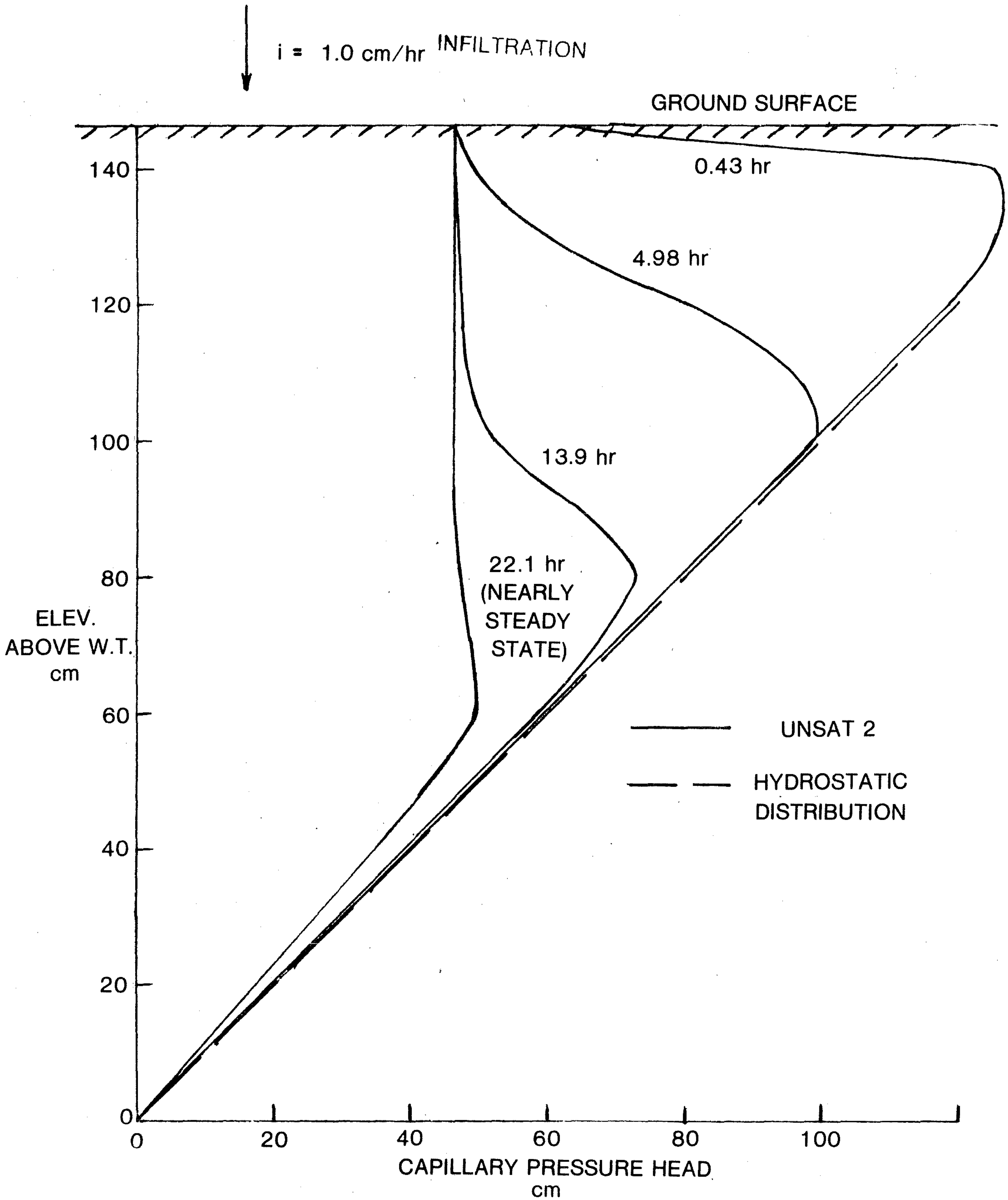

FIGURE I-3 DOWNWARD FLOW-INITIALLY HYDROSTATIC

I-1.3 Evaporation from the Soil Surface

A network consisting of eight vertical elements was used to determine upward movement from a water table due to evaporation at the soil surface. The top six elements were 10 cm wide by 5 cm high and the bottom two were 10 cm by 10 cm. The initial condition of the soil was saturation with a potential capillary pressure (tension) of 140 cm at the soil surface. As evaporation occurred the soil dried, increasing the capillary pressure to the specified maximum as shown in Figure I-4. The dimensionless evaporation rate from the computer solution agreed well with the corresponding experimental value given by Anat et. al. (1965).

I-1.4 Infiltration into a Dry Soil

The mesh for this problem consisted of six elements. The lower five were 5 cm by 5 cm and the top was 0.4 cm high by 5 cm wide. The initial condition was a moisture content of 0.132 which is quite dry. The top boundary was ponded to a depth of 1.6 cm. Figure I-5 shows a comparison of the computer output with experimental data from McWhorter (1971). The verification here is poorer than most of the problems, probably because the initial moisture content for the experimental problem was not given and an assumed value was used for the program. At larger times, the initial moisture content would have little effect on the infiltration rate and the agreement with experimental data is reasonably good.

I-1.5 Two-Dimensional Drainage

This was run for an area 122 cm high by 610 cm long which represented the flow into one side of a drain. One end of the model represented the drain and the other end represented the midpoint between the parallel drains. The finite element mesh included 60 elements and 75 node points. The soil was initially saturated to two-thirds of the total depth of the profile and drainage was toward the end with the drain. Figure I-6 compares experimental data from Hedstrom, et al. (1971) with the computer output.

I-1.6 Downward Flow in Two-Layered Material

This was a one-dimensional downward flow problem through two different materials. A great deal of trouble was encountered running this problem with actual soil properties. The numerical solution became unstable during the iteration procedure and the program would not run. When hypothetical soil properties were used, good runs were obtained. There were no experimental data that could be used for verification of this problem.

I-2 MODIFICATION OF PROGRAM FOR AIR FLOW

Detailed study of UNSAT2 showed that modification of the program to consider air flow would require major changes in data input form and there was considerable doubt that the present formulation based on the Galerkin method would even work for two-phase flow. Therefore, modification of this program for airflow is not feasible.

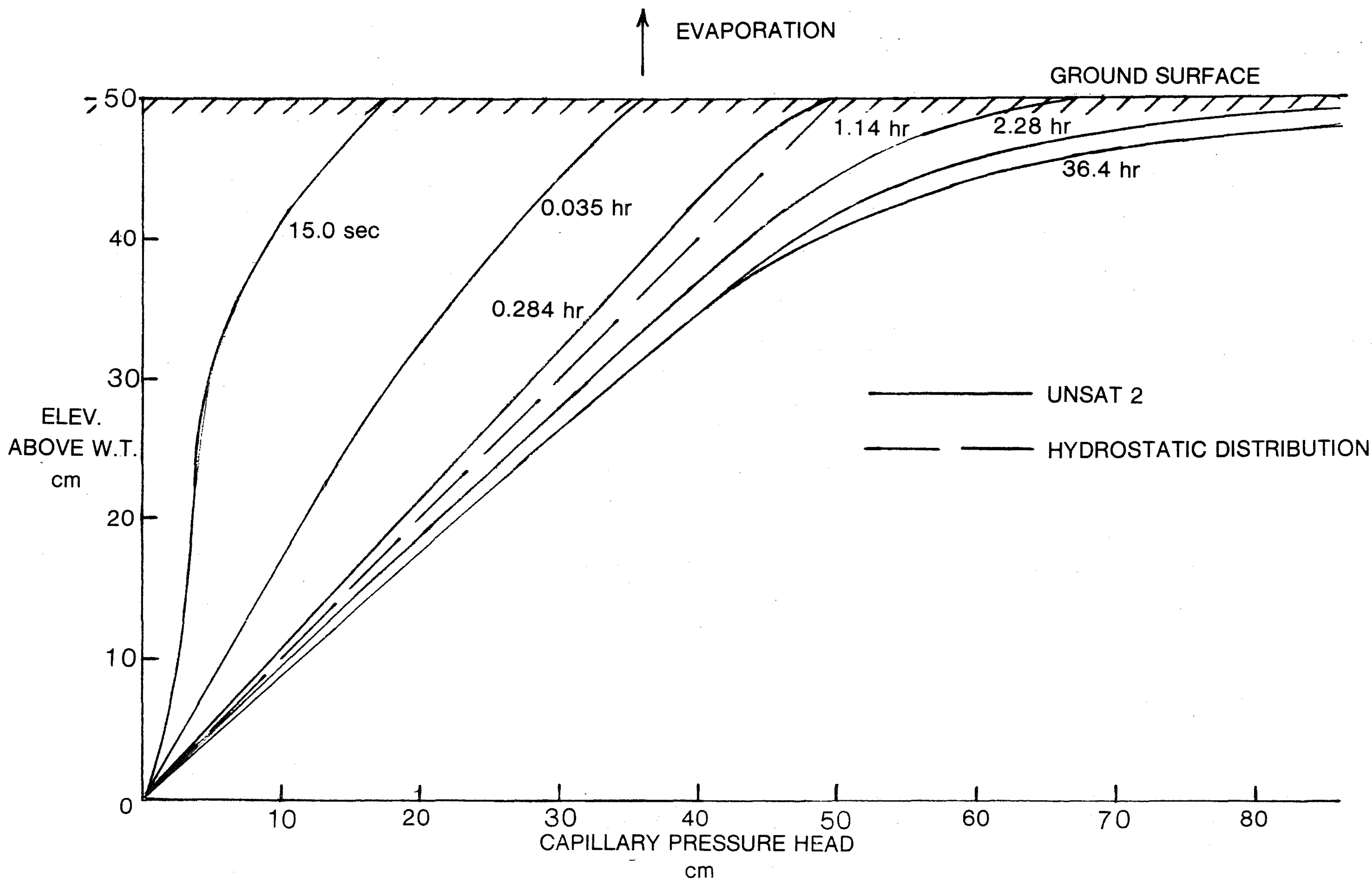

FIGURE I-4 CAPILLARY PRESSURE DISTRIBUTION-EVAPORATION FROM POUDRE SAND

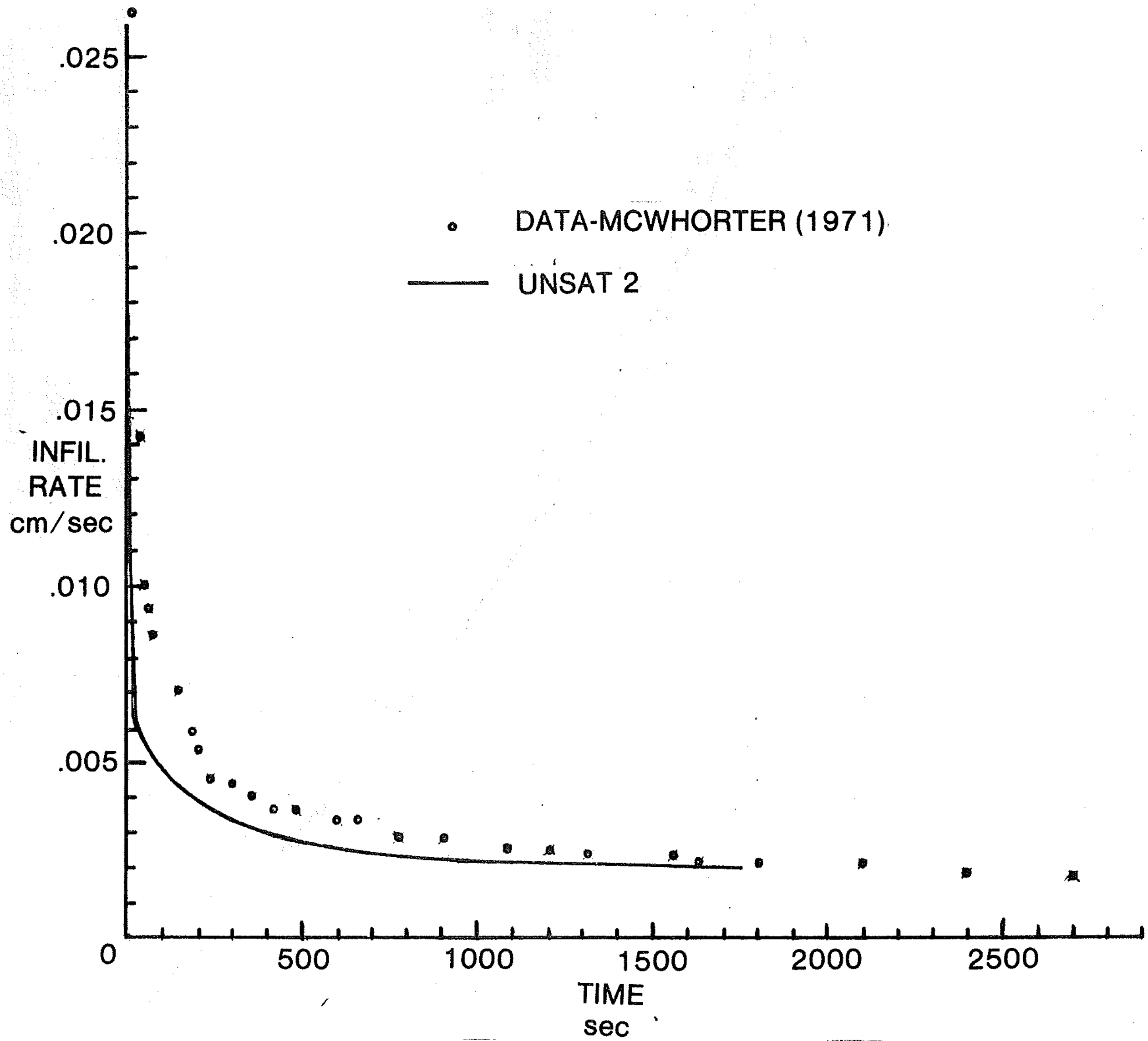

FIGURE I-5 INFILTRATION INTO DRY SOIL

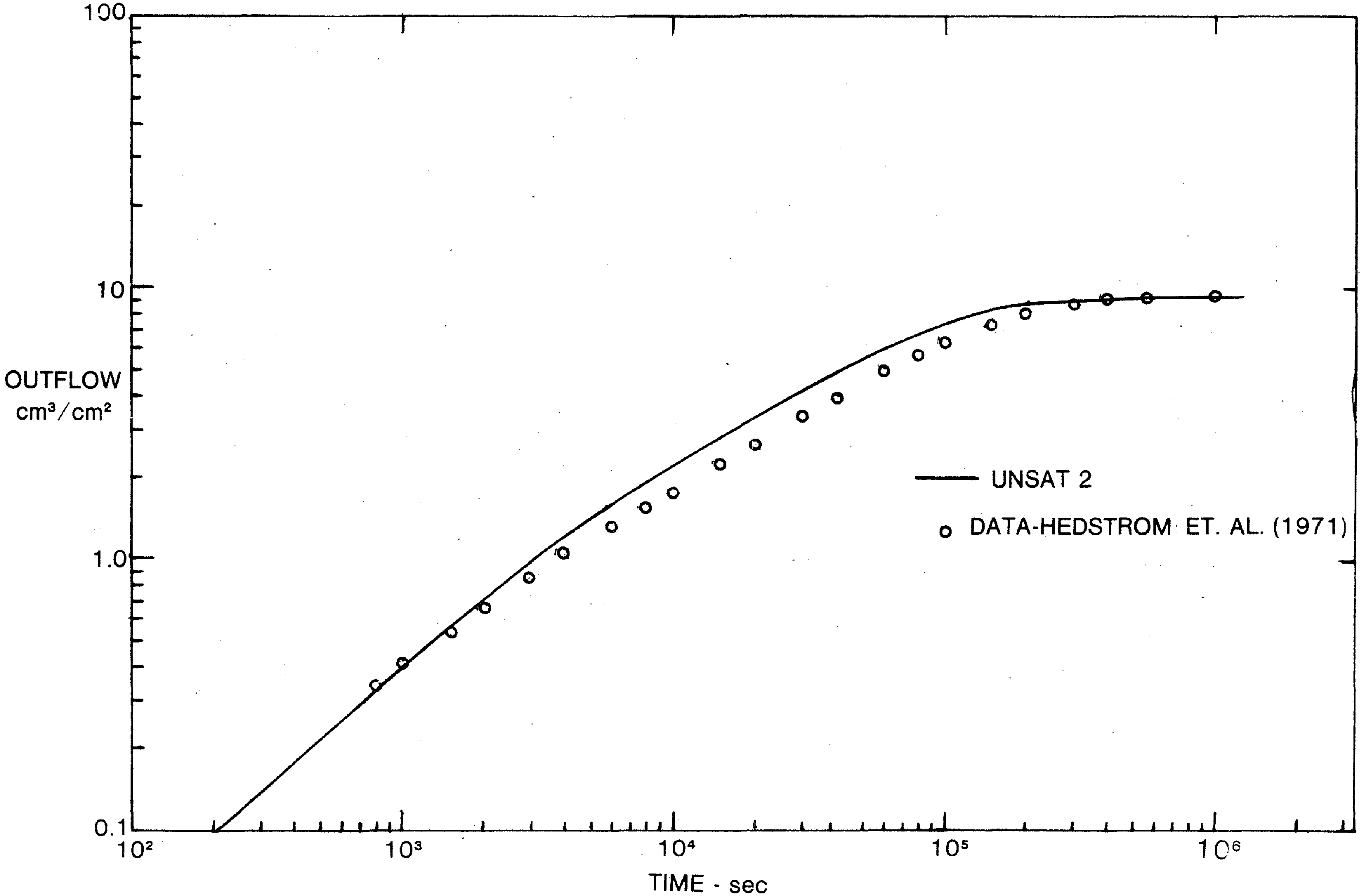

FIGURE I-6 TWO-DIMENSIONAL DRAINAGE

In the theory of two-phase flow, a so-called fractional flow function is introduced which couples the wetting and nonwetting fluid flow characteristics. A total flow variable (sum of wetting and nonwetting fluid fluxes) may also be introduced into the continuity equation giving an equation similar in form to the continuity equation for steady, saturated flow. An attempt was made to introduce this total flow variable into a saturated flow finite element program from the Corps of Engineers Waterways Experiment Station. However, this program did not operate satisfactorily even without modification so this goal was abandoned.

It appears that the introduction of air flow will require a different formulation for the finite element procedure than has appeared in the literature. It is almost certain that the petroleum industry does have finite element programs which consider the flow of both wetting and nonwetting fluid phases; however, this is proprietory information and is therefore, not available.

I-3 SUMMARY

The completion of Phase I showed that the program UNSAT2 was operational and could be used for a number of unsaturated flow problems with good agreement between experimental data and the computer simulation.

PHASE II

The work under this phase will not be discussed in the order listed in the scope of work, rather the determination of hydraulic properties of shale will first be considered, then comparison between data from the field seepage ponds and computer simulation will be made.

II-1 SHALE HYDRAULIC PROPERTIES

Laboratory procedures and data are given in Appendix B. The data which were used in running UNSAT2 are given rather than original laboratory data. The values for hydraulic properties have in some cases been averaged and interpreted as explained in Appendix B. The data presented make up the best current information concerning the hydraulic properties of waste shale. Some of the analysis of data is based on theory of Brooks and Corey (1964) and Laliberte, et al. (1968). The term "hydraulic properties" includes values of saturated hydraulic conductivity and relationships between relative conductivity, capillary pressure (tension), and saturation or moisture content. The purpose of this is to provide sufficient data on retorted shale that it will be possible to design shale piles and predict the hydraulic properties such that a complete analysis of the flow in the pile can be done with no additional lab work. In the analysis, the emphasis was on whether the values are reasonable and it is recognized that there was considerable variation between samples.

II-2 SIMULATION OF SEEPAGE PONDS WITH UNSAT2

The properties of the soil which are required for the computer simulation are porosity, saturated hydraulic conductivity, relative conductivity as a function of volumetric moisture content and capillary pressure as a function of moisture content. Volumetric moisture content, θ, is determined from saturation by the equation

$$\theta = S\phi$$

where S is saturation and ϕ is porosity.

For both ponds, the field data consisted of the ponded depth and the quantity of water that was lost from the pond in a particular time as measured by the drop in the water surface. For simulation, it was necessary to use the average depth over a time period as a constant potential and compare the total volume of inflow from simulation with that from the field data. The data presented consists of a plot of actual and assumed pond depth versus time, and a plot of inflow versus time, with both field and simulated values.

The finite element networks for both ponds were set up as axial symmetrical problems with the bottom area of the ponds the same as in the field. This would not give the same perimeter and area of the sides for simulation as occurred in the field, but this is a minor error.

II-2.1 Pond 1

The finite element mesh for this pond is shown in Figure II-1. The axis of symmetry for the pond is on the left side. The area of the bottom of the pond is 280.3 m^2 (3017 sq ft), there are 104 node points and 81 elements.

During all periods of testing in this pond, free flow was allowed from the drain. The lower boundary was, therefore, treated as a seepage surface which allowed outward flow when the water pressure was greater or equal to atmospheric pressure. The seepage surface extends from node 1 to node 96.

The average density of the shale in the pond was 1613 kg/m^3 (100.6 pcf) and the average moisture content when compacted was 22.1 percent by weight. The pond was initially filled to 1.07 m (3.5 ft) and kept near this depth from December 8, 1975, to February 25, 1976. Staff gauge readings were taken periodically during this period. The simulation of the pond was from December 16 to January 31. The period from January 31 to February 25 was not simulated because the field data were inconsistent. The staff gage reading on both February 2 and 25 is given as 1.07 m, yet at the start of a 19-day period ending March 15 (which was February 25), the reading is given as 0.91 m (3.0 ft). During this time, there was no loss of water recorded for the pond.

Figures II-2 and II-3 show the comparison between simulated and field values for the December-January and the March-April periods, respectively. In the upper part of the figures, the depth of ponding as a function of time is given and in the bottom part, the cumulative loss from the pond as a function of time is given. The agreement is very good except for the two periods from 0 to 550 hours in Figure II-2 and from 800 to 960 hours in Figure II-3.

Probably the most important reason for the discrepancy up to 550 hours is related to the initial moisture condition. According to the average density of 100.6 pcf, the porosity or void space would be 0.398. A moisture content of 22.1 percent would give a volume of water per unit volume of 0.356. When the pond was filled there would therefore be considerable trapped air in the shale and the conductivity would be considerably less than the saturated value.

For this reason the initial conductivity was taken as 55 percent of the saturated conductivity. The value of .55 is a typical value for many materials, but could be considerably in error. Trapped air will eventually (several months) dissolve in the water and escape either by diffusion or by being carried out by the flowing water as explained by Adams et al. (1969). It was arbitrarily decided to assume the initial hydraulic conductivity was (.55)(.00024) = .000134 m/hour. At the end of the 1079 hour period, the shale was assumed to be completely saturated, or K = .00024 m/hour. The average of these two values, or .000189 m/hour was, therefore, used for the 1079 hour period. For the remainder of the simulation K = .00024 m/hour was used. Very likely the effect of trapped air was more severe than thought and a lower value of conductivity should have been used.

Another possible reason for poor agreement could have been the effect of temperature on viscosity. During the initial 1079 hours, the temperature was always very near 0°C. The later measurements, during which the value of hydraulic conductivity was determined, were during the spring but temperature was not recorded. If the water temperature at this time was as high as 20°C, the hydraulic conductivity at 0°C would have been approximately half of that

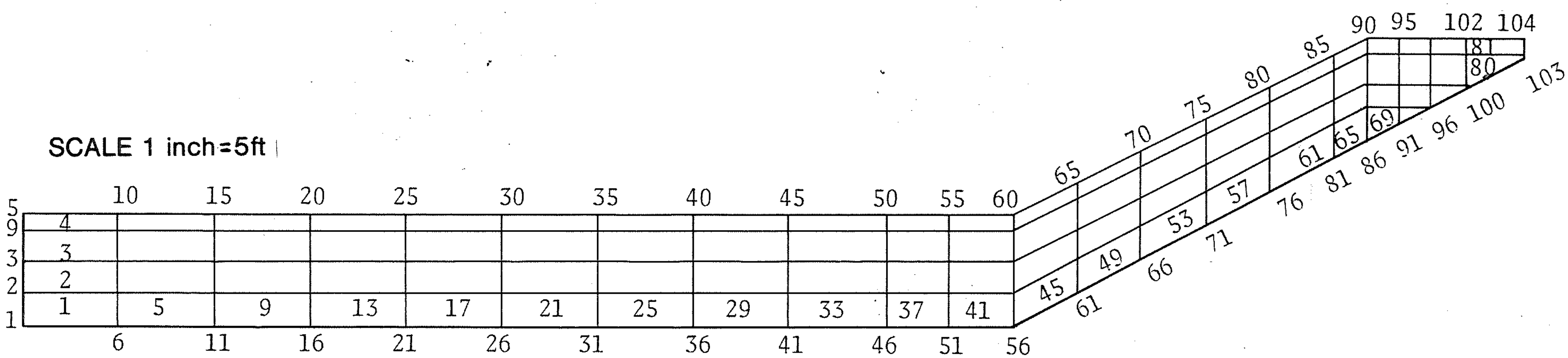

FIGURE II-1 FINITE ELEMENT MESH FOR POND 1

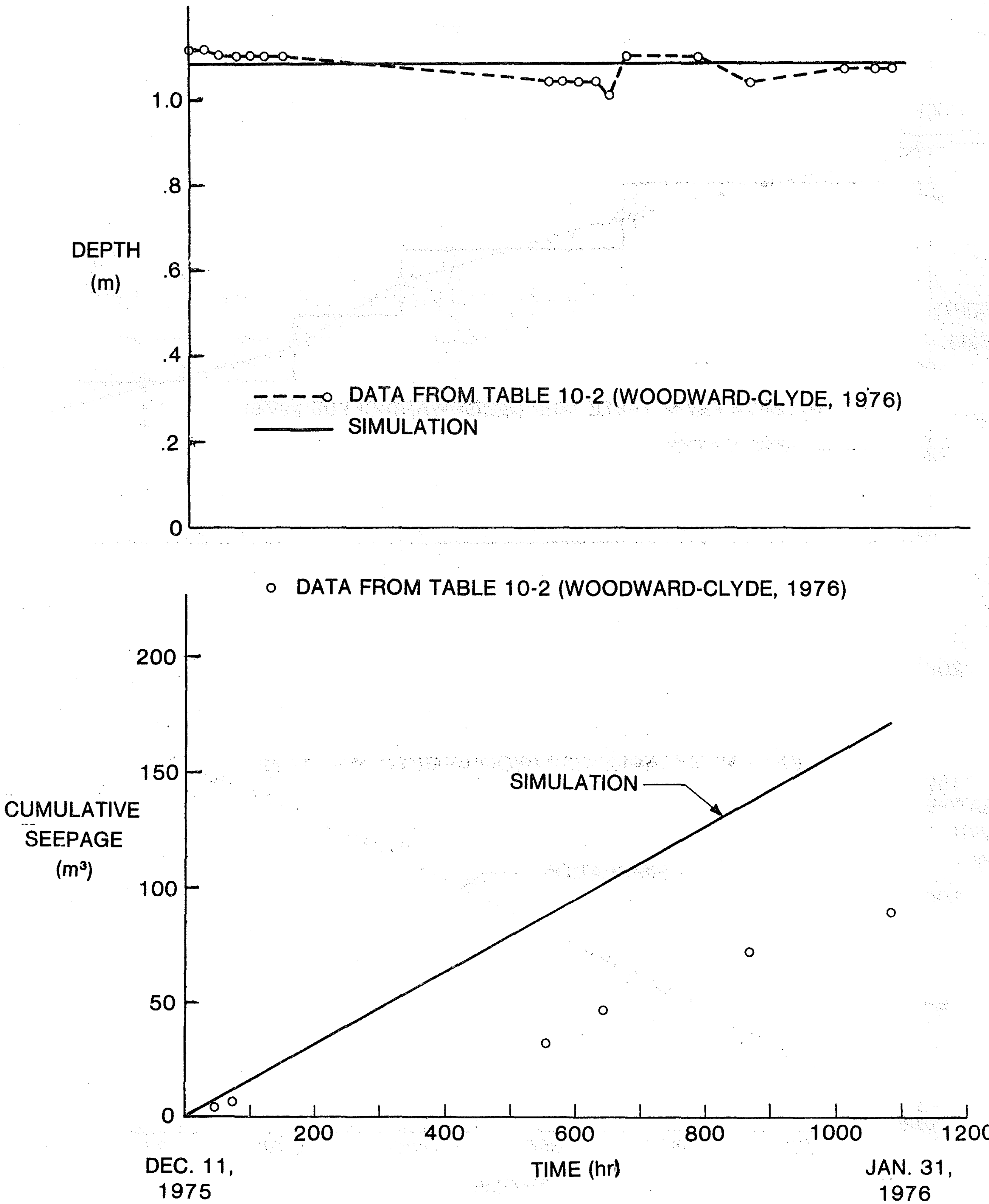

FIGURE II-2 SIMULATION OF POND 1 DEC. 1975-JAN.1976

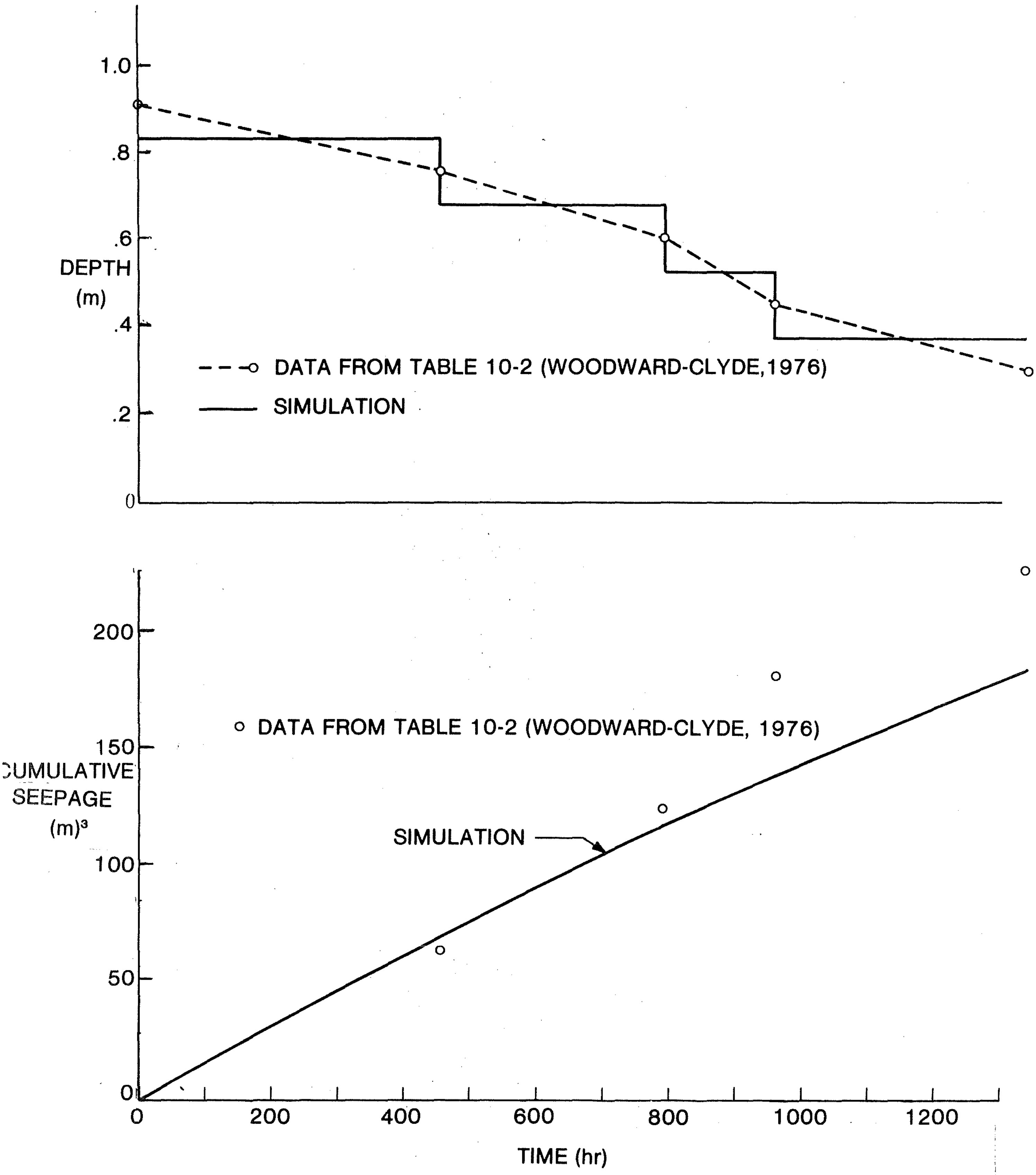

FIGURE II-3 SIMULATION OF POND 1 FEB-APR,1976 at the warmer temperature considering only the effect of temperature on viscosity. No correction was made for temperature since the necessary data were not available.

The poor agreement from 800 to 950 hours in the March-April period is probably due to a leak in the pond which could have closed up temporarily during the 950 to 1350 hour period before washing out completely about April 21. The leak was due to a tear in the pond liner caused by settlement of the fill under the pond. It appears that the field data during the short period is not consistent with that either before or after.

There is no doubt that better agreement could have been reached between simulated and field values by adjusting the values of hydraulic conductivity periodically. Unless there are reasons, backed up by data, as to how much the conductivity should be changed, nothing is really proved by doing this, however.

II-2.2 Pond 2

The finite element mesh for this pond is shown in Figure II-4. The axis of symmetry for the pond is again at the left side, the area of the bottom is 187 m^2 (2017 sq ft); there are 130 node points and 106 elements.

This pond had a wide range of boundary conditions. At various times, as shown in Table II-1, the upper boundary had conditions of constant potential, no flow, infiltration, or evaporation. The lower boundary was either a seepage surface or a no-flow boundary at all times. The seepage surface extended from node 1 to node 103.

The hydraulic properties of the shale for the pond again were not considered constant over the entire period of simulation. When the pond was initially filled, the average moisture content on a volume basis was 0.054 and the average porosity was 0.453 which would indicate considerable trapped air in the shale.

During the initial period of simulation, imbibition data for the shale were used. From laboratory data on imbibition, the moisture content was estimated to go to 0.412 without any influence of trapped air. Thus, the porosity used with the imbibition data was 0.412 for the first 30 hours. After this time, a porosity of 0.453 was used so that the shale could become completely saturated. It is realized that the shale would possibly not have been completely saturated after only 30 hours and a correction could have been applied over a longer time period.

The value of hydraulic conductivity used varied from 37.9 m/yr to 68.0 m/yr over the initial simulation period of 287 hours. The reasoning for this is the same as above; that initially the material contained trapped air but eventually it became completely saturated. The value of 68.0 m/yr was the value actually measured in the field in December when the water temperature was 1°C. This is not the value from the line in Figure B-10 which has been adjusted to a temperature of 10°C. The other values in Figure B-10 were measured in the summer when the water temperature was considerably higher but was not recorded. To calculate these conductivities, the temperature was assumed to be the average for the particular month when the measurements were made.

Figure II-5 shows the simulation for pond 2 during December, 1975. The agreement between simulation and field data is excellent except after 265 hours when the measured flow was less than predicted.

SCALE 1 inch=5 ft

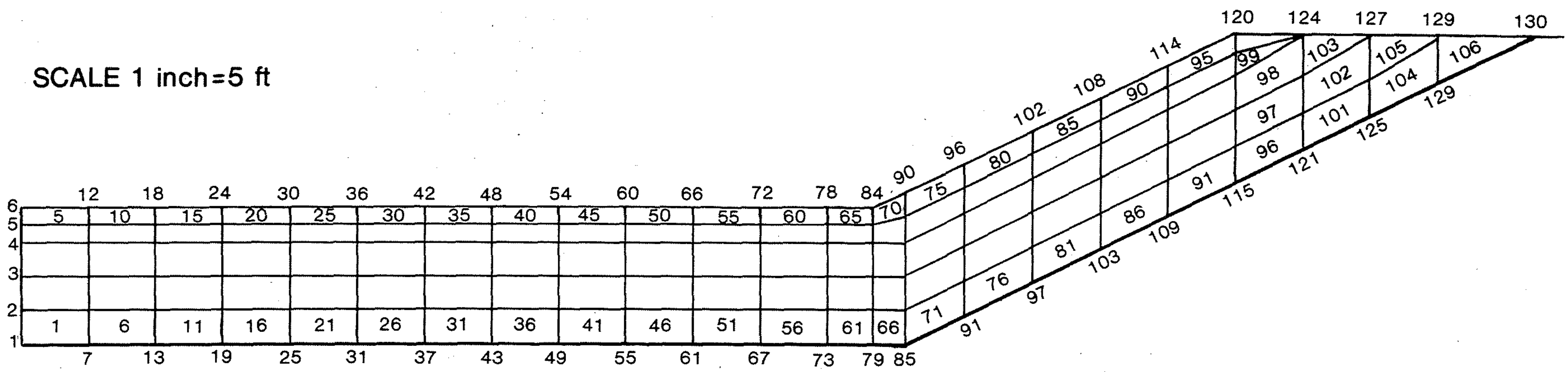

FIGURE II-4 FINITE ELEMENT MESH FOR POND 2

TABLE II-1

Boundary Conditions and Values of Parameters for Simulation of Pond 2

Date	ΔT	Top Boundary Condition	Bottom Boundary Condition	Conductivity Used m/yr	Porosity
Dec. 10, 1975					
	30 hours	H = 0.277 m	Seepage Surface	37.9	0.412
Dec. 11, 1975					
	120 hours	0.357 m	No flow	44.8	All other porosities were 0.453
Dec. 16, 1975					
	21 hours	0.282 m	Seepage Surface	52.9	
Dec. 17, 1975					
	21 hours	0.183 m	No flow	60.6	
Dec. 18, 1975					
	50 hours	0.171 m	No flow	60.6	
Dec. 20, 1975					
	21 hours	0.366 m	No flow	60.6	
Dec. 21, 1975					
	24 hours	0.259 m	Seepage Surface	68.0	
Dec. 22, 1975					
May 11, 1976					
	196 hours	0.817 m	No flow	All other conductivities were 200 m/yr	
May 19, 1976					
	7 hours	0.817 m	Seepage Surface		
May 19, 1976					
	7 hours	0.488 m	Seepage Surface		
May 20, 1976					
	6 hours	0.223 m	Seepage Surface		
May 20, 1976					
June 8, 1976					
	170 hours	0.924 m	No flow		
June 15, 1976					
	6 hours	0.677 m	Seepage Surface		
June 15, 1976					
	16 hours	0.283 m	Seepage Surface		
June 16, 1976					
	8.5 hours	0.030 m	Seepage Surface		
June 16, 1976					
	961 hours	No flow	Seepage Surface		
July 26, 1976					
	2424 hours	Evaporation	No flow		
Nov. 4, 1976					
	95 hours	Infiltration	Seepage Surface		
Nov. 6, 1976					

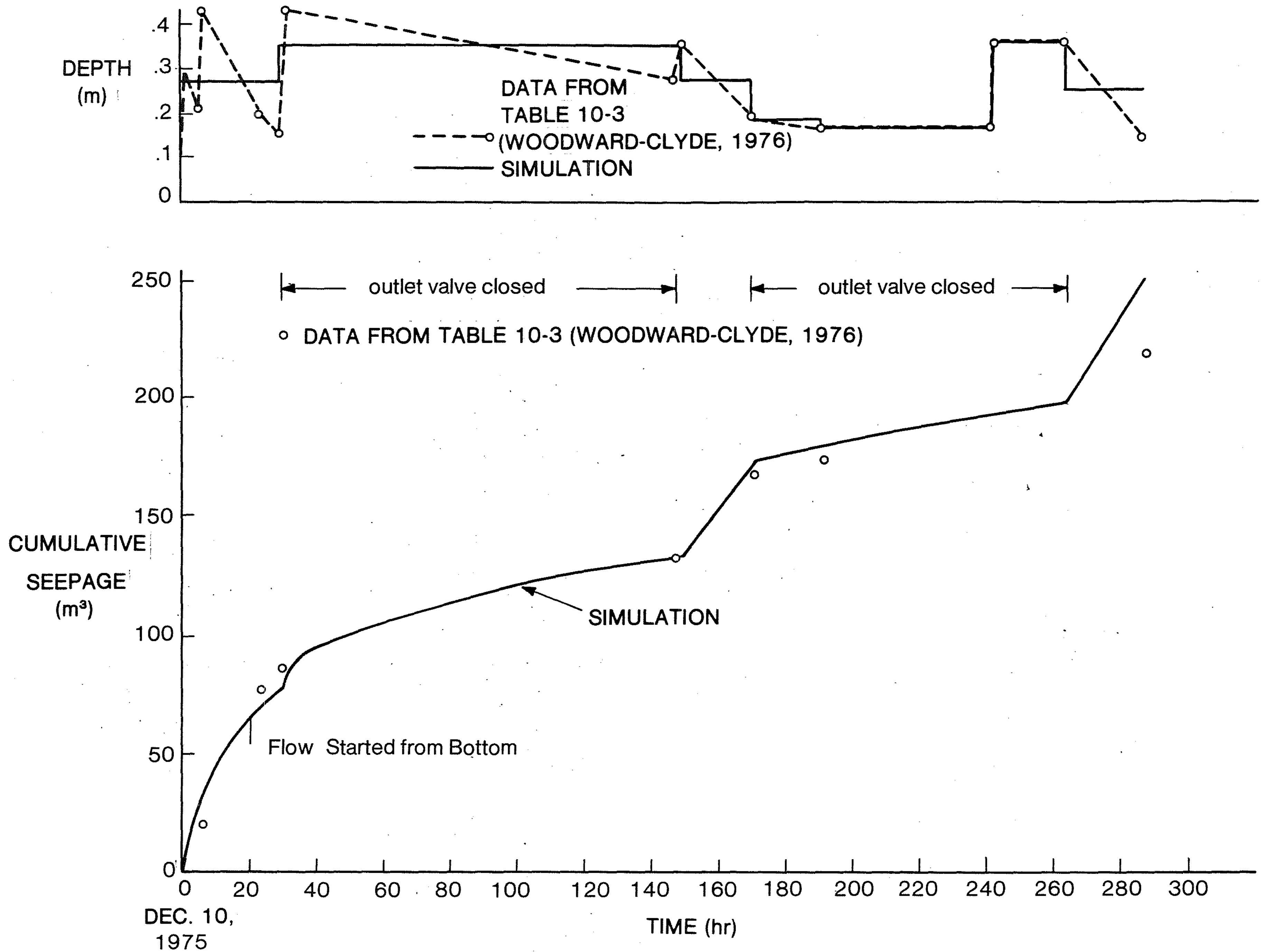

FIGURE II-5 SIMULATION OF POND 2-DEC, 1975

The next period during which field data were taken was in May, 1976, when the pond was filled to a depth of 0.98 m. After 8 days it had dropped 0.3 m, even though the outlet valve was closed. It was apparent the water was simply moving into the shale which had dried due to evaporation from December to May. The program could have been run for this period to determine the evaporation to have the proper moisture content in May. It was decided, however, to simply estimate the evaporation from the average evaporation figures for western Colorado. This estimate was a total of 40 m^3 of water which, when removed from the shale, left a moisture content of 0.260. This was the initial moisture content used for the May period. This correction is somewhat arbitrary, but appeared to be satisfactory since detailed weather records were not available. An evaporation of 3.3 mm per day for 9 days or 8.1 m^3 was also applied as a correction to the field data for water loss from the pond.

The simulation for this period is shown in Figure II-6. Agreement between the simulation and data is reasonably good with some difference toward the end of the 9-day period. Seepage from the pond was somewhat greater than that from simulation. During this period the value of hydraulic conductivity used was 200 m/yr which was a value determined during June. This is a larger value than one would have obtained from the line in Figure B-10, but again the actual temperature is unknown.

The next period of field data was from June 8 to July 26, followed by evaporation until November 4 when the pond was sprinkled and allowed to drain until November 6. The simulation for June 8 to June 16 is shown in Figure II-7. The agreement here is quite good especially for the amount that had infiltrated at 198 hours. Table II-2 compares the actual discharge from the drain in the field and from simulation during the period of June 16 to July 26 after inflow stopped. The simulated drainage is somewhat higher initially and then decreases faster than that measured in the field. It is unknown how accurate the field data are since the data sheet states the flow was estimated. One reason that the simulated flow would show a quicker response time is that in the field the water would drip from the shale and then run out through the gravel layer and the drain pipe, whereas the simulation gives the time at which water leaves the shale.

From June 26 to November 4, the program was run to simulate evaporation at a rate dependent on atmospheric conditions and the rate at which the water moved to the surface of the shale. During this time, a total evaporation of 113 m^3 was calculated which is about 0.20 m over the area of the entire pond. This compares with an average evaporation from a free water surface of about 0.43 m during this period.

The last period simulated was November 4 to 6, 1976, when the pond was sprinkled with 17,400 liters of water during a 30-minute period. For simulation, the initial moisture distribution was set at that which existed at the end of the evaporation period. The infiltration occurred at a varying rate as determined by the flow into the shale. The maximum specified rate was that at which the water was applied or about 50 mm in 30 minutes. The maximum infiltration rate that occurred during simulation was 44 mm per hour. The field data do not indicate whether infiltration occurred as fast as the

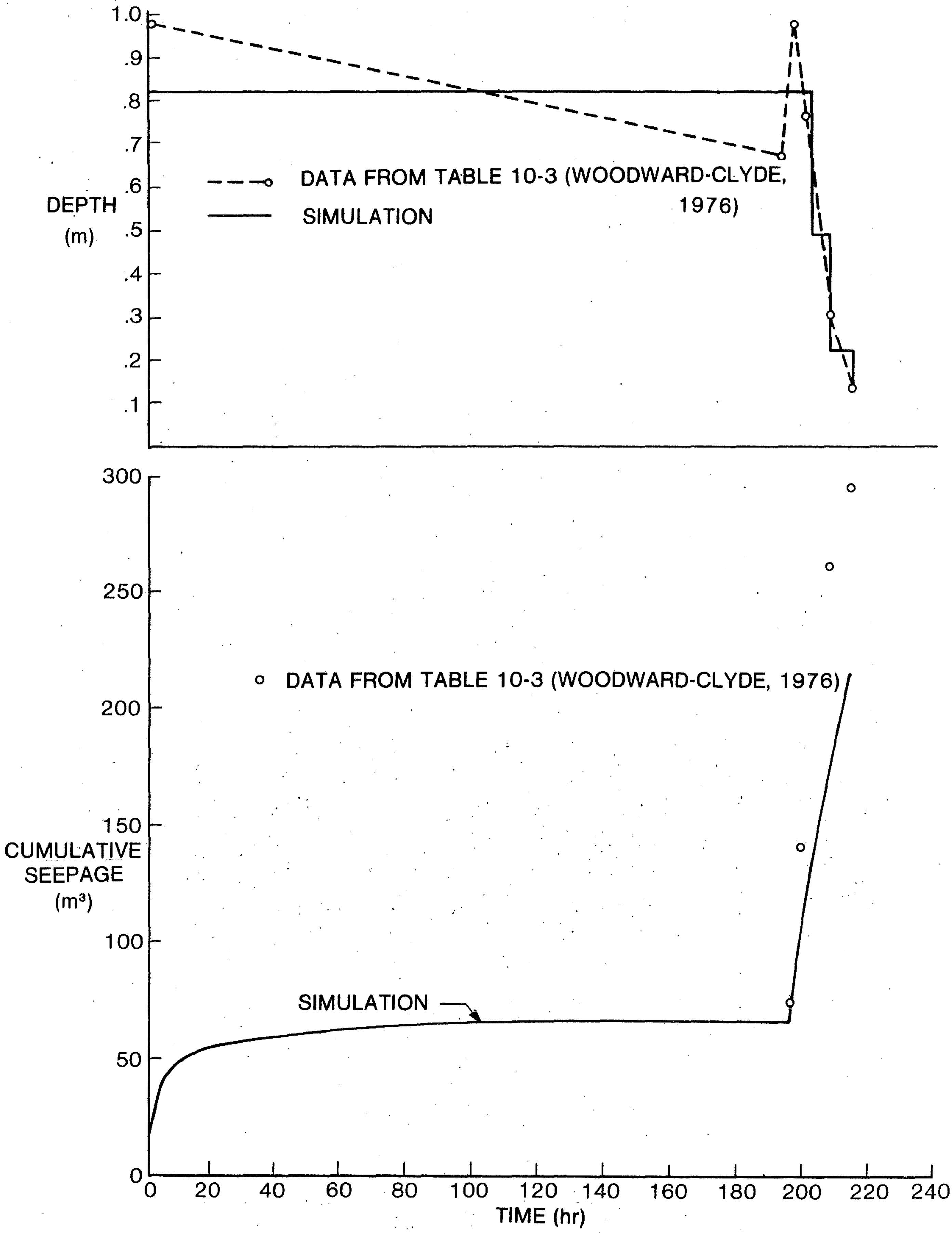

FIGURE II-6 SIMULATION OF POND 2 MAY, 1976

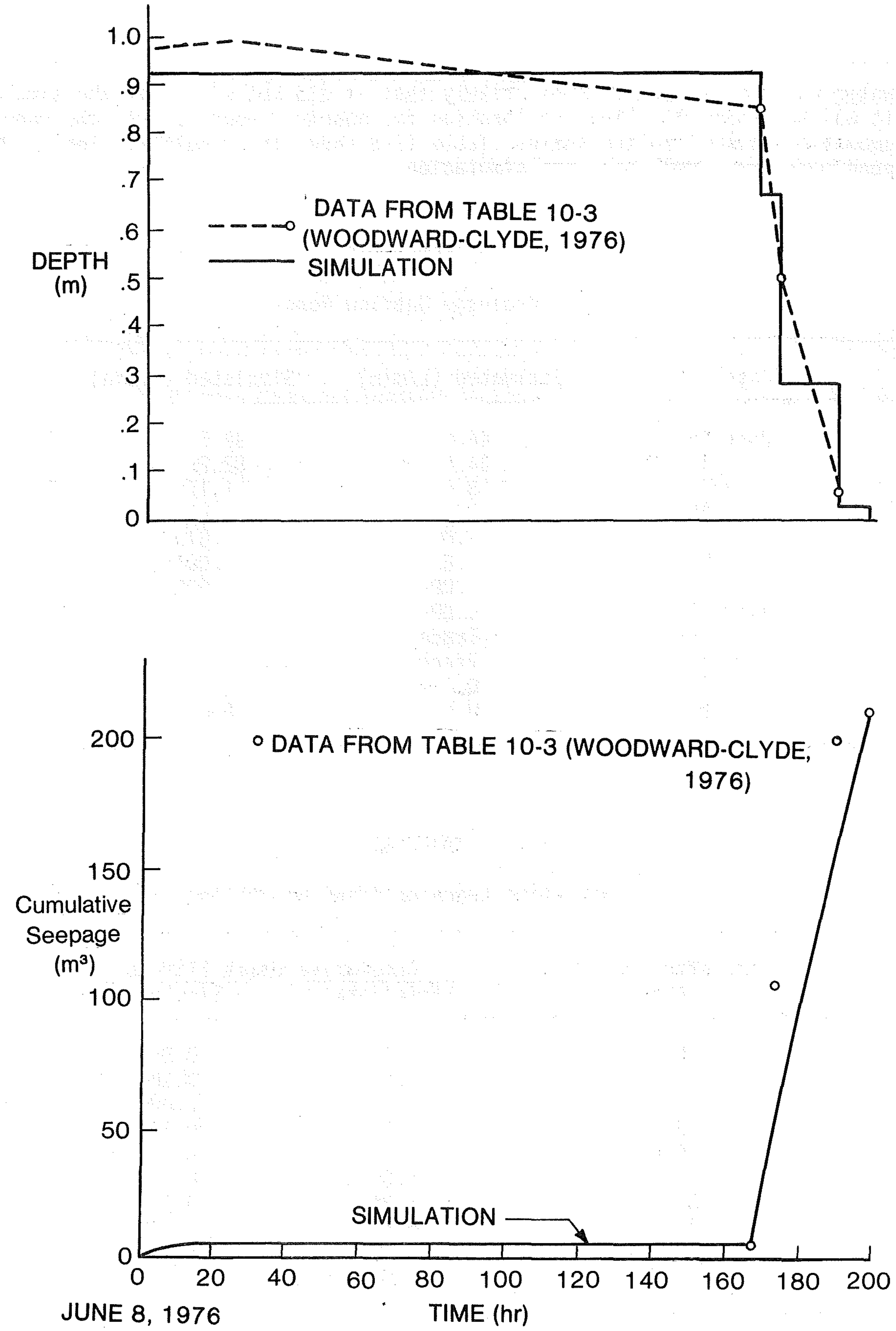

FIGURE II-7 SIMULATION OF POND-2 JUNE-JULY, 1976 water was applied but it seems likely that it did not since, in the simulation, it was necessary to allow infiltration for nearly 2 hours to get the required amount of water into the shale. Table II-3 shows the cumulative leach from the pond both from field data and simulation.

TABLE II-2

Drainage Outflow Pond 2

Date	Estimated (L/min)	Simulated (L/min)
June 16	46.6	97.55
16	24.6	82.26
17	3.4	1.17
18	2.4	.42
23	.08	.019
25	.03	.0019
29	.004	.0002
July 2	<.004	
9	Trace	
16	Trace	
23	0.0	
26	0.0	0.0

TABLE II-3

Cumulative Leaching After Sprinkling

Time after rainfall (hrs)	Cumulative Leach (liters)	
	Field Data	Simulation
0.0	.00	0.000
.6	.02	0.000
1.9	.06	0.000
3.2	.09	0.71
6.0	.15	0.71
22.7	5.59	0.71
30.2	6.30	0.71
46.7	6.99	0.71
70.7	6.99	0.71
94.7	6.99	0.71

Although there was approximately 10 times as much water drained from the pond in the field as occurred in the simulation, the correlation is very close since over 17,000 liters of water were applied. When it is considered that the simulation occurred over a 4-month period which included evaporation and sprinkling and the amount of water which leached is only 6.28 L more than predicted (from a volume of over 680 m^3 of shale) the agreement is excellent.

II-3 SUMMARY

In summary, the work under Phase II showed that:

1) The computer program UNSAT2 will satisfactorily simulate unsaturated flow of water in waste shale under various boundary conditions.

2) The hydraulic properties of waste shale have been determined with sufficient accuracy for prediction of flow in waste shale with the above computer code.

3) Waste shale appears to have a high moisture holding capacity somewhat similar to silt loam soils.

PHASE III

This portion of the project involved the use of the program UNSAT2 to study the flow of water from precipitation both in a natural geologic profile of the Green River Formation and in a hypothetical profile of retorted shale. A comparison is also made between the use of this program and conventional (saturated) flow finite element programs.

The first objective in Phase III was to conduct a rainfall intensity-duration-frequency analysis for Western Colorado. This information was readily available for the weather station at Grand Junction and is given later in Table III-3. Grand Junction is at a lower elevation than either Rifle or the Piceance Basin and the annual rainfall is therefore somewhat less. The intensity-duration-frequency curves would not be identical for Grand Junction and higher elevations but there was not sufficient data readily available to develop such curves for other locations. Since this study was to investigate the application of intensity-duration-frequency data and UNSAT2 to shale profiles, the Grand Junction data were used.

The storm intensities which were used were all for a 100 year return period as this is the most extreme case given. The actual intensity values used are given in the following sections of the report.

In the future, if an actual waste shale pile is being designed, a detailed frequency analysis could be carried out for that particular location by the procedures developed here.

III-1 SIMULATION OF NATURAL PROFILE - PICEANCE BASIN

A north-south cross-section of the Piceance Creek basin shown as Section A'-A' in Figures III-1 and III-2 was simulated. The total length of the section is about 53 km (33 miles) and the total thickness about 760 m (2500 ft). For the finite element mesh there were 103 node points, 88 elements (arranged in general in 5 rows and 17 columns) and 4 different materials. (Figure III-3) On the average the elements were elongated in the horizontal direction by a ratio of 20:1. Some finite element programs will not run with this degree of elongation of the elements but it caused no particular problems here. The shaded area in Figure III-2 and that area above it to the ground surface were simulated.

The locations of surface streams appear as single node points with a "seepage surface" boundary condition. This allowed flow into the stream as long as the water table was as high as the channel bottom. The boundary nodes in between surface streams were either infiltration or evaporation nodes.

The conductivity, porosity, and specific storage values used were those given by Golder Associates (1977) shown in Figure III-4. The values for other hydraulic properties (capillary pressure-saturation-relative conductivity data) were obtained from data on sandstone cores of corresponding conductivities (Bloomsburg and Corey, 1964), and are shown in Table III-1.

The use of these data at best is a gross approximation but we feel under the circumstances it is justified since the problem was only being run to show the applicability of UNSAT2 to a natural profile.

The initial conditions used for all runs of this problem was the water table at the location given by Golder Associates (1977) with a pressure

FIGURE III-1 LOCATION OF THE PICEANCE CREEK BASIN AND STUDY SITES

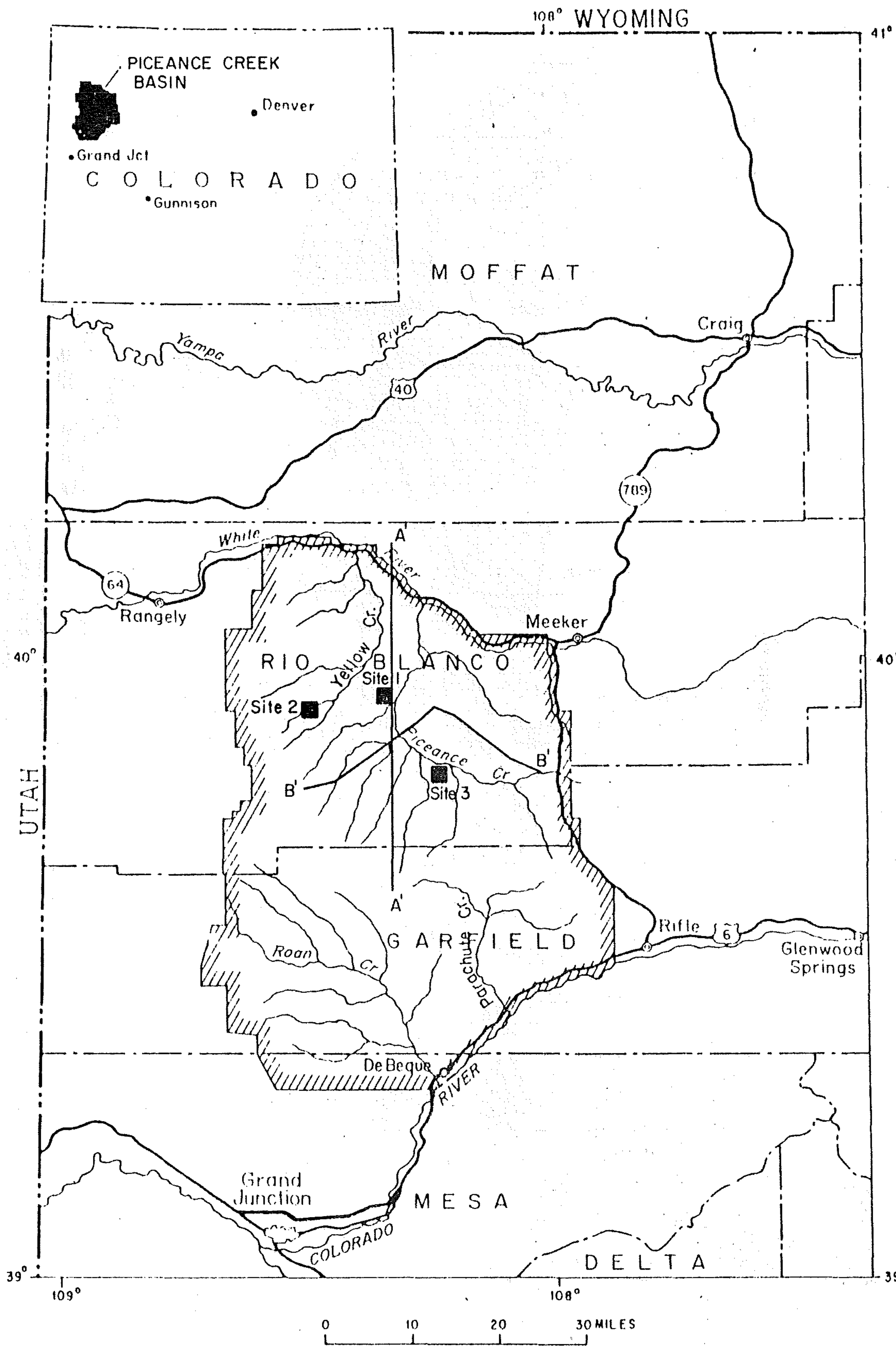

After Coffin, et al., 1971

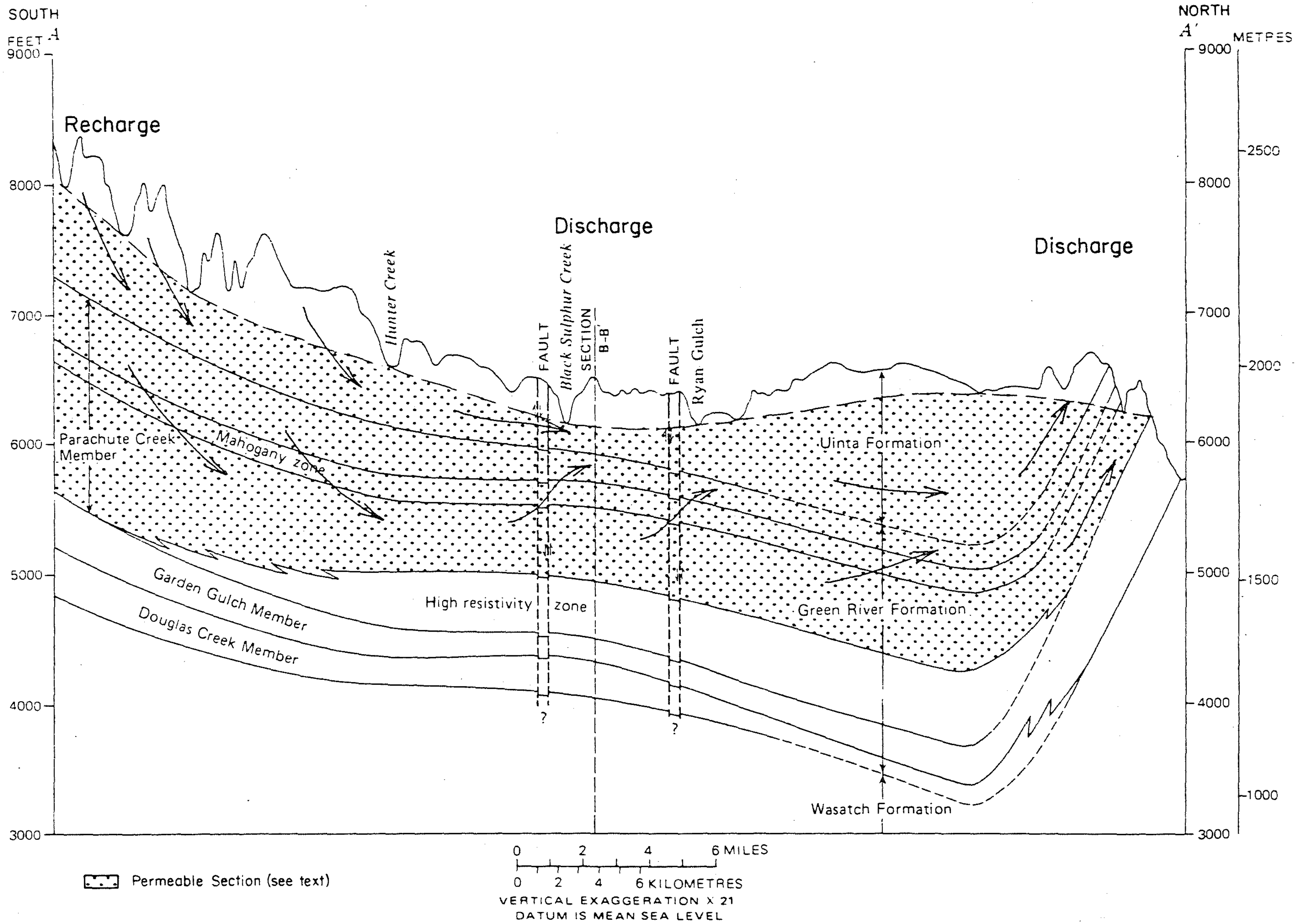

After: Weeks, et al., 1974, p.6.

FIGURE III-2 GEOHYDROLOGIC SECTION THROUGH THE PICEANCE BASIN (Section AA' in

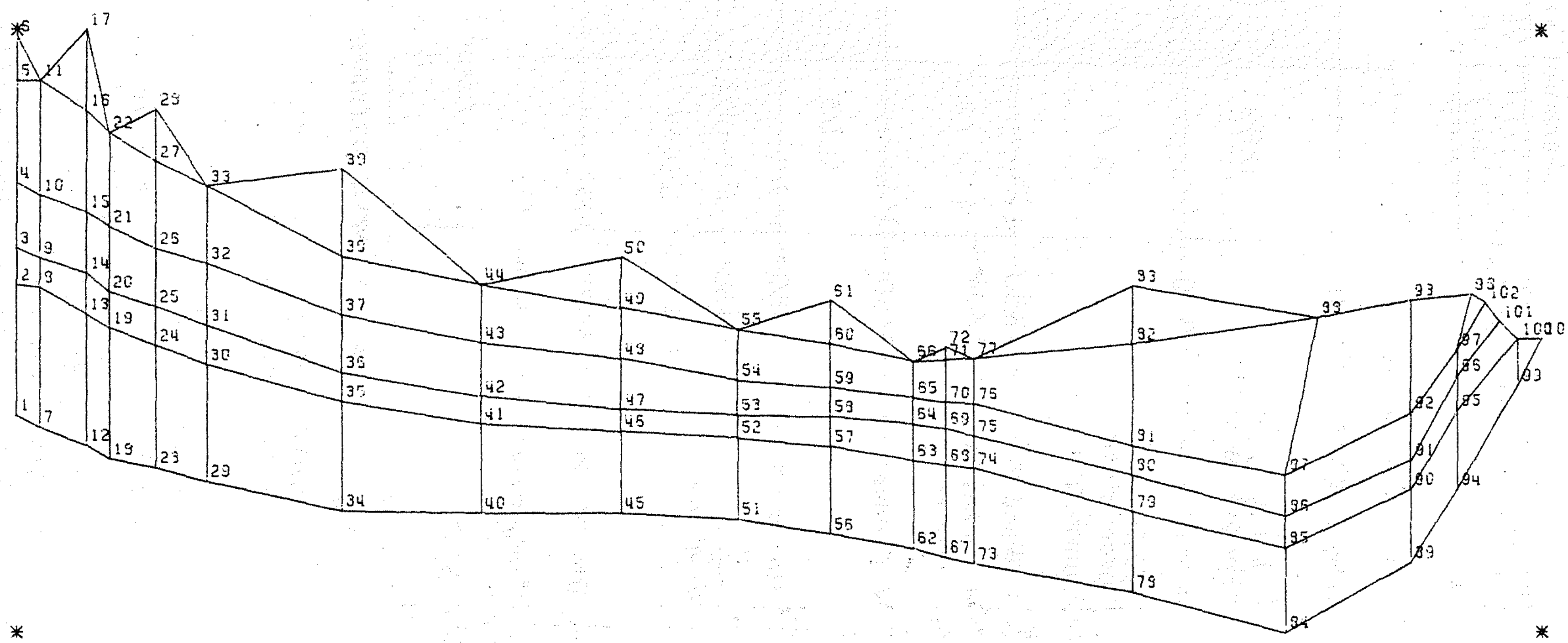

FIGURE III -3

FINITE ELEMENT MESH - PICEANCE BASIN XSCALE = 20000.00 YSCALE = 1200.00

FIGURE III-4 GEOHYDROLOGY MODEL OF SITE I

Geol. Unit		Feature Description	Elevation (Above M.S.L.)	Permeability Horizontal (ft./day)	Permeability Vertical (ft./day)	Drainable Porosity	Specific Storage ($ft.^{-1}$)
Uinta Formation		Ground Surface	6225				
Uinta Formation		Water Table	6100				
Uinta Formation		Uinta Sandstone		0.89	0.03	0.10	3×10^{-7}
GREEN RIVER FORMATION	Parachute Creek Member		5500				
GREEN RIVER FORMATION	Parachute Creek Member	Upper Parachute Cr. Member		5.71	0.03	0.01	3×10^{-7}
GREEN RIVER FORMATION	Parachute Creek Member	A Groove	5350				
GREEN RIVER FORMATION	Parachute Creek Member	Mahogany Marker	5300	1.74	0.009	0.01	3×10^{-7}
GREEN RIVER FORMATION	Parachute Creek Member	B Groove	5150	0.53	0.003	0.025	3×10^{-7}
GREEN RIVER FORMATION	Parachute Creek Member	Horizon X	4850				
GREEN RIVER FORMATION	Parachute Creek Member		4450	0.003	0.0003	0.01	3×10^{-7}
GREEN RIVER FORMATION	Parachute Creek Member	R-4 Zone	4200				
GREEN RIVER FORMATION	Garden Gulch Member	Blue Marker	3925				
GREEN RIVER FORMATION	Garden Gulch Member	Orange Marker	3750	Assumed Functionally Impervious			

NOTES: **FROM GOLDER ASSOCIATES, 1977**

1. Geology based on USBM 01-A and USBM 02-A
2. Hydrology data primarily from USBM 01-A, USBM 02-A, and USBM pilot hole "X" testing.
3. All elevations rounded to nearest 25 feet
4. Not to scale.
5. Quality of information for the purposes of this study:
   - (blank box) "Based on acceptable test data"
   - (hatched box) "Estimated or based on poor data"
   - (cross-hatched box) "Experiential guess"
6. Available data indicates that this model is not valid at points 3 to 4 miles distance from Horse Draw. It should be used only with great caution, and with a complete understanding of the data upon which it is based.
7. Horizon X is defined in section 4.5.1.

TABLE III-1

Hydraulic Properties Used for Piceance Basin

Material	K_H (ft/day)	$\frac{P_d}{\rho g}$ (ft)	η	$*K_r$	$\frac{P_c}{\rho g}$ (ft)	θ
4	.89	4.92	11.4	1.0 8.3×10^{-14}	0 100	.1 .01
3	5.71	3.15	13.5	1.0 9.6×10^{-16}	0 100	.01 .001
2	1.74	4.92	11.4	1.0 8.3×10^{-14}	0 100	.01 .001
1	.53	5.25	5.7	1.0 1.6×10^{-13}	0 100	.025 .0025

* The values of K_r were calculated from the Brooks-Corey relationships

$$K_r = \left(\frac{P_c}{P_d}\right)^{\eta}$$

and

$$S_e = \left(\frac{P_c}{P_d}\right)^{\frac{\eta-2}{3}}$$

where S_e is the effective saturation, and η and P_d are as given in columns 3 and 4.

at the upper boundary nodes of -20.48 m (-100 ft). The soil at these points would be quite dry because that pressure represents a tension of approximately 3 atmospheres.

The first run of the problem consisted of having maximum infiltration at the average annual precipitation for the watershed or 40 cm (16 inches) per year. This was run for a period of 60 days, during which the general flow was down the piezometric gradient toward the center of the profile. Typical inflows into the streams during this time were a cubic foot per hour or approximately 1.5 cfs per mile of stream. This value appears to be within reason in comparison to the mean annual flows in Piceance Creek of 24 cfs. This comparison at best, says the results are not unreasonable. The stream at Node 11 ceased flowing in less than a day after the start as the water table dropped about 1.2 m (4 ft) at the left end of the mesh. The pressure increased at most nodes to the right of Node 21 except for a few nodes at the right end of the mesh.

During this time period, there did not appear to be any tendency for perched water tables to form. This was expected because of the short time simulated and because the vertical conductivities in the profile in general get smaller with increased depth. A perched water table tends to develop where a less permeable layer is above a more permeable layer and the general flow direction is downward. As pointed out by Golder Associates (1977) the Green River Formation has innumerable "highly impervious, but very thin, rich oil shale stringers", which cause the formation of perched water tables. However, geologic information is not available in sufficient detail to delineate these layers and their effect is therefore not simulated.

The second run of this problem was with evaporation occurring at all upper boundary nodes except the stream nodes. This was run for only an 8 day period to see whether the streams would dry up. Most of them did dry up within a six month period.

The maximum evaporation used was 86 cm (34 inches) per year. This is the actual pan evaporation for the Piceance Basin as given in Climatic Atlas of the United States (1968). This is considerably greater than the actual rate from the soil because rainfall is only about 40 cm (16 inches). It does not really matter what is used for the maximum rate because evaporation in an arid region such as Piceance Basin is limited by the available water and the rate of water movement up through the soil profile.

The third run on this profile was with a 100 year - 24 hour storm. The intensity given for this storm at Grand Junction is 0.254 cm (.1 inch) per hour. Since we were attempting to simulate a storm over the entire Piceance Basin ($\approx$ 900 mi^2) the point value of precipitation should be reduced by 10 per cent (Linsley, et al., 1975). Thus the maximum infiltration rate used was 5.5 cm (2.16 inches) per day. This infiltrated at all points in the watershed and there was no runoff. In actual practice, a rain of this magnitude would probably have surface runoff due to areas of lower permeability than were used in this study. To get better simulation we would have to delineate surface variations in more detail than has been done here.

In summary, it has been demonstrated that UNSAT2 can be applied to a profile of the Green River Formation with several infiltration conditions and evaporation. The runs that were made were for relatively short time periods to keep computer costs down. At such time as a particular problem is to be solved, more detailed geologic data should be obtained, better capillary pressure-saturation-relative conductivity data should be obtained and in many cases a considerably longer time of solution would be required. It would also be desirable to use a smaller cross-section so that better delineation of shale lenses could be obtained without using an extremely large number of node points.

III-2 COMPARISON OF UNSAT2 WITH CFLOW

CFLOW is a finite element program which was originally developed at the University of California - Berkeley and has been used in simulation of flow through various types of tailings dams. Corp (1974), Kealy (1972), Kealy and Williams (1971) are only a few of the studies that have made use of CFLOW.

The data input for UNSAT2 and CFLOW is in essentially the same form. The specification of the elements and node points is identical. UNSAT2 does require data on the capillary pressure - saturation - relative conductivty relationships for the porous material. However, using assumed values for these relationships gives better results than assuming completely saturated flow as in CFLOW.

UNSAT2 does not have a collapsing mesh for free surface flow problems so will treat problems which have a change of materials in a vertical direction (i.e., the plane of discontinuity is horizontal). As shown in the example problem in a typical tailings pond it is possible to have a material under the dam with different permeability than within the dam. UNSAT2 will consider unsteady flow problems and will predict the formation of perched water tables and unsaturated regions. This is a condition that is very likely to occur when there is horizontal layering in the tailings dam. Most boundary conditions can be changed at particular times, such as changing the potential at constant potential boundaries or changing to or from constant flux. Infiltration and evaporation can be considered where the actual rate is determined by exterior conditions such as rainfall and evapotranspiration.

The output from UNSAT2 is somewhat different from CFLOW in that the velocity of flow in a particular element is not given. However, if this type of information is needed it can be easily calculated from the pressures at the node points. Output consists of a complete listing of pressures at each node point at each increment of time. The flux at all node points which have flow in or out of the material is also given.

CFLOW is limited to use in steady saturated flow problems and therefore does not handle flow through the unsaturated zone above the water table. In situations such as tailings ponds where there is less permeable material at the bottom of the pond and more permeable material below, it is very common to have unsaturated flow in the more permeable material. This type of problem is shown in Figure III-5. This is a tailings pond located about 1524 m (5000 ft) from an open pit mine. The pond consists of 0.9 m (3 ft) of slimes with 6.1 m (20 ft) of ponded water. By separating the problem into various segments and using a pseudo steady state analysis, it was determined that after about 20 years the region beneath the pond would be saturated.

To run the problem with UNSAT2 a mesh consisting of 120 node points (19 columns by 5 or 6 rows) and 95 elements as shown in Figure III-6 was used. The elements are elongated as much as 3:500 in the horizontal. The initial conditions were a water table at an elevation of 42.7 m (140 ft), a negative pressure of 27.4 m (90 ft) at the bottom of the slime layer and a ponded depth of 6.1 m (20 ft) in the pond.

The problem was run for a period of five years. The region beneath the pond was still unsaturated at that time but the water table beneath the pond had increased in elevation approximately 2.7 m (8.9 ft) due to downward flow. The original water table and final water table are also shown in Figure III-6.

Another thing shown by this analysis was that the effect of seepage at the open pit mine had affected the water table for a distance of only about 304 m (1000 ft). Therefore, the assumption made in the pseudo steady state analysis that the flow out into the open pit would have no effect on the flow under the seepage pond is certainly valid. The time required for the drawdown from the outflow surface to reach the region of the seepage pond would be over 100 years, assuming that the drawdown effect moves back at a rate proportional to the square root of time.

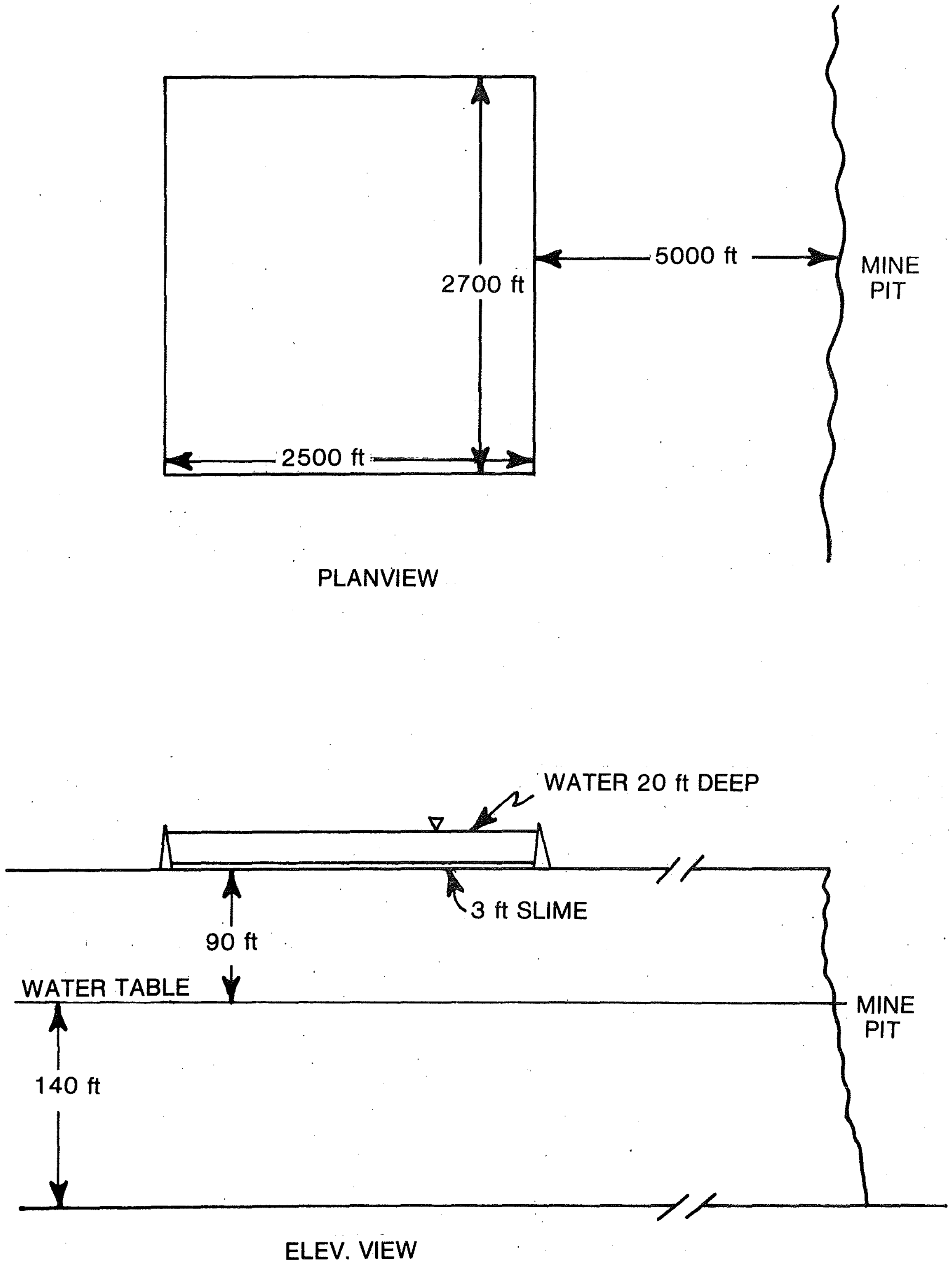

FIGURE III-5 TAILINGS POND

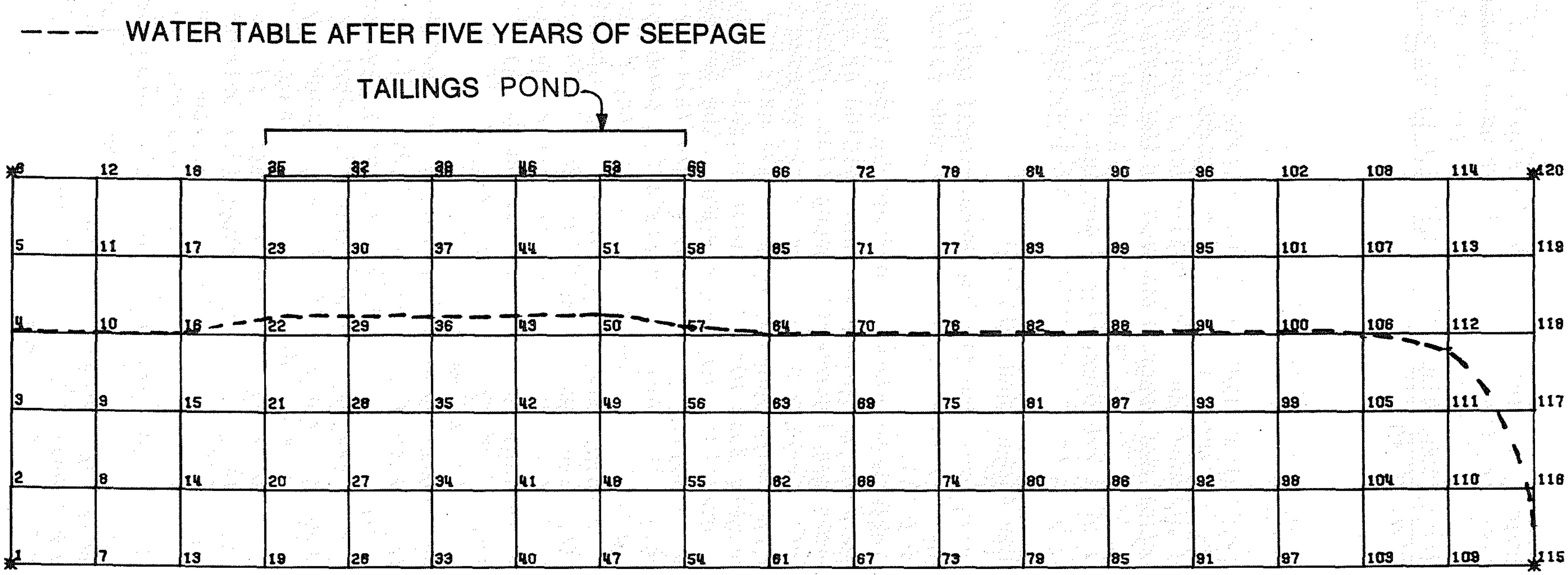

FIGURE III-6
FINITE ELEMENT MESH - TAILINGS POND XSCALE = 1000.00 YSCALE = 100.00

In general, we feel that UNSAT2 should be a very useful tool in many waste disposal problems that involve flow of water through the unsaturated or saturated portion of the soil profile. In some cases it is rather difficult to get a solution for a long time period without using a lot of computer time. A reasonable understanding of the physics of unsaturated flow is also necessary to use the program effectively.

III-3 ANALYSIS OF WASTE SHALE PILES

The initial analyses were run as one dimensional problems to determine what actually would happen to water from storms of various intensities followed by periods of evaporation. The reason for a one dimensional analysis was to simplify the running of the program and reduce the costs so that a large number of runs could be made. The latter part of this work involved analysis of a hypothetical shale pile as a two dimensional problem. This problem was run with a ponded depth of 1.52 m (5 ft) of water as well as several different storm intensities.

III-3.1 One Dimensional Analysis

The mesh used for the one dimensional analysis is shown in Figure III-7. It consists of 21 square elements, 44 node points and represents a depth of 5.25 m (17.2 ft).

The surface boundary is defined by the line between nodes 22 and 44; it was specified as either an infiltration or evaporation boundary. The element sides are impermeable boundaries. Between nodes 1 and 23 was a "conditional" seepage surface; no water entered but if internal moisture conditions allowed, seepage water could exit the system.

There were four materials used in this analysis: oil shale of 75, 85, and 95 pcf densities and Poudre sand. The permeability-capillary pressure-saturation characteristics for all materials are listed in Tables B-2, B-3, B-4, and B-5. The shape of the relative permeability curve was determined from the mean of two experimental secondary desaturation curves for 85 pcf density. The same relative curve has been applied to densities of 75 and 95 pcf. The saturated permeability for 75, 85, and 95 pcf densities was determined from a least squares regression analysis of available experimental data shown in Table B-1. Since secondary capillary pressure-saturation values were used, the effective porosity was specified to account for entrapped air. Hysteresis is not accounted for in UNSAT2.

Initial moisture distribution in the profile was generated by specifying a uniform capillary head of -4.743 m (15.6 ft) at all nodes and allowing evaporation for 720 hours with an evaporation potential of -150 m (492 ft); this generated a moisture distribution unique to each profile. The selection of -150 m (-492 ft) was somewhat arbitrary. The permanent wilting point of many plants is in the range of 15 atmospheres. This potential and greater would develop in a shale pile with a decreasing moisture content. The -150 m (-492 ft) evaporation potential pressure head limits the amount of this depletion. Table III-2 shows some representative evaporation potentials as a function of relative humidity and temperature at standard pressure as well as average values for evaporation at Grand Junction. A potential of -147 m (-482 ft) is developed at a temperature of 10 degrees centigrade and 98 percent relative humidity. During this investigation, four separate analyses were performed on a uniform 85 pcf density profile varying only ψ_L, the atmospheric evaporation pressure potential. The moisture

FIGURE III-7

FINITE ELEMENT MODEL GENERAL DESIGN

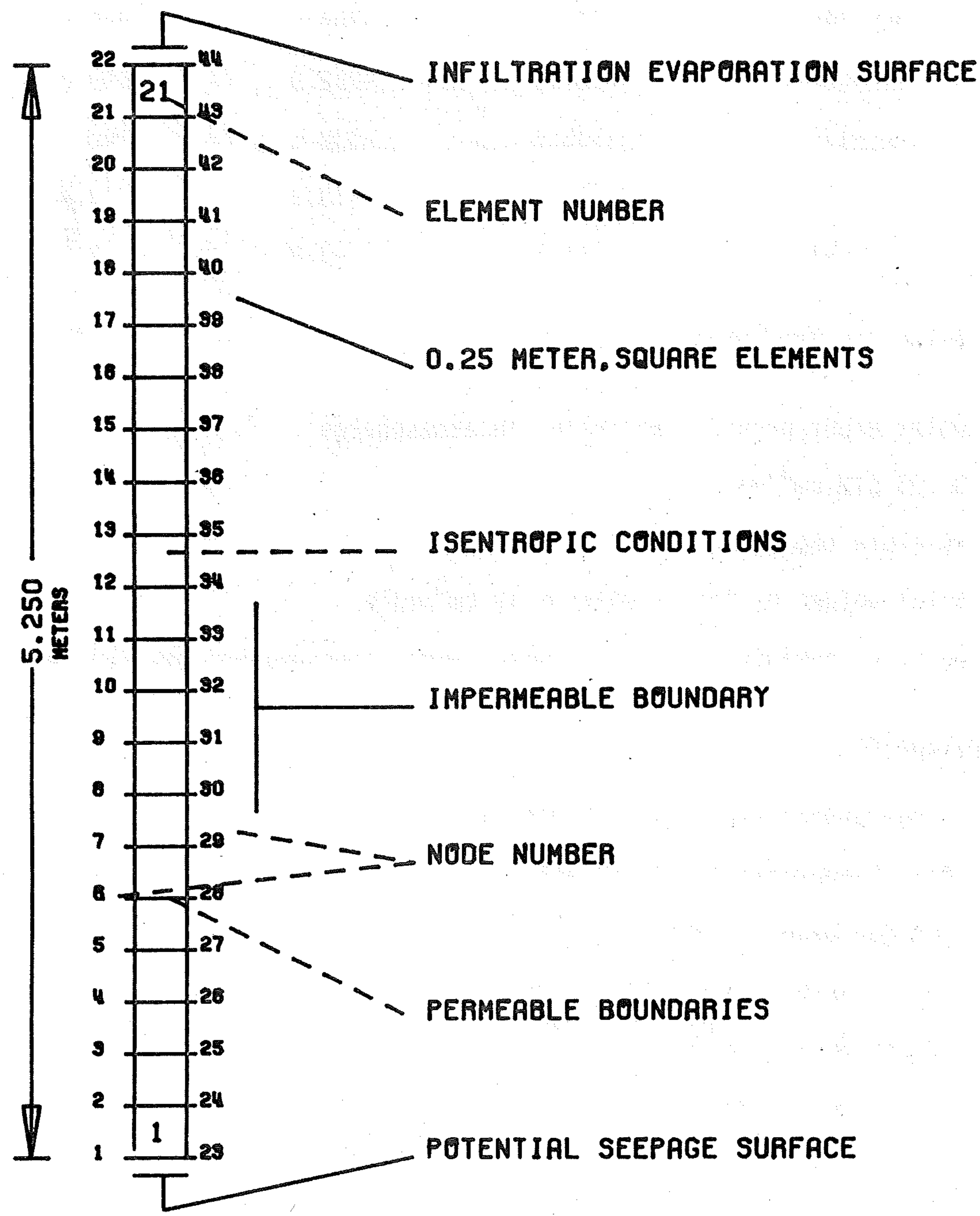

TABLE III-2

Evaporation Potential and Data

$$\psi_L = \frac{RT}{\overline{V}} \ln (R.H.)$$

RH	T = 0°C	10°C	15°C	20°C
.40	-1140.3	-1182.0	-1202.9	-1223.8
.55	-744.3	-771.2	-784.8	-798.5
.80	-277.7	-287.9	-292.9	-298.0
.90	-131.1	-135.9	-138.3	-140.7
.990	-12.51	-12.97	-13.2	-13.42
.999	-1.3	-1.3	-1.3	-1.3

Table Values in Atmospheres

ψ_L = water vapor pressure potential in atmospheres

R = 82.05 ATM.cm^3/mole °K

T = absolute temperature in °K

$\overline{V}$ = total volume of liquid water = 18 cm^3/mole

RH = relative humidity = ratio of water vapor pressure to saturated value

Evaporation Data[1]

Class A Pan evaporation rate = 1.3208 m/yr

May - Oct. Evaporation = 77% of annual,

180 day mean = 2.3542×10^{-4} m/hr

Nov. - April Evaporation = 23% of annual,

180 day mean = 0.7032×10^{-4} m/hr

Evaporation, annual mean = 1.529×10^{-4} m/hr

---

[1] Evaporation Maps for the United States, 1959. Technical Paper #37, U.S. D.O.C., Weather Bureau (NOAA-NWS).

distribution and total evaporation were identical for ψ_L = -150, -75 and -25 meters. At ψ_L = -5 m, the potential in the profile was greater than the atmospheric potential and "negative evaporation" occurred; that is, there was an accumulation of moisture in the system. Desiccation of air by soil does occur but its relative contribution to the bulk of soil moisture is small. The selection of the -150 m value seems to be reasonable.

A representative moisture distribution had to be established for each profile so that the results could be compared. Disturbed retorted shale in the laboratory dried at room temperature has a moisture content of less than 5 percent by weight. Core samples from the test pond lining contained 16 to 18 percent moisture by weight. From Table B-3, a value of 37.8 percent was arbitrarily selected as the initial moisture content; the corresponding capillary pressure head of -4.743 m (-15.6 ft) was assigned to all materials in all profiles after which evaporation was allowed to take place for a period of 720 hours. The moisture distribution at the end of this period was assumed to be the initial condition.

In addition to specifying a minimum evaporation potential it is necessary to specify a maximum or potential rate of evaporation. This maximum rate is dependent on atmospheric conditions whereas the actual rate is dependent on the rate at which water moves up through the soil profile.

Potential evaporation or evapotranspiration may be estimated by several methods depending on surface cover and available meteorological data. A lake evaporation rate could have been used in the analysis except that a well constructed profile would have little ponding and associated cooling due to evaporation. In addition, black oil shale would tend to have a low albedo and high energy absorption, producing potential evaporation rates closer to class A pan values. A yearly mean pan evaporation value was selected as opposed to a seasonal mean. Schleusener and Corey (1959) state that rapid initial drying tends to conserve soil moisture and that pan evaporation represents potential evaporation rates. The summer rate is 27 percent higher and the winter rate is equally lower than the yearly mean. The distribution of the yearly precipitation is fairly uniform and since the profile does have storage capacity, the yearly mean would seem to be a reasonable estimate of average normal conditions.

Five hypothetical profiles are shown in Figure III-8. Three uniform profiles were used to identify trends in moisture distribution under varying atmospheric conditions, but results from only two of these (85 and 95 pcf) are presented here because they are more realistic than 75 pcf.

Of the five profiles, the three density profile is probably most realistic. If waste is placed by conveyor it will be quite "loose" at the surface with densities of perhaps 75 to 85 pcf. As more shale is placed and machinary is routed over the surface, there will be consolidation to densities of 85 to 95 pcf.

The 85 pcf profile with a sand layer was thought to be an alternative to profiles constructed with high density liners. If the unconsolidated sand layer would effectively retard moisture movement because of unsaturated flow, an economical flow control method would have been identified.

The 85 pcf density was selected as the major component for composite profiles because it offers a permeability-capillary pressure-saturation relationship conducive to moisture mobility. It possibly represents a typical profile near the surface.

DENSITY	EFFECTIVE POROSITY	PERMEABILITY
75 PCF 1202 KG/CU.M	.468	6.716E-03 M/HR
85 PCF 1362 KG/CU.M	.447	2.376E-04 M/HR
95 PCF 1522 KG/CU.M	.3995	2.657E-05 M/HR
INDICATED	---	---
POUDRE SAND 1619 KG/CU.M	.396	9.498E-02 M/HR

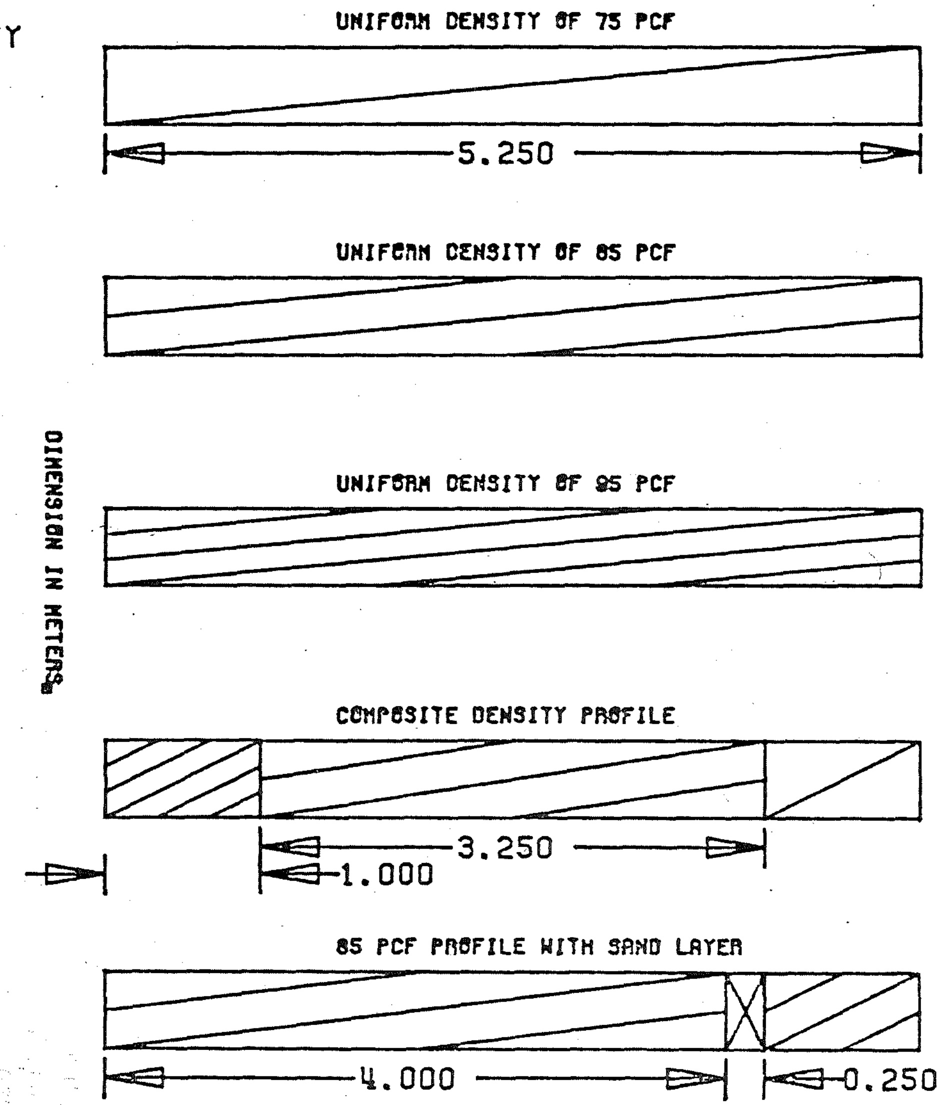

FIGURE III-8
PROFILE CONSTRUCTION

Storm intensity and duration applied at the surface boundary was of a 100 year frequency. If there is a reasonable chance of deep percolation or run-off, these storm intensities should identify under what conditions they would occur. Data on storms of this frequency are listed in Table III-3. A single 24 hour storm yield represents 13 percent of the yearly mean precipitation at Grand Junction, Colorado. A five minute storm intensity is 4100 times the saturated permeability of oil shale compacted to 95 pcf. Storm durations of 5 and 30 minute, and 1, 6, 12, and 24 hours were applied to uniform profile surfaces; simulated post storm evaporation periods of 720 hours were conducted for 5 minute, 6 and 24 hour storms. A 24 hour storm with post storm evaporation was applied to two composite profiles. Five, 1 hour storms, each of which was followed by a 120 hour evaporation period, were applied to composite profiles and one uniform profile. Values in Table III-3 are characteristic of climate at Grand Junction, Colorado. If ponding or soil moisture accumulation were to occur due to direct storm effects, it should have happened under the above conditions. After the storm, evaporation immediately began and continued to the next event or terminated at the end of computation. The evaporation potential was -150 m after every storm. In all the moisture distribution figures, time is cumulative within a single storm series. For example, a storm ended at 24 hours after which evaporation immediately began and continued to time 24 + 720 or 744 hours.

The storm sequence used here was very arbitrary; however, the purpose of this work was to develop a method by which infiltration from various storms followed by evaporation periods could be analyzed to investigate the disposition of natural precipitation. This objective could be accomplished with an arbitrary storm sequence. At such time as an actual waste pile is being designed, a more extensive probability analysis may be conducted using alternative design storms and modified sequencing during storm events.

Many of the input parameters were arbitrarily selected but they appear to be reasonable estimates and should give some insight into the direct effect of storms on moisture distribution in processed oil shale profiles.

III-3.1.1 Discussion of Finite Element Analysis Results

Figures on the following several pages give the results selected from detailed analyses of hypothesized profiles under varying atmospheric conditions. The figures are of two types. Comparison plots show the moisture distribution of two or more profiles at a particular time. Time series plots show a series of moisture distributions of a single profile at several points in time.

III-3.1.2 Multi-Profile, Single Time Comparisons

The following fourteen figures are comparison plots and have been selected because they show initial, final or significant intermediate developments during an event. An event is at least one infiltration period resulting from a 100 year frequency storm of a 5 minute, 6 or 24 hour duration and of characteristic intensity. The infiltration phase has been immediately followed by an evaporation phase as previously described. This immediate succession of phases during an event does not allow for post storm infiltration. If ponding occurred during an event, it has been assumed that immediate run off resulted, and water was not available for infiltration later.

TABLE III-3

Climatological Data

Grand Junction, Colorado

Precipitation Data - 100 Year Frequency[1]

Duration	Intensity m/hr	Elapse Time (hours)	Storm Yield (m)
5 min.	1.092×10^{-1}	0.0833	.00910
30 min.	3.937×10^{-2}	0.500	.01969
60 min.	2.413×10^{-2}	1.000	.02413
2 hour	1.397×10^{-2}	2.000	.02794
6 hour	6.35×10^{-3}	6.000	.03810
12 hour	3.810×10^{-3}	12.000	.04572
24 hour	2.540×10^{-3}	24.000	.06096

[1]Rainfall Intensity - Duration - Frequency Curves, 1955. Technical Paper #25, U.S. Dept. of Commerce, Weather Bureau (NWS) Superintendant of Documents, U.S. Government Printing Office, Washington D.C. 20402.

Note that the smooth curve through the data points in all of the plotted figures has been generated by a routine using spline theory. The line does not represent an infinite number of data points. UNSAT2 treats each element's characteristics as a separate set; at the junction of two dissimilar elements, there is a moisture discontinuity and two computed moisture values result. One value has been omitted and the interpolated curve has been plotted between the remaining successive data points. Physically, this would represent a gradual rather than a sudden change from one layer to the next as might be expected in nature. However, in several figures, one section of the interpolated curve is clearly not physically correct.

Figure III-9 shows the initial conditions for the beginning of a storm event described in the previous section. The uniform 95 pcf density profile is extremely dry at the surface ($\theta = 0.164$, $P_c = -96.6$ m) due to the low permeability of the underlying layers. The greater moisture mobility in the 85 pcf profile allows more general profile drying during evaporation and less surface drying. This is the initial condition for moisture contained in the profile so these numbers on the figure are zero.

Figure III-10 shows the effect of a 5 minute storm on the moisture distribution for uniform profiles. Figure III-11 represents the distribution 720 hours after the storm ended. As might be expected, there is less infiltration in the 95 pcf profile which indicates the earliest ponding and the most potential runoff. Both the 85 and 95 pcf profiles pond during the storm. The total storm yield in a five minute or 0.083 hour storm is .91 cm and the 0.138 cm potential runoff of the 95 pcf profile would probably infiltrate in a level disposal area. However, the total evaporation during the following 720.0 hours is 11.009 cm and the storm yield and runoff is small in comparison. The 95 pcf profile is more dry at the surface ($\theta = 0.128$) at the end of the evaporation phase after the storm than at initial conditions.

In these and the following comparisons, the evaporation from all profiles over equal time periods is equal to the potential rate, 0.01529 cm per hour, specified in the input.

A six hour storm was selected as an intermediate storm and applied to uniform profiles. The 95 pcf profile ponded before 2.3 hours and the 85 pcf profile ponded before 4.2 hours. Figures III-12, 13, and 14 show the moisture distributions at 2.34, 6.0 (end of rainfall) and 726.0 hours. At 6 hours (Figure III-13) the moisture had moved down approximately one meter but again, after the 720 hour evaporation (Figure III-14) the soil was considerably drier than the initial condition in Figure III-9. Potential run off values from the 85 and 95 pcf profiles are 0.909 cm and 1.279 cm respectively.

The results of a twenty four hour storm even are shown in Figures III-15, 16, and 17. The 95 pcf profile was first to pond at 7.6 hours, and the 85 pcf profile ponded before the end of the storm. The potential runoff was 0.66 and 0.34 cm respectively. Figure III-17 shows that at the end of the evaporation period there is a net loss of moisture of over 5 cm from each profile.

FIGURE III-9

MOISTURE DISTRIBUTION IN PROCESSED OIL SHALE

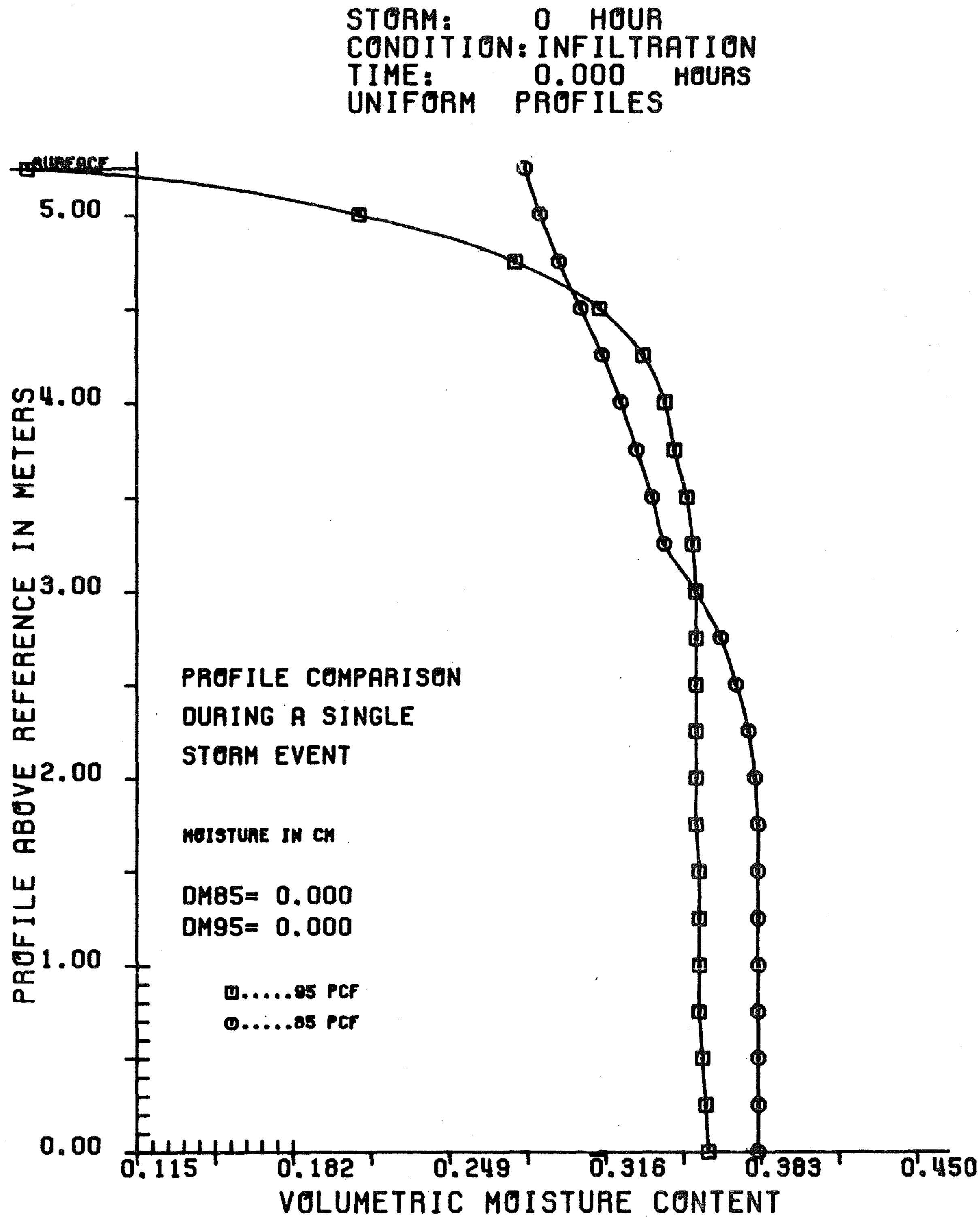

ERRATA - Seepage Through Partially Saturated Shale Wastes.

Figure III-9 through III-17 bottom scale numbers should be 0.2, 0.25, 0.30, 0.35, 0.40 and 0.45

FIGURE III-11

OISTURE DISTRIBUTION

N PROCESSED OIL SHALE

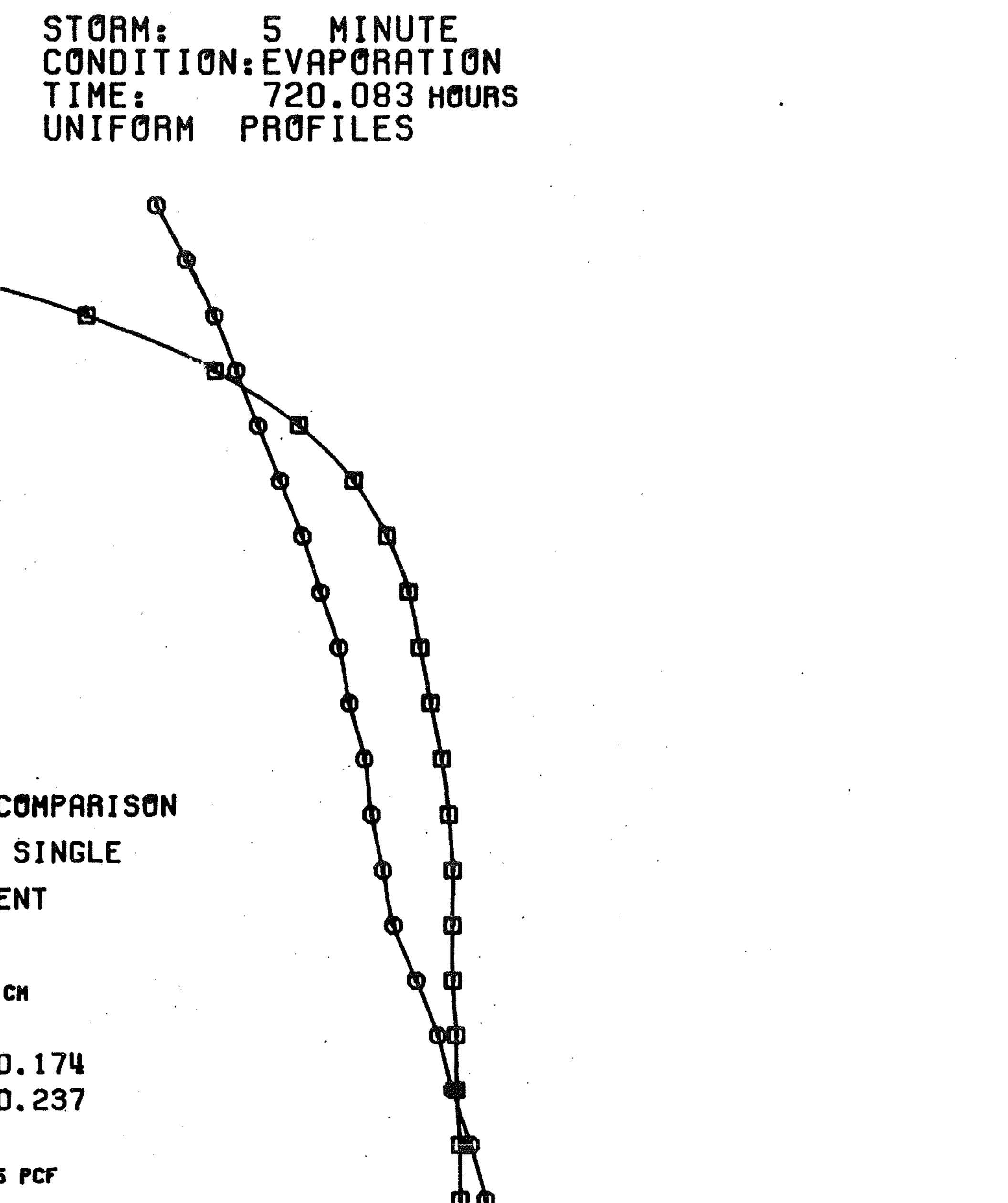

FIGURE III-12

MOISTURE DISTRIBUTION

IN PROCESSED OIL SHALE

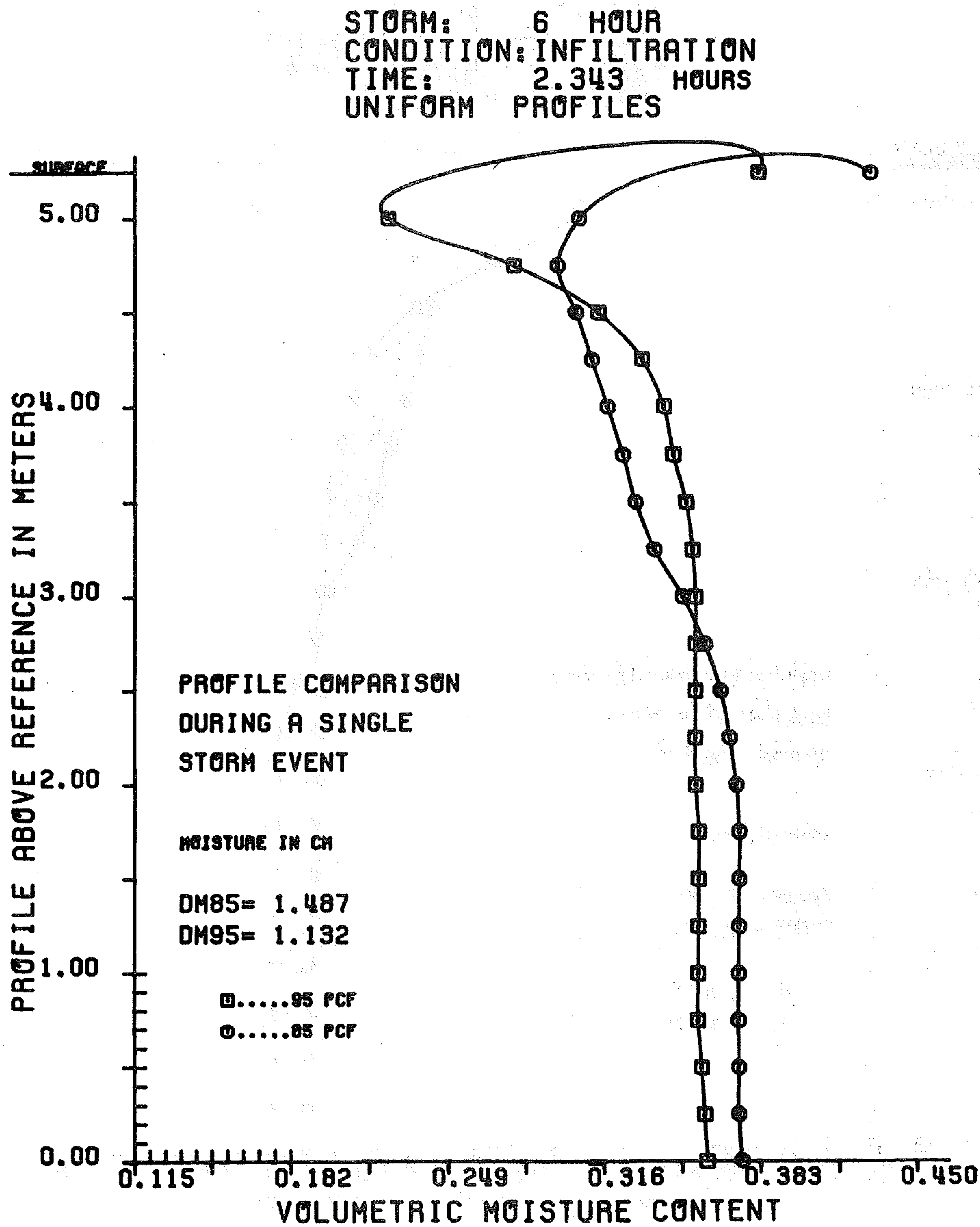

FIGURE III-13

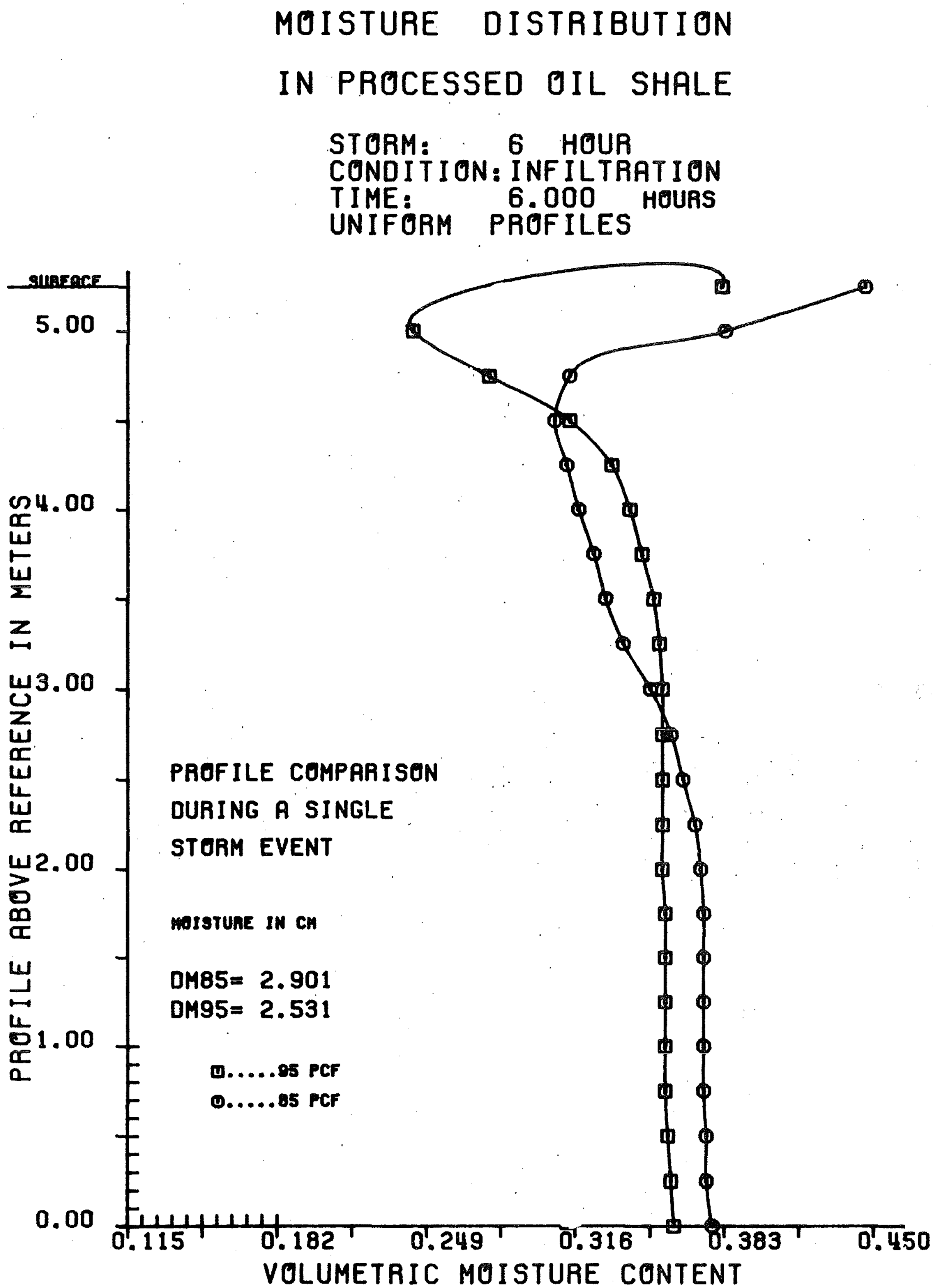

FIGURE III-14

MOISTURE DISTRIBUTION

IN PROCESSED OIL SHALE

STORM: 6 HOUR
CONDITION: EVAPORATION
TIME: 726.000 HOURS
UNIFORM PROFILES

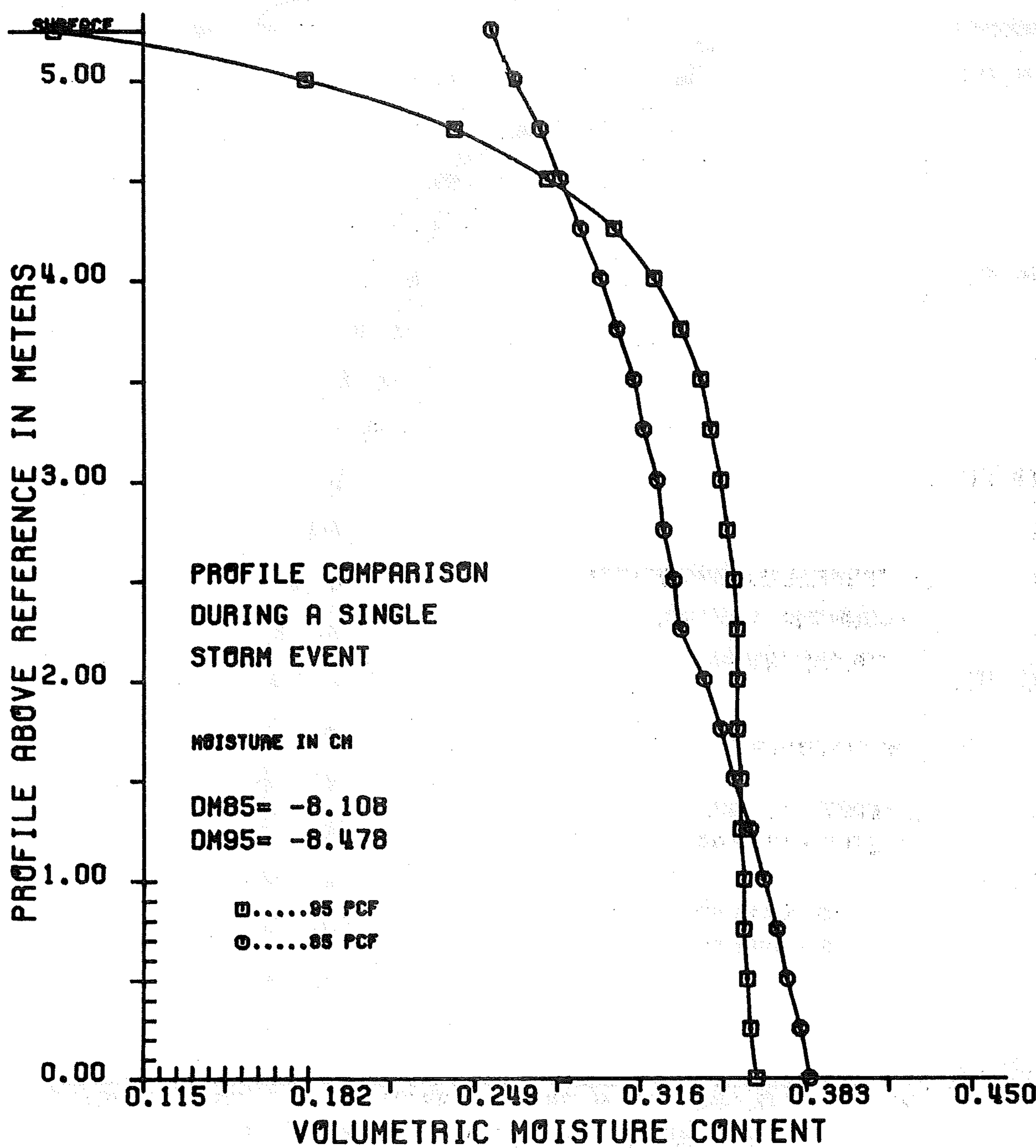

FIGURE III-15

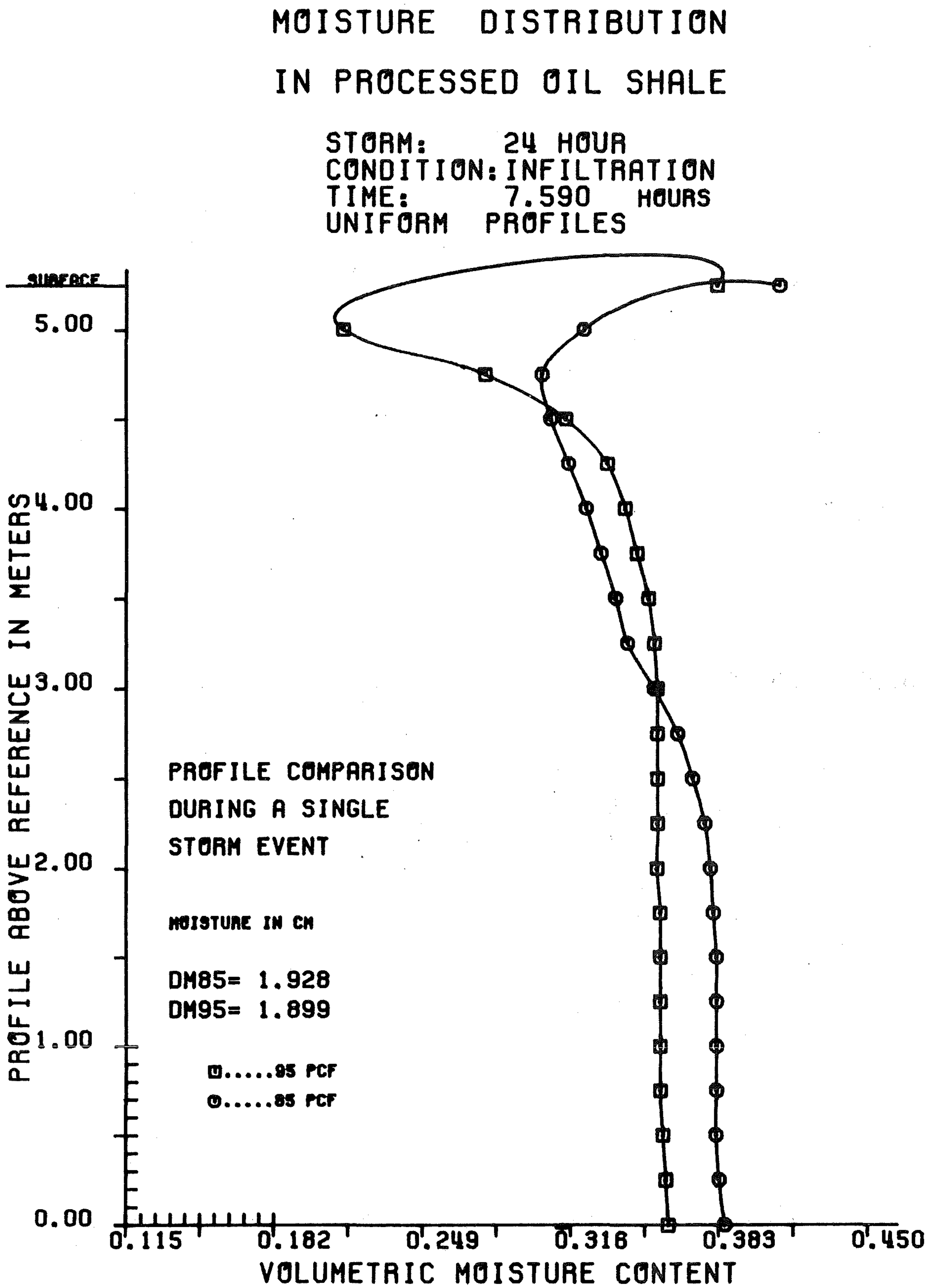

FIGURE III-16

MOISTURE DISTRIBUTION IN PROCESSED OIL SHALE

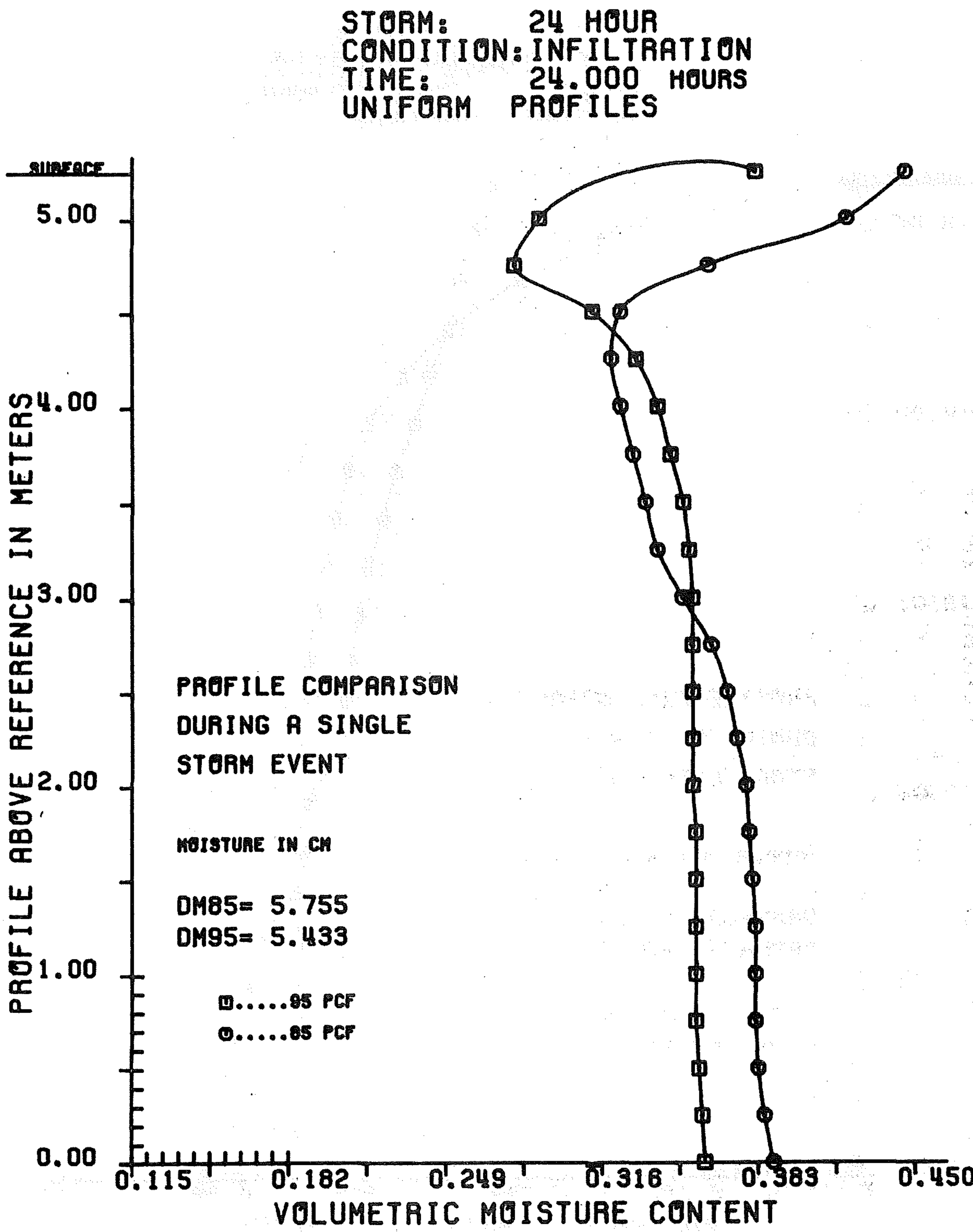

FIGURE III-17

MOISTURE DISTRIBUTION

IN PROCESSED OIL SHALE

STORM: 24 HOUR
CONDITION: EVAPORATION
TIME: 744.000 HOURS
UNIFORM PROFILES

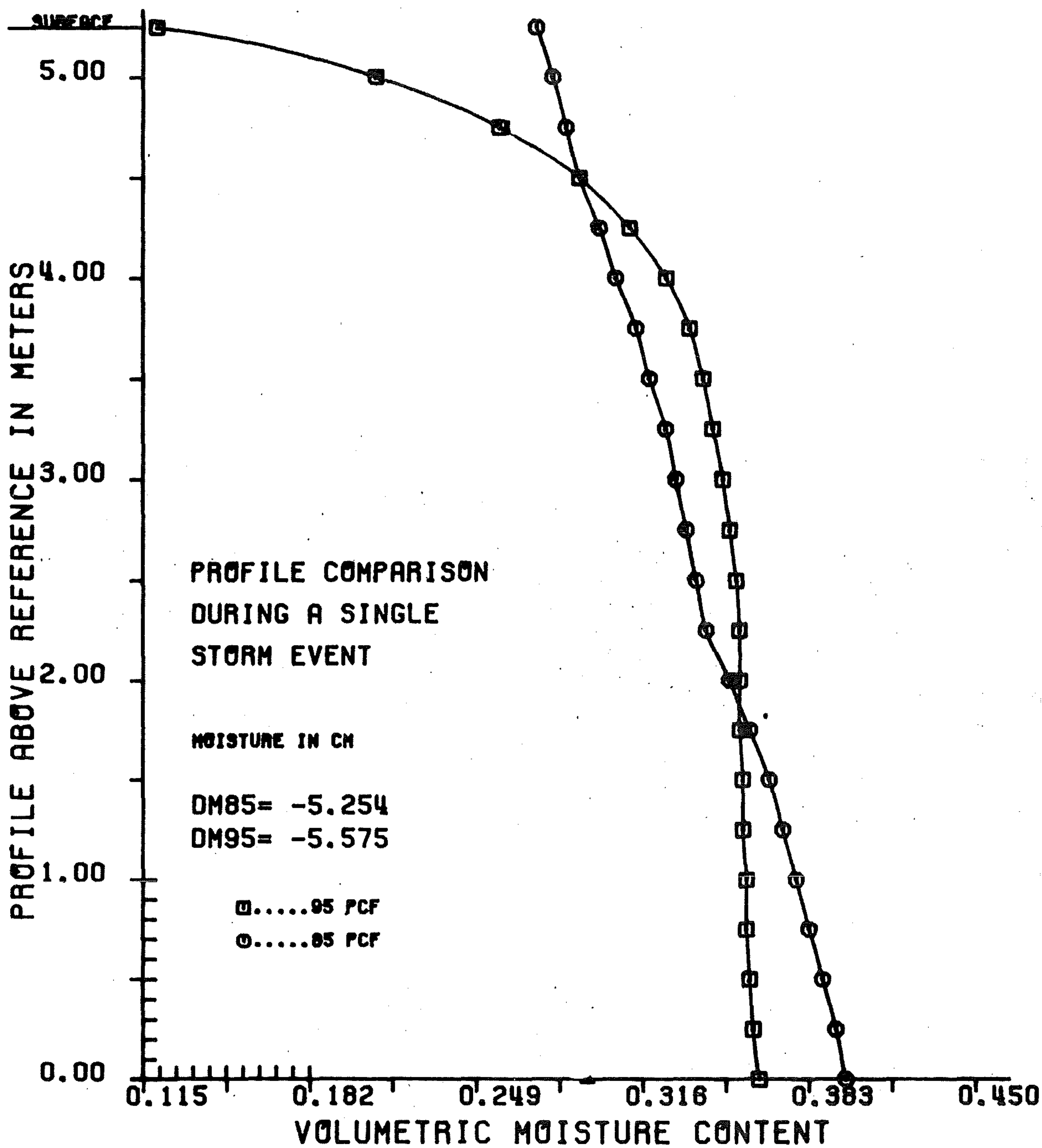

ERRATA - Seepage Through Partially Saturated Shale Wastes.

Figure III-9 through III-17 bottom scale numbers should be 0.2, 0.25, 0.30, 0.35, 0.40 and 0.45

FIGURE III-18

OISTURE DISTRIBUTION

N PROCESSED OIL SHALE

STORM: 0 HOUR
CONDITION: INFILTRATION
TIME: 0.000 HOURS
COMPOSITE PROFILES

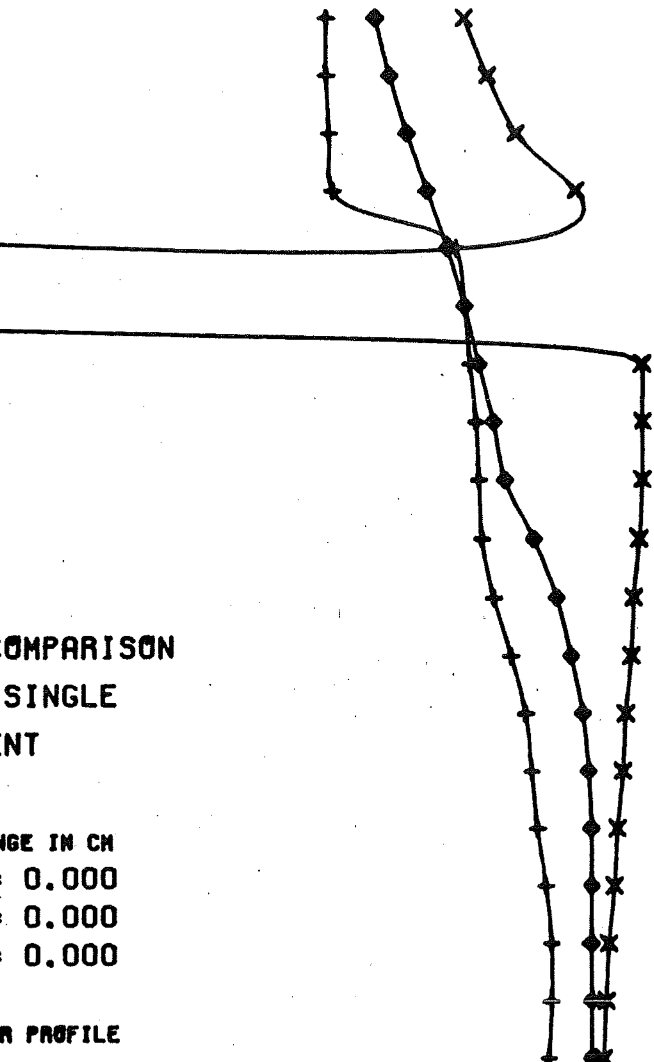

FIGURE III -19

MOISTURE DISTRIBUTION IN PROCESSED OIL SHALE

STORM: 1 HOUR
CONDITION: INFILTRATION
TIME: 1.000 HOURS
COMPOSITE PROFILES

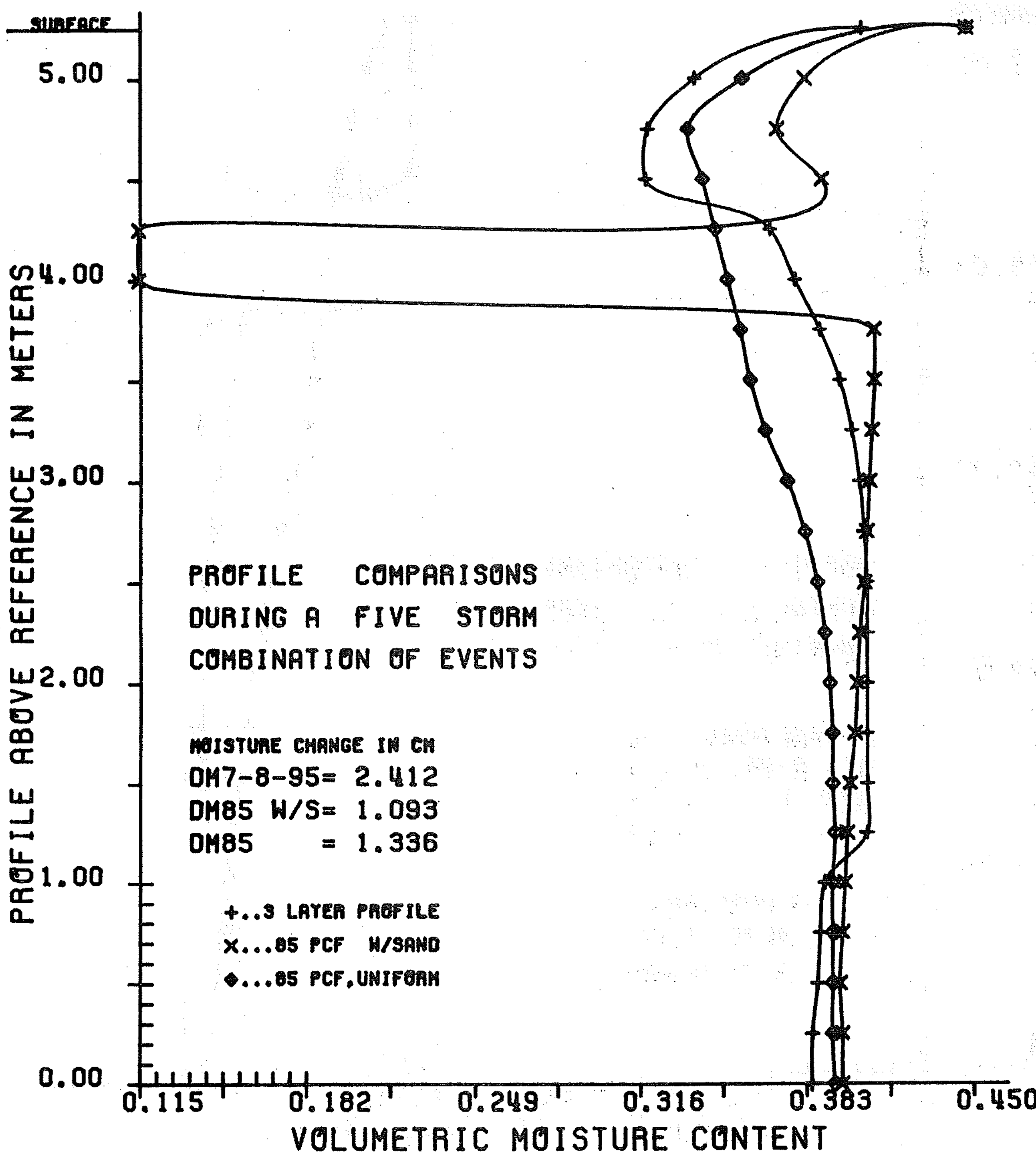

FIGURE III-20

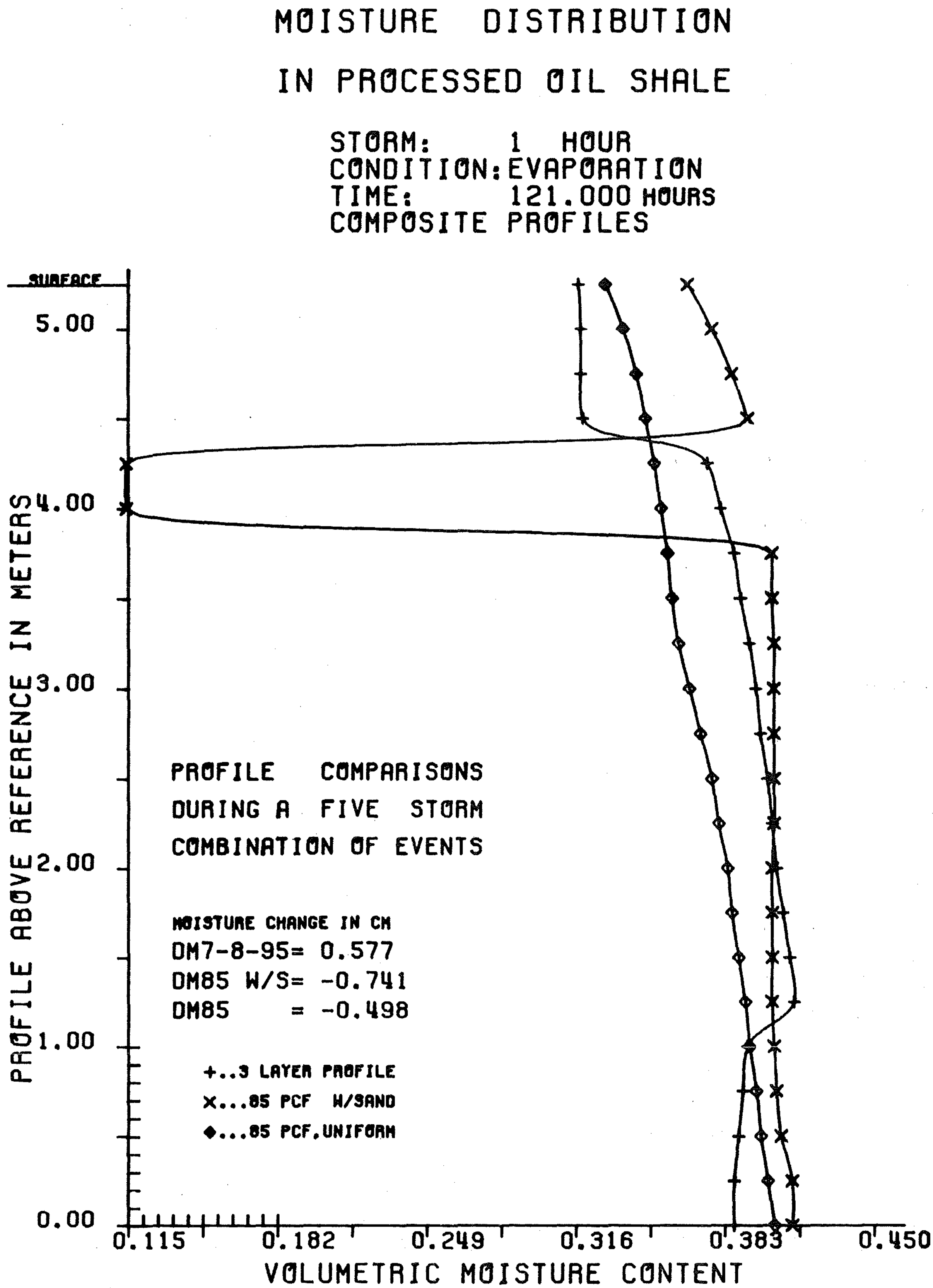

FIGURE III-21

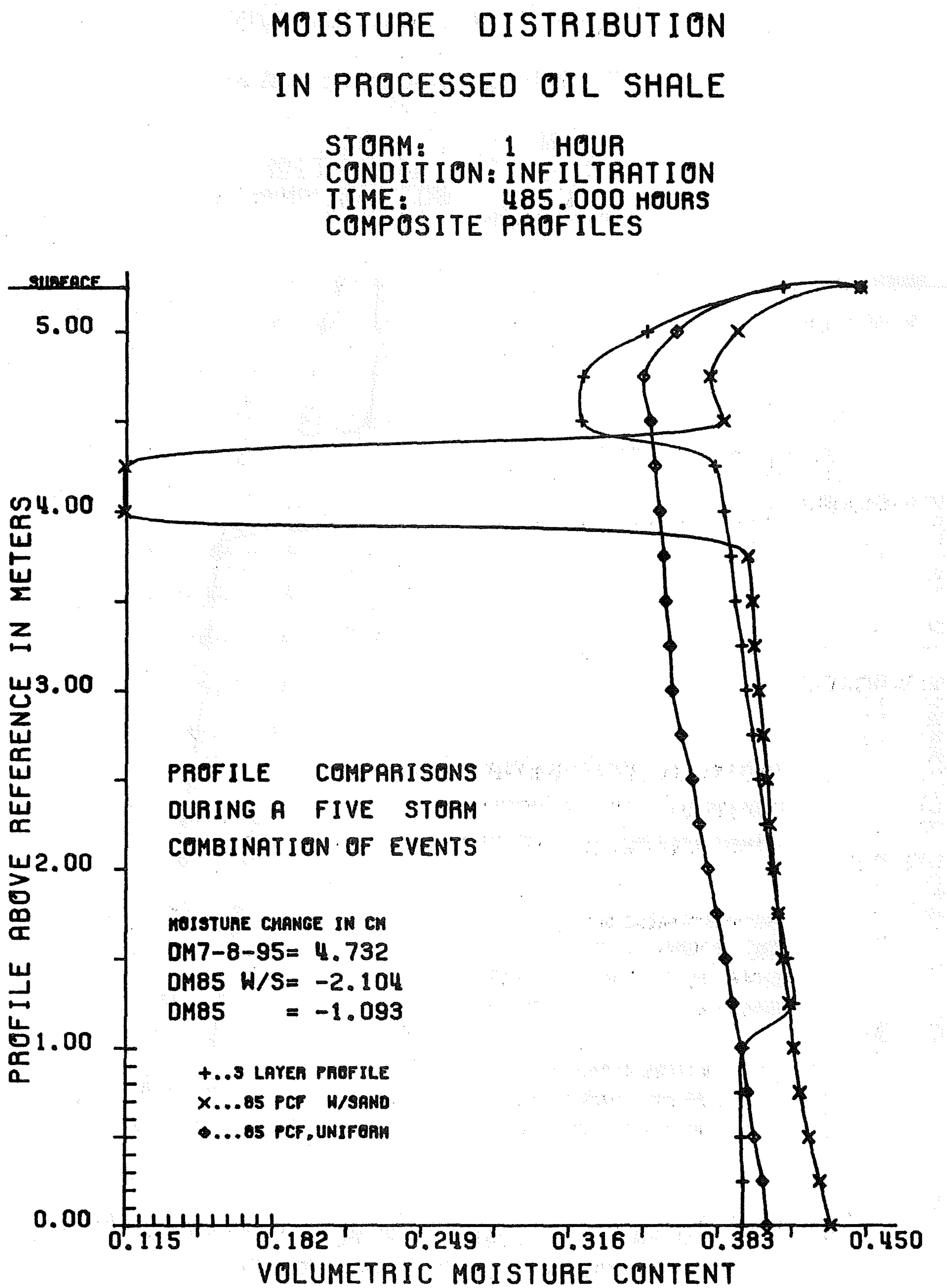

FIGURE III-22

MOISTURE DISTRIBUTION IN PROCESSED OIL SHALE

STORM: 1 HOUR
CONDITION: EVAPORATION
TIME: 605.000 HOURS
COMPOSITE PROFILES

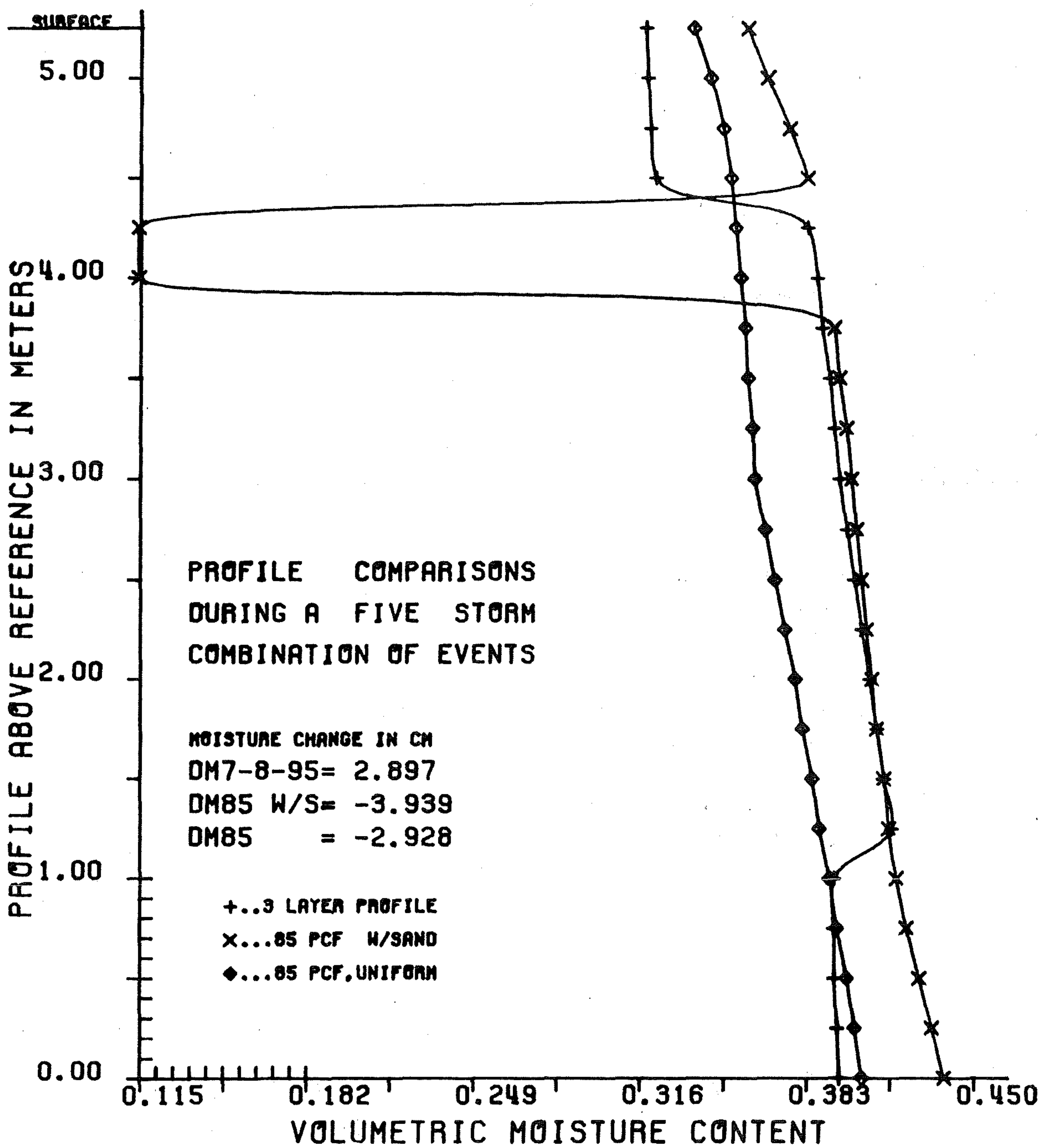

FIGURE III-23

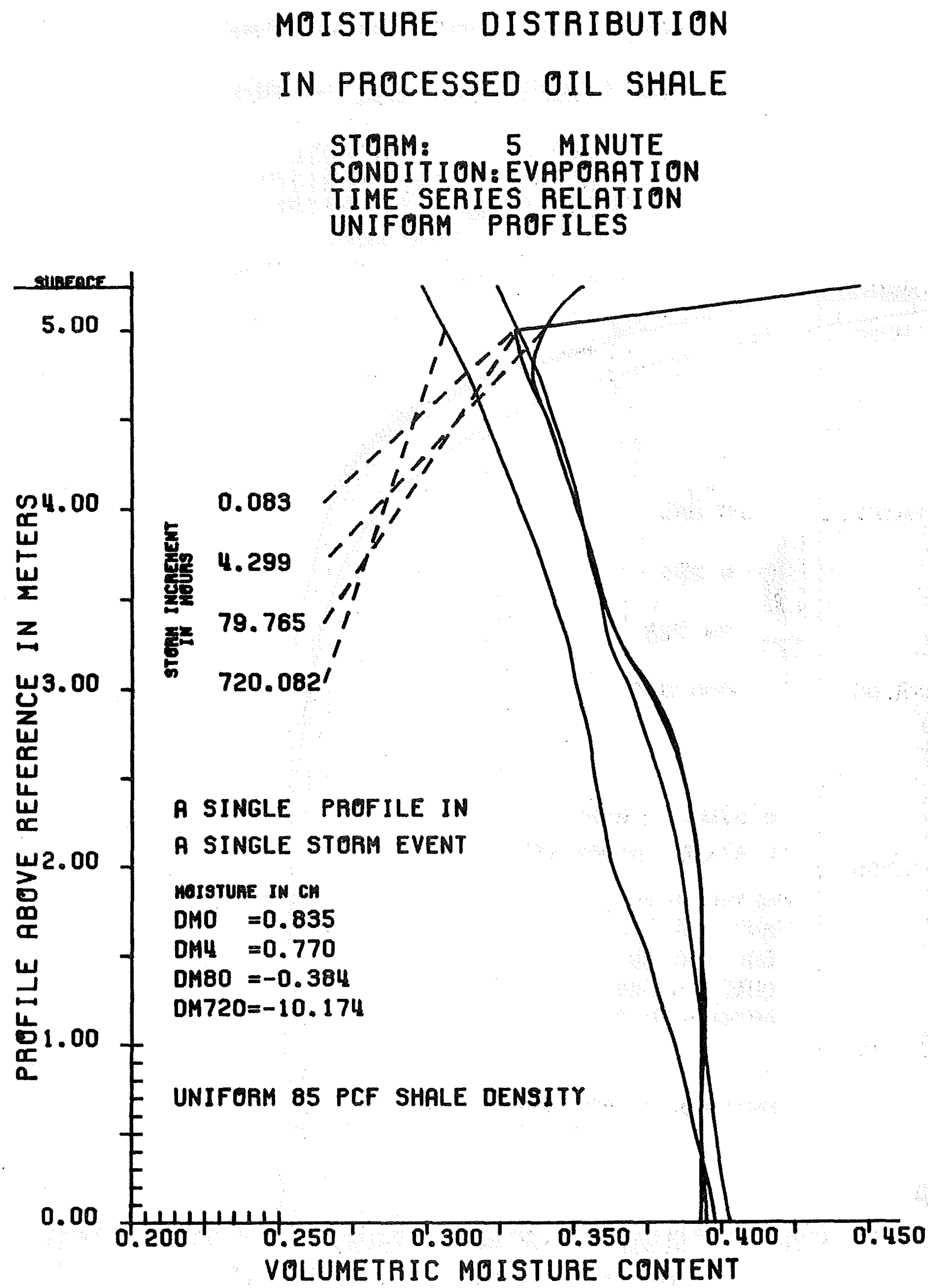

FIGURE III-24

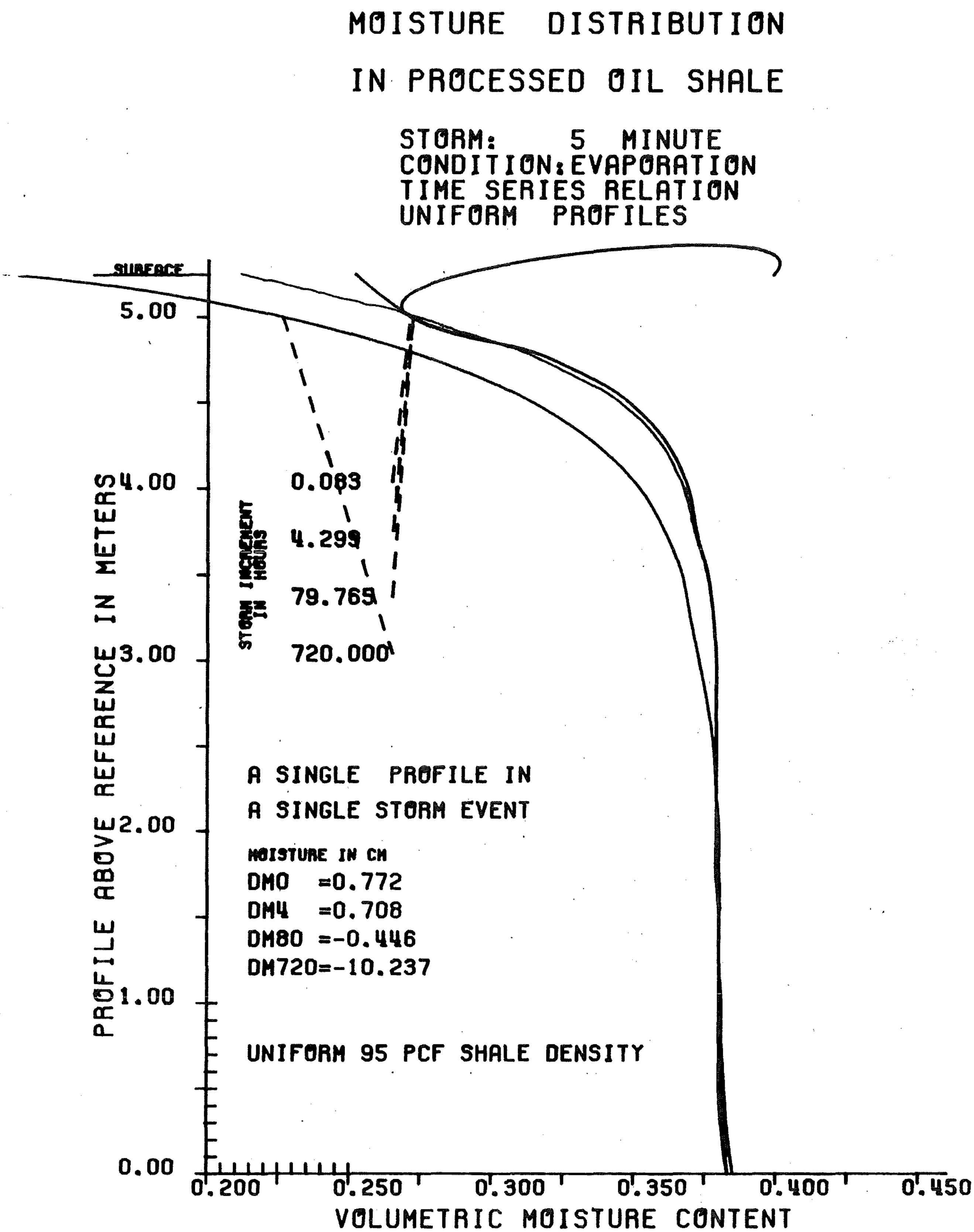

FIGURE III-25

MOISTURE DISTRIBUTION

IN PROCESSED OIL SHALE

STORM: 24 HOUR
CONDITION: INFILTRATION
TIME SERIES RELATION
UNIFORM PROFILES

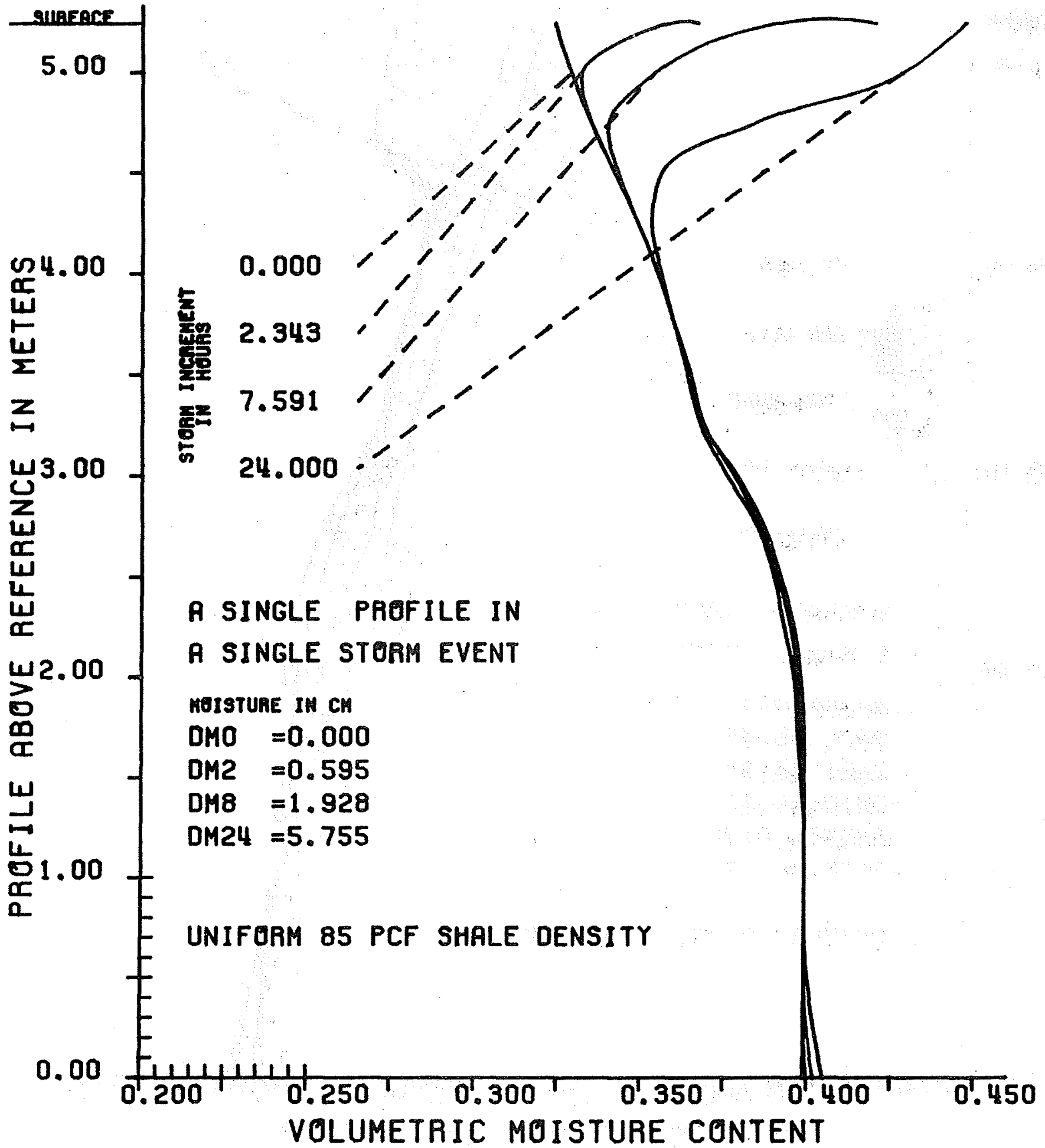

FIGURE III-26

MOISTURE DISTRIBUTION

IN PROCESSED OIL SHALE

STORM: 24 HOUR
CONDITION: EVAPORATION
TIME SERIES RELATION
UNIFORM PROFILES

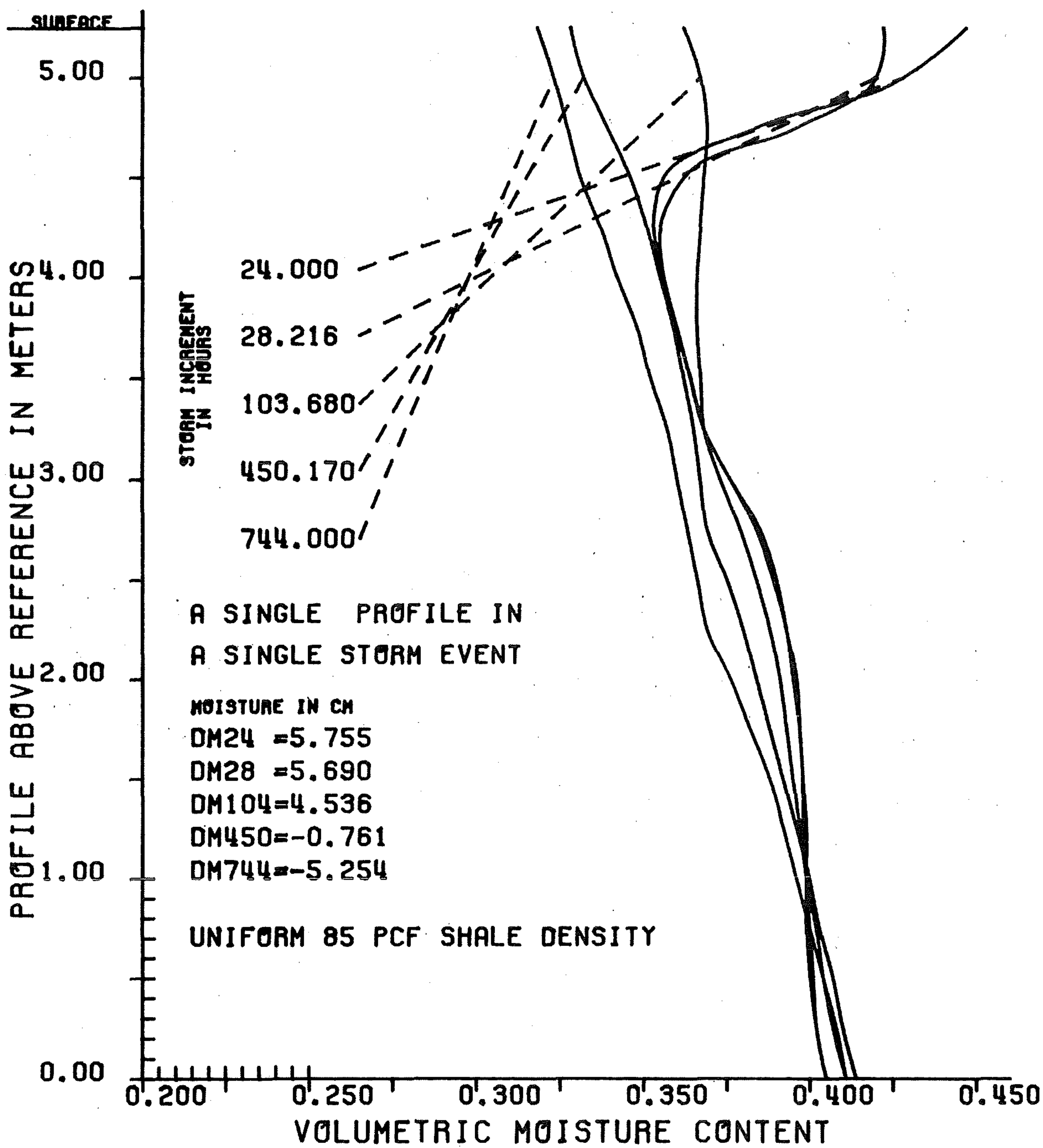

FIGURE III-27

MOISTURE DISTRIBUTION

IN PROCESSED OIL SHALE

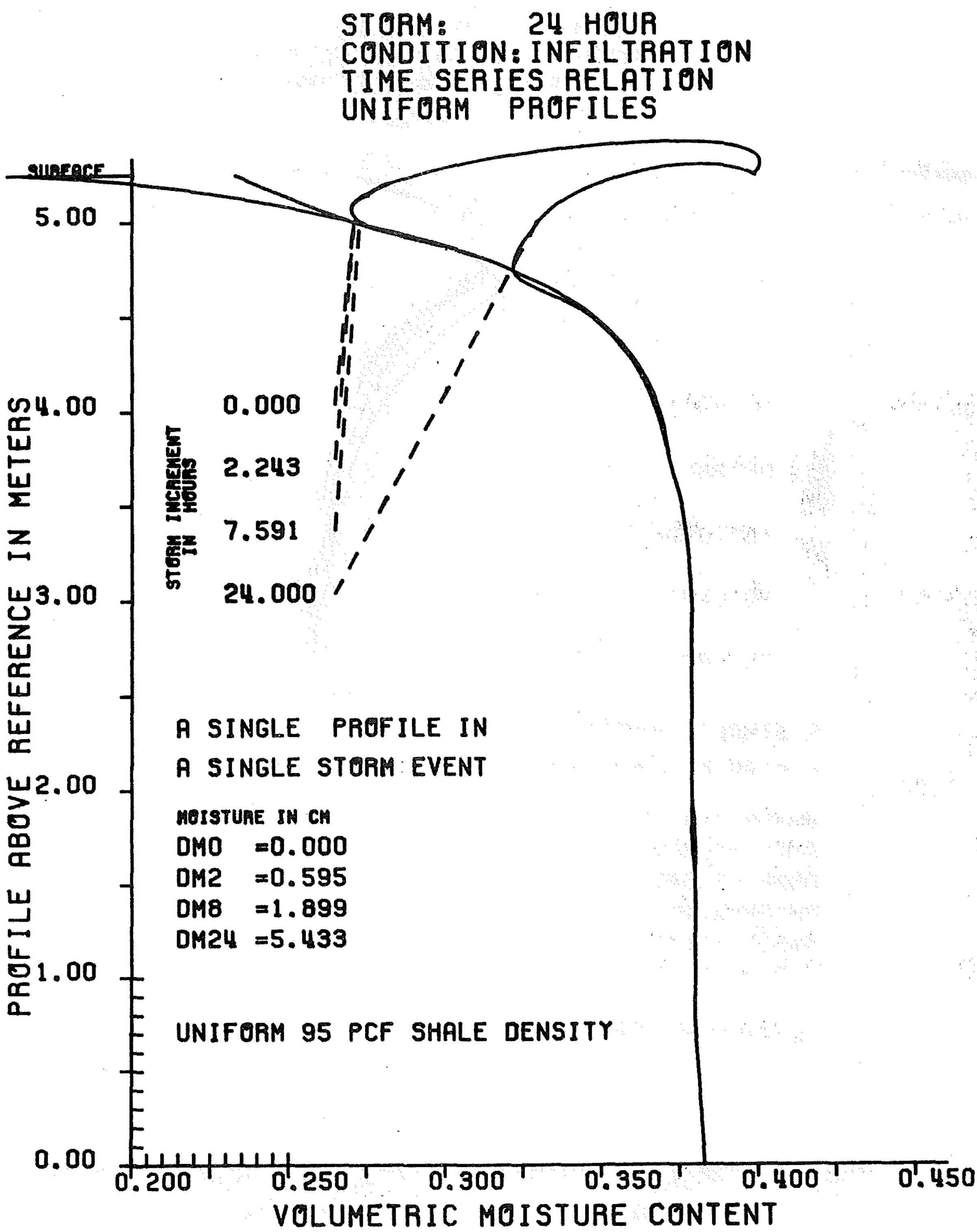

FIGURE III-28

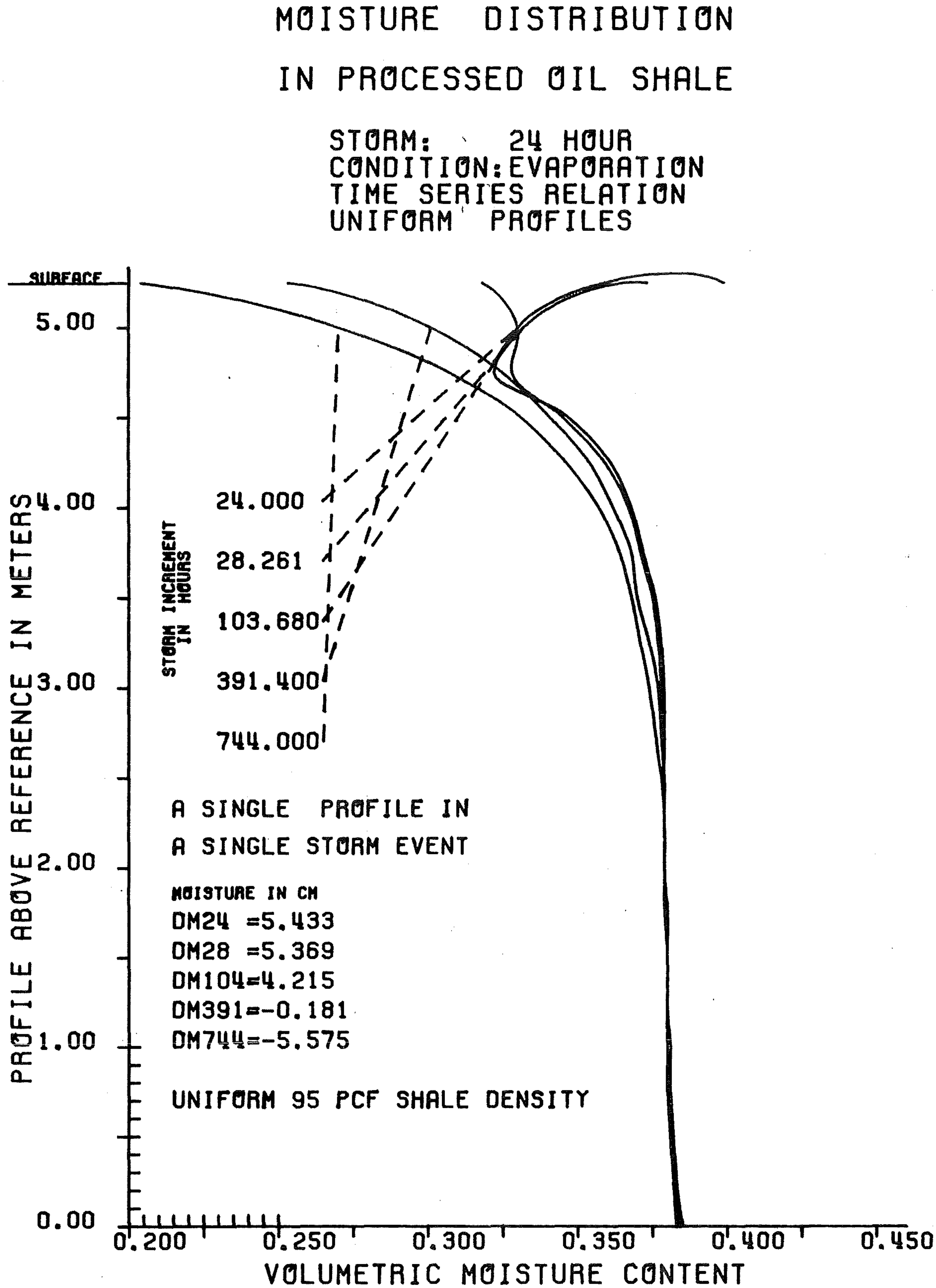

Figures III-27 and 28 display very little lower layer reaction to the drastic changes in upper layer moisture content in the 95 pcf profile. The capillary pressure head was -52.7 m at the surface at 744.0 hours.

The remaining figures show the moisture distribution in the two layered profiles and the 85 pcf profile which were subjected to a set of 5 one hour storms; each followed by 120 hours of evaporation. All of the intermediate storms are shown in these figures. Only the first and last storm sets were included in the previous plots of these data. The total five storm yield was 12.06 cm and the total potential evaporation from each profile was 9.16 cm.

The 75, 85, 95 pcf profile distribution shown in Figures III-29 and 30 evidently had not reached equilibrium conditions before the first storm. However, even with initial excess mid layer moisture, only 0.55 cm had entered the 1.00 m thick base layer after 605 hours. During the same period, there was no runoff. At 605.0 hours, storage in the upper 4.25 m zone had increased 2.35 cm.

The moisture distribution for this storm series on the sand layer profile is shown in Figures III-31 and 32. The profile above the 2.50 meter level lost 5.13 cm to deep percolation and 6.84 cm to run off for a total of 11.97 cm. Because of the excessive run off and deep percolation, storage in the upper zone decreased 9.07 cm by the end of the fifth evaporation phase. The curves also show the steady decrease in the amount of upper zone moisture and increase in the amount of lower zone moisture.

Figures III-33 and 34 have been included as a comparison to Figures III-29 through III-32. This profile did not have a restricting sand layer or an unconsolidated surface layer to promote infiltration. In all five storms, ponding occurred and there was a total of 5.825 cm run off. There was some lower zone storage but the moisture distribution was essentially stabilized during the period 121 through 605 hours. Moisture did not accumulate in the uniform profile due to runoff and upward moisture movement. Material with the characteristics of that represented in Figure III-34 will probably be the major component in the upper zone of real shale profiles with dynamic moisture distributions.

In these analyses the largest single storm yield was 6.1 cm in 24 hours and the total yield of the combination storms was 12.1 cm. No water was lost from the system as deep percolation because a seepage face (between nodes 01 and 23) did not develop. This is not to suggest that, in a real system, where the profile does not end at the reference datum, there will not be moisture movement across this interface. Conclusions may be drawn based on trends within the profile, however.

It is important to recognize the ability of the capillary potential to move water against gravity and to allow the effects of the evaporative potential to be transmitted deep into the profile and work to reclaim infiltrated surface water as demonstrated in Figure III-32. As much as any factor, permeability controls the effectiveness of the evaporative potential. The composition and the order of these profile constituents may act to enhance or detract from the ability of the atmosphere to reclaim precipitation where it falls.

FIGURE III-29

MOISTURE DISTRIBUTION

IN PROCESSED OIL SHALE

STORM: 1 HOUR
CONDITION: INFILTRATION
TIME SERIES RELATION
COMPOSITE PROFILES

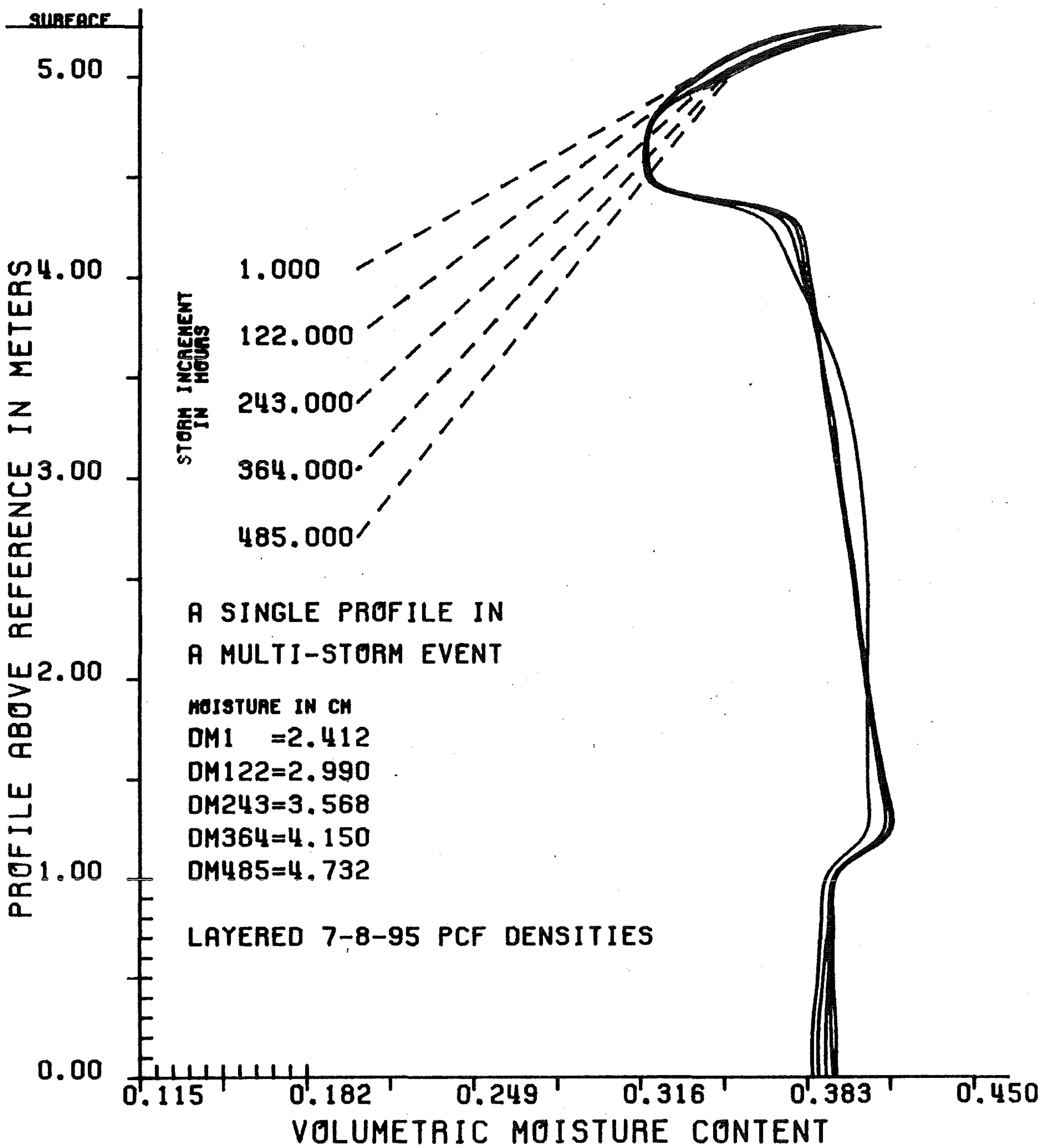

FIGURE III-30

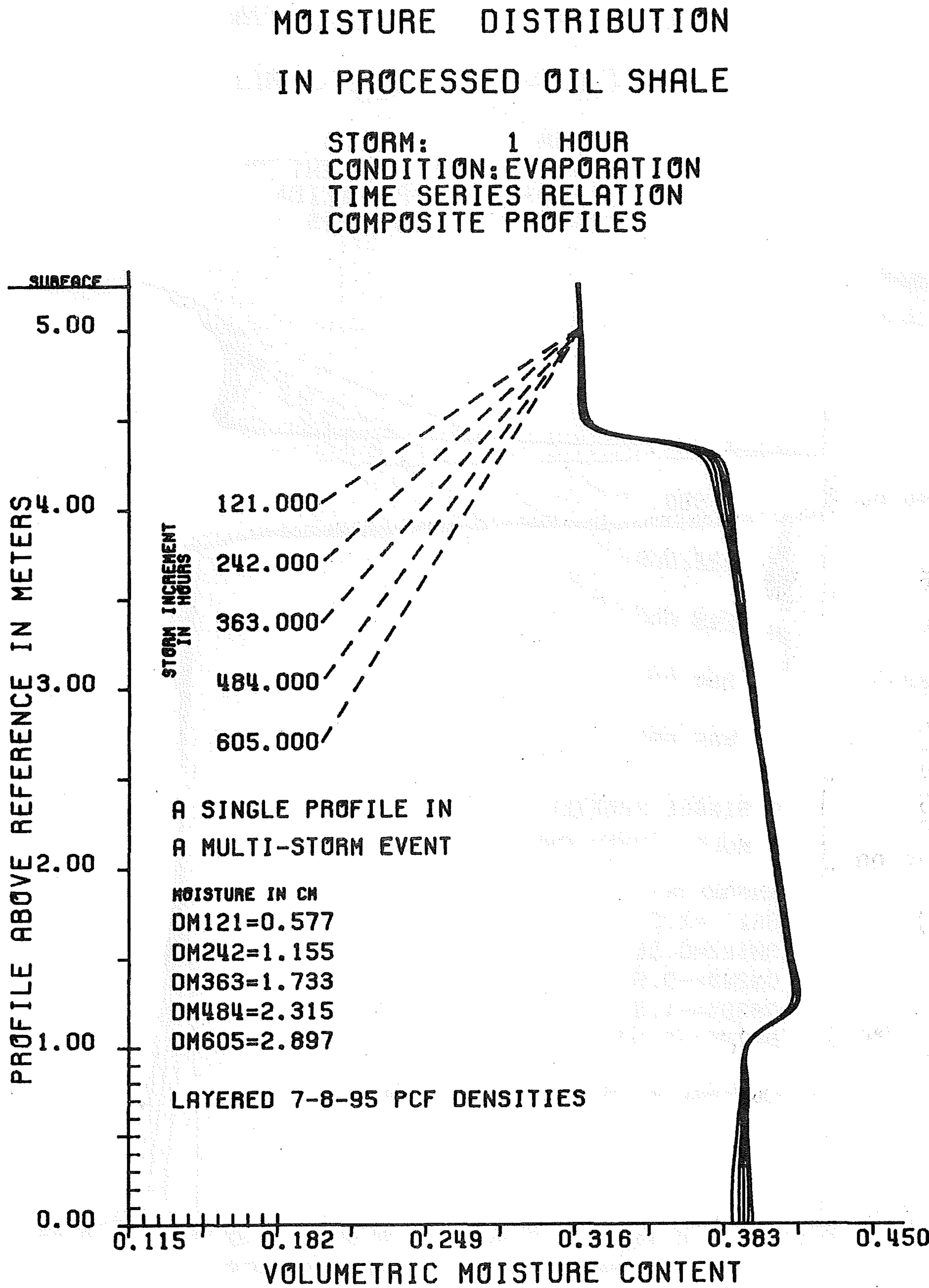

FIGURE III-31

MOISTURE DISTRIBUTION

IN PROCESSED OIL SHALE

STORM: 1 HOUR
CONDITION: INFILTRATION
TIME SERIES RELATION
COMPOSITE PROFILES

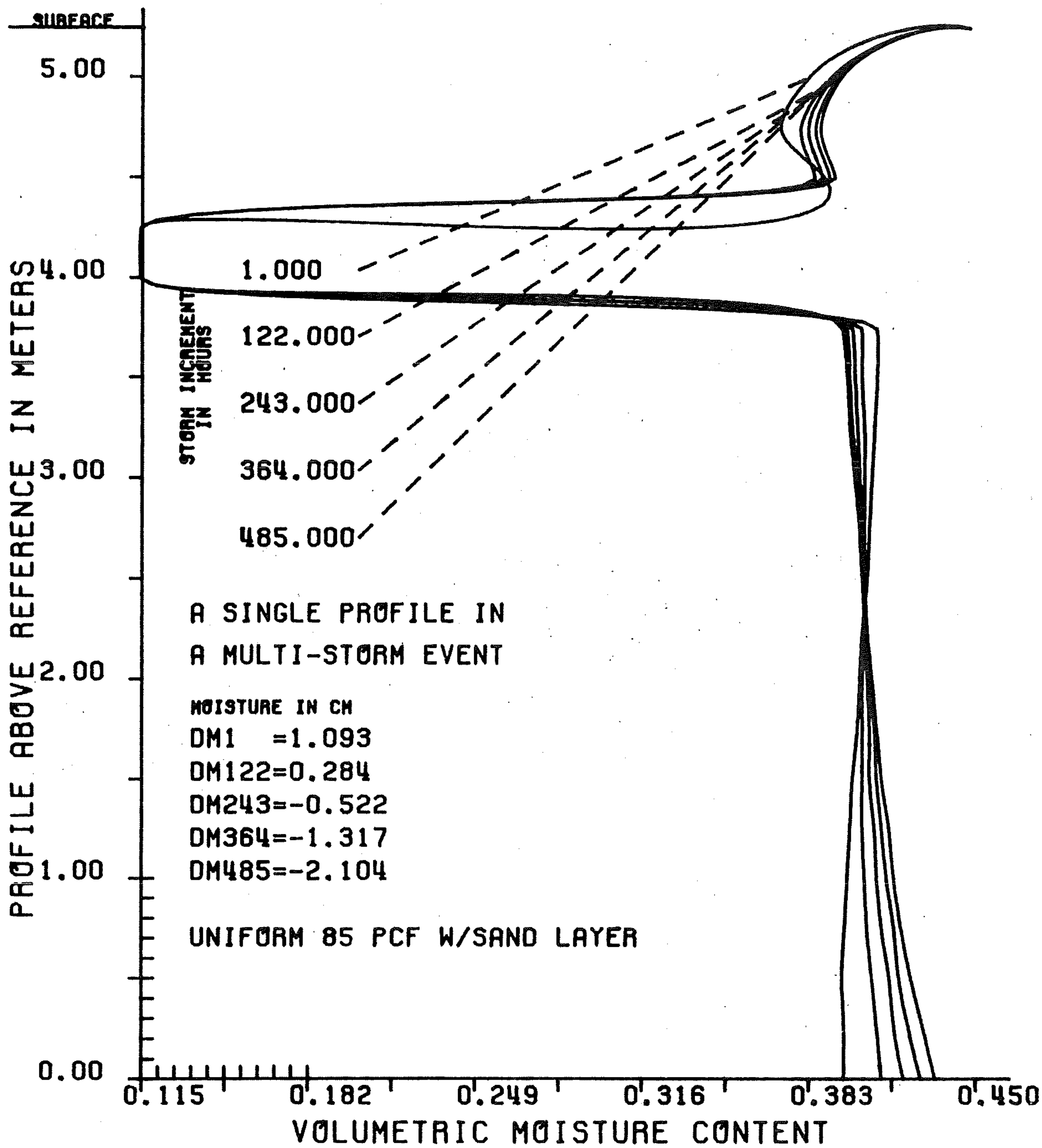

FIGURE III-32

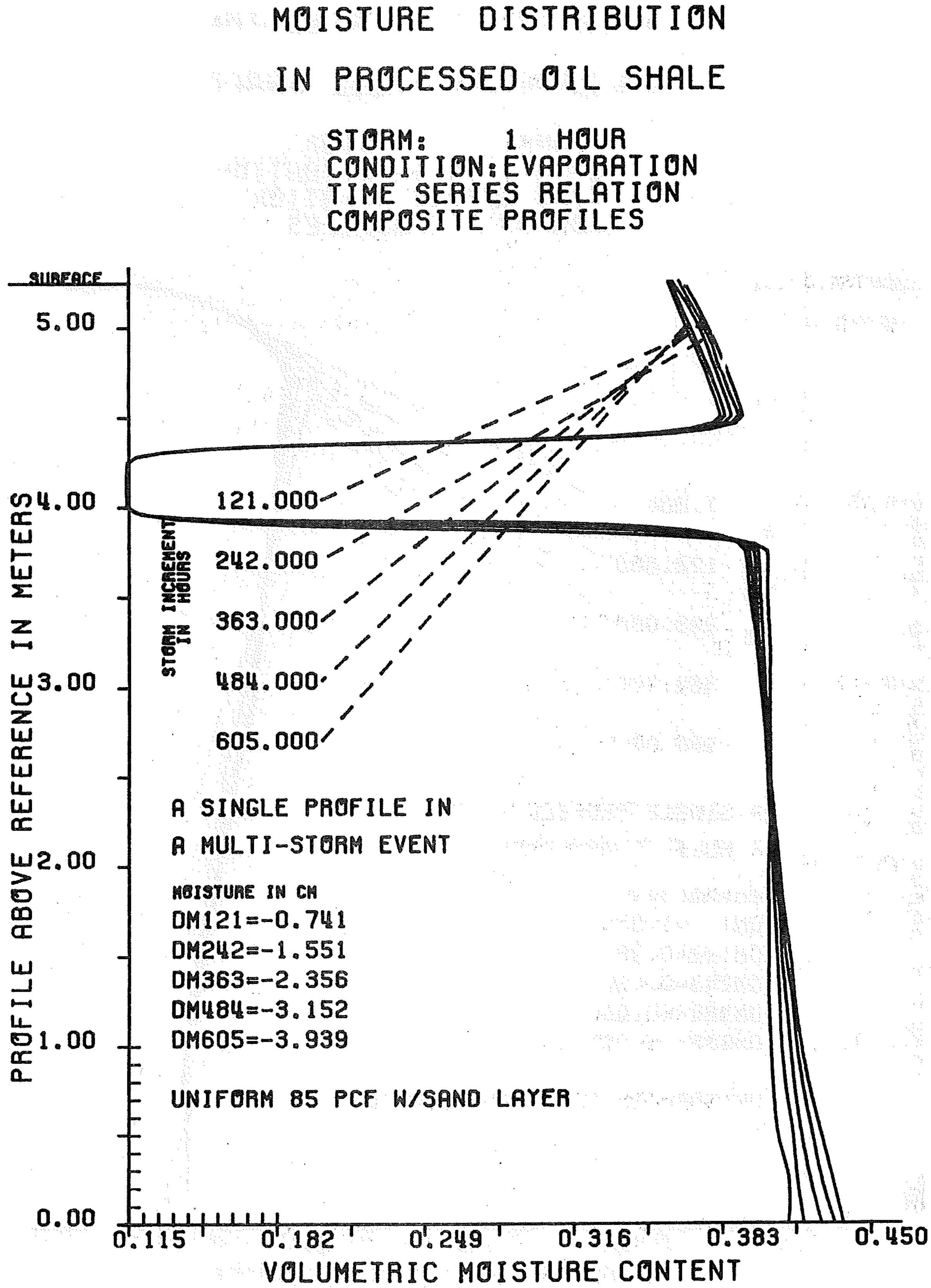

FIGURE III-33

MOISTURE DISTRIBUTION IN PROCESSED OIL SHALE

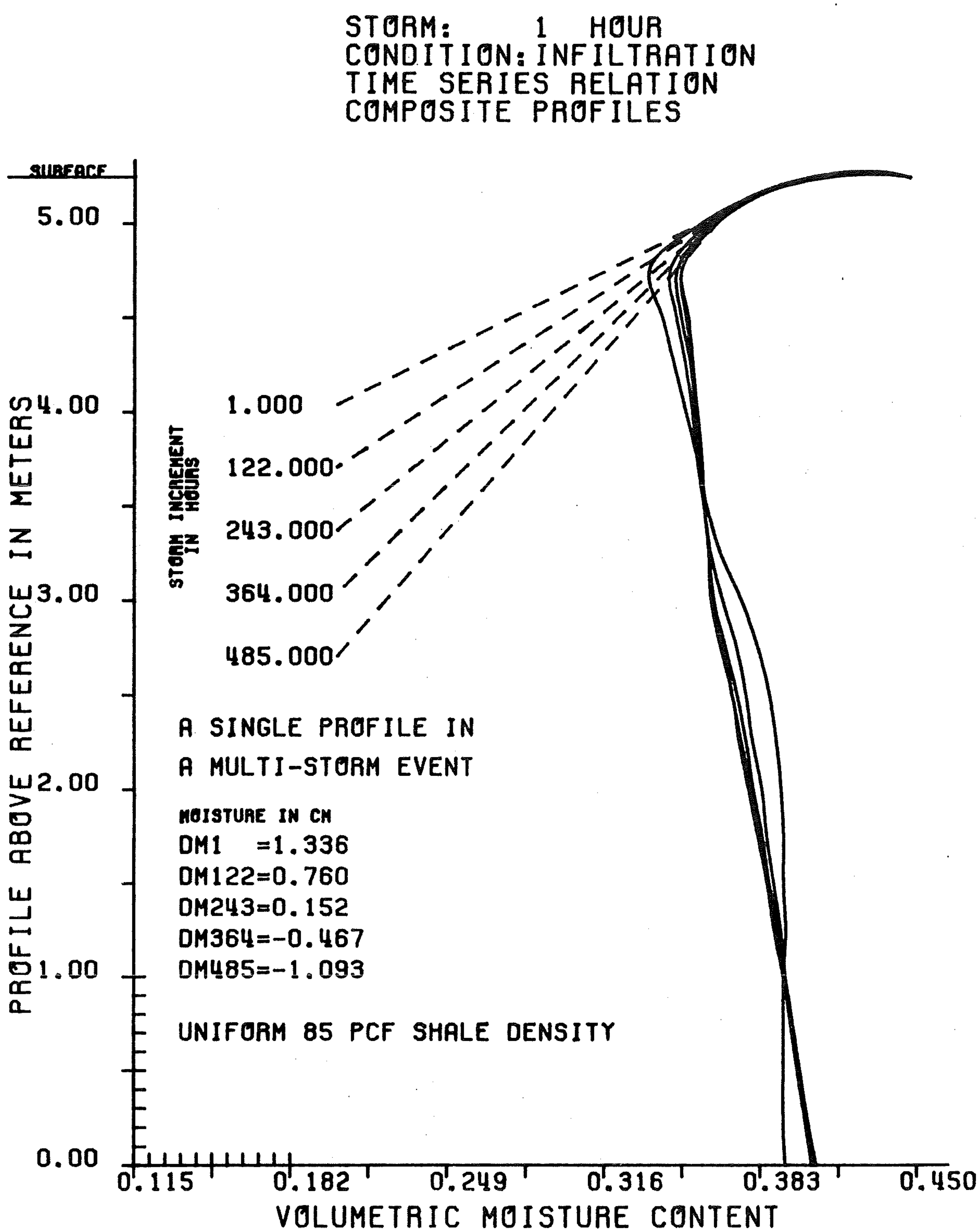

FIGURE III-34

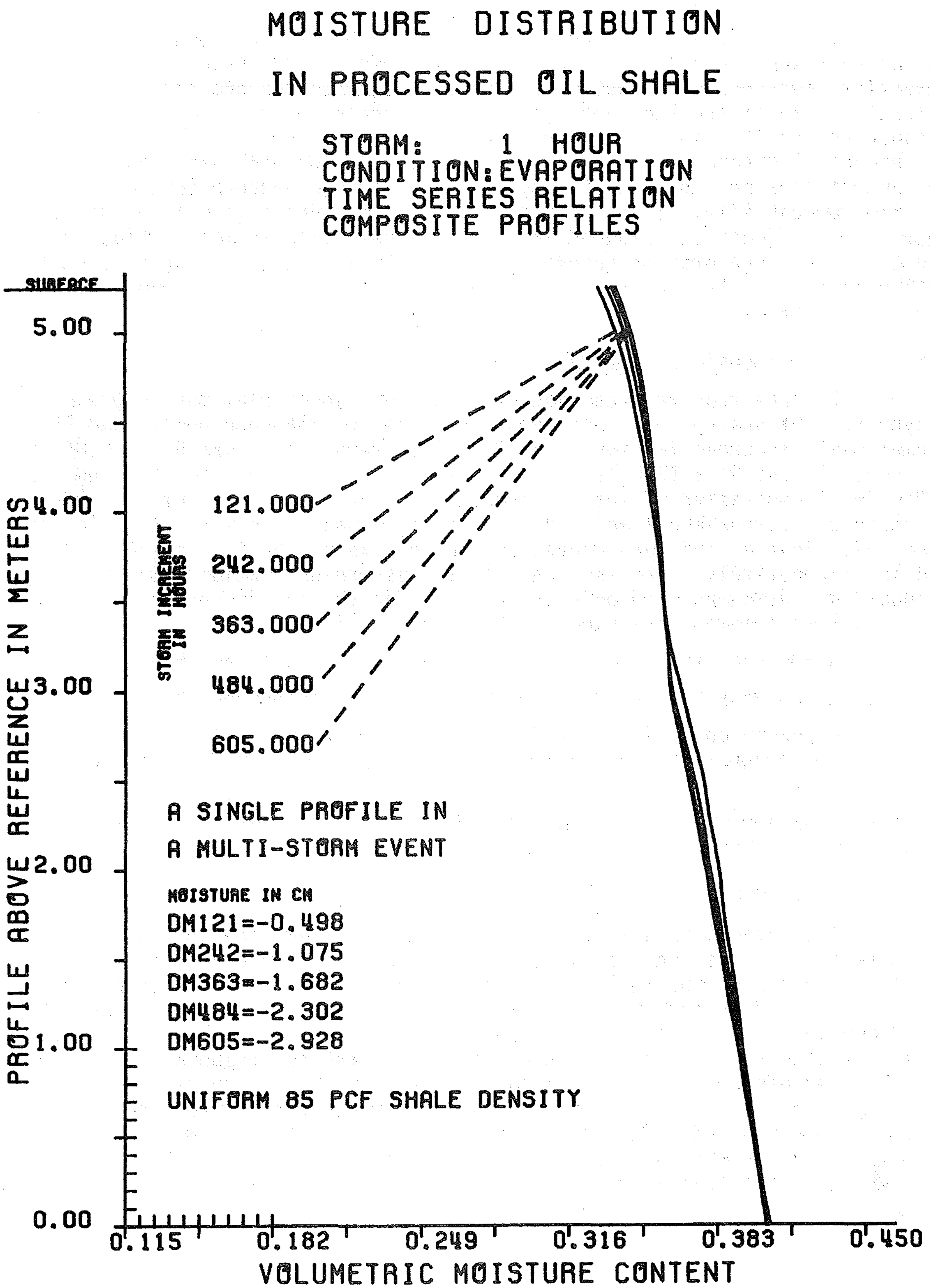

The effect of having a sand layer slightly below the ground surface was not as expected and yet is easily explained. When unsaturated conditions exist the pressure in the water is less than atmospheric and sand will be relatively dry at the same pressure at which shale would be quite wet. Thus during infiltration the sand impedes water flow because it is relatively dry and has low permeability. Some water does get through the sand, however, and it does not move back up through the sand during evaporation because of the low permeability. Thus the sand layer at this depth (1.5 m) had two undesirable effects: 1) reduced infiltration resulting in more surface runoff and 2) reduced evaporation resulting ultimately in water seeping through the entire pile. If the sand layer had been at a greater depth it would not have been as harmful.

III-3.2 Two Dimensional Analysis

A series of runs were carried out on a two dimensional mesh representing a hypothetical shale pile. This mesh consisted of 168 node points and 149 elements and is shown in Figure III-35. The overall size was 573 m (1880 ft) horizontally and 91 m (300 ft) vertically. The right side (to the right of nodes 76-84) consisted of shale compacted to 95 pcf. To the left of this line was 85 pcf shale and under the entire pile was a 1.5 m (5 ft) layer of sand. The initial moisture conditions (on dry weight basis) were 25%, 20% and 13% respectively. The same capillary pressure-saturation relative conductivity data was used here as was used for the one dimensional analysis.

This problem was run under 3 boundary conditions:

1. A 100 year 1 hour storm (intensity of .95 inches per hour)
2. A 100 year 6 hour storm (intensity of .25 inches per hour)
3. A ponded condition of 1.5 m (5 ft) of water on surface nodes 3 through 84 and no infiltration or evaporation on the remainder of the pile.

A seepage surface was allowed at the right side of the mesh (nodes 166 and 167) under all these conditions.

III-3.2.1 One Hour Storm

The two intensities of storms were run to get some idea of what storm intensity would cause surface runoff. This is highly dependent on the initial moisture content of the shale. In the one dimensional analysis evaporation was run for 30 days before a storm was put on but this was not done for the two dimensional analysis. It is probably more realistic to have evaporation since over the years during which a pile is constructed evaporation will occur.

This problem was run for one hour and at no time was there runoff from the 85 pcf shale. There was, however, considerable runoff from the 95 pcf shale because the infiltration rate varied from 2.54 to 3.18 mm/hour (.1 to .125 inches/hour) whereas the rainfall rate was 24.13 mm/hr. The moisture content at the surface nodes with 85 pcf density increased from 0.188 to about

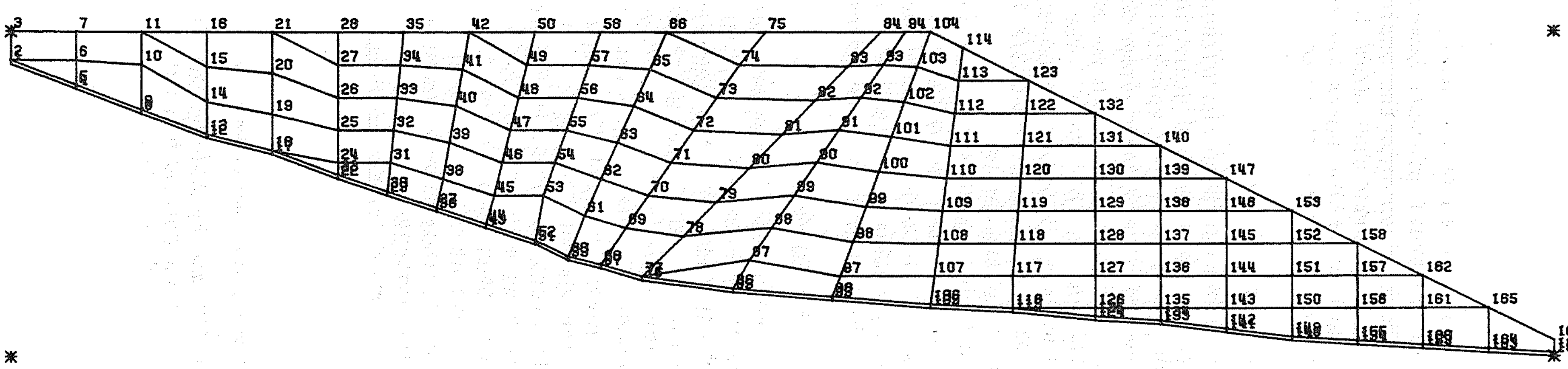

FIGURE III-35

FINITE ELEMENT MESH 2-D WASTE SHALE PILE XSCALE = 200.00 YSCALE = 200.00

0.191 while those with 95 pcf density increased from 0.3779 to 0.3784. There was also some internal moisture movement not related to rainfall as water moved from the sand up into the shale because the initial moisture content of the sand was greater than could be maintained in contact with the shale. The shale, having smaller pores and being dryer than the sand, attracted the water from the sand. There was no flow from the seepage surface.

III-3.2.2 Six Hour Storm

This problem was also run without an evaporation period. The results were similar to the one hour storm in that there was no runoff at any time from the 85 pcf shale (i.e. infiltration was equal to rainfall rate) and there was runoff at all times from the 95 pcf shale (i.e. infiltration was always less than rainfall). In no case in either problem were there any saturated regions in the shale. The moisture content at the boundary nodes with 85 pcf density increased from 0.188 to about 0.194 while those with 95 pcf density increased from 0.378 to 0.379. Again, moisture moved from the sand up into the shale.

There are two reasons for the wide difference in the infiltration characteristics of the two materials: 1) The moisture content was less in the 85 pcf shale which provides more available volume for water storage and 2) The conductivity is greater in the 85 pcf shale at high moisture contents allowing water to move more rapidly from the surface.

III-3.2.3 Ponded Surface

The ponded surface extended over the entire surface of the 85 pcf shale (nodes 3 through 84). This was run for a period of 1 year during which there was flow from the seepage surface at node 166. This flow started during the first day which was entirely unexpected. However, after noting the pressures in the sand layer to the left of the seepage surface it was apparent that the water was simply draining out of the sand layer and was not moving through the shale. This rate of drainage was 0.0283 m^3/d (1 cfd) at the end of the year. The regions that became saturated are indicated by cross-hatching in Figure III-36. The saturated zone had moved into the shale as much as 12.2 m (40 ft) from the surface and moved considerably deeper than that at the left end of the 95 pcf shale. There is also a saturated zone at the right end of the sand layer.

In general, these three problems with the 2-dimensional mesh ran very well with few unsuccessful runs. The total cost for the problems was about $80 or 20 minutes of computer time.

II-4 SUMMARY

In summary, the work done in Phase III demonstrates the following:

1. UNSAT2 may be applied to large sections of natural profiles. Whether it will predict perched water tables depends on the degree of delineation of various geologic formations.

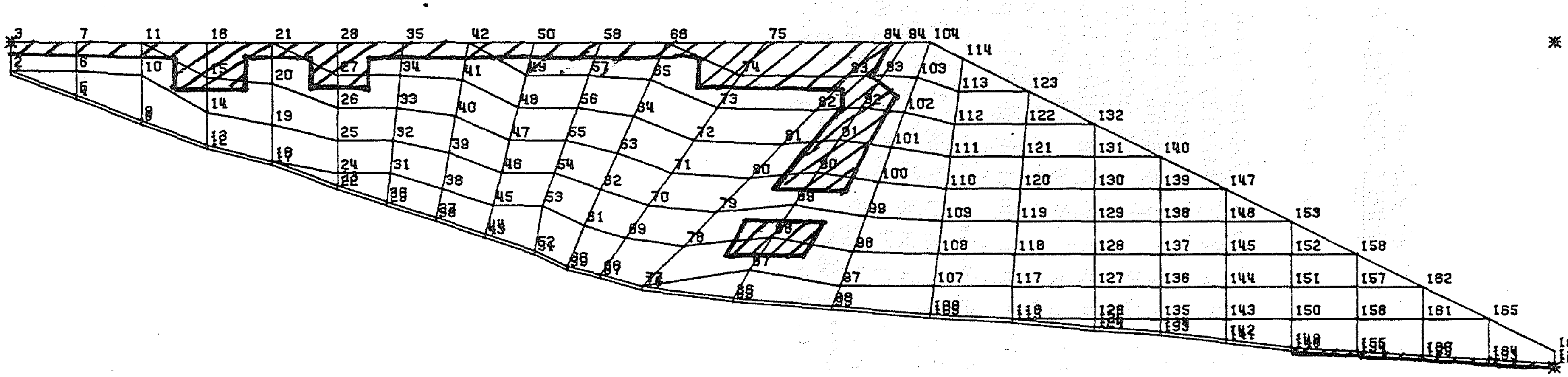

FIGURE III-36

SATURATED ZONES AFTER ONE YEAR OF PONDING XSCALE = 200.00 YSCALE = 200.00

2. UNSAT2 can be used on infiltration or evaporation problems concerned with unsteady, unsaturated flow that conventional saturated flow programs cannot be used on.

In addition, we have the following results common to Northwestern Colorado:

3. Surface and groundwater effects originating from waste shale piles and resulting from low intensity, low yield storms will be insignificant. Evaporation will completely reclaim most common storm yields. Most low intensity storms will completely infiltrate with no special profile preparation. Groundwater will not accumulate as a result of common storms.

4. High intensity, low yield storms may require a disposal zone border or an unconsolidated, low density surface layer to contain surface water until it can be infiltrated. Evaporation will prevent groundwater accumulation with no special profile preparation.

5. High intensity, high yield storms may require borders or unconsolidated, low density surface layers to contain runoff. During the construction of the profile, care should be taken to produce a uniform profile so as not to restrict upward moisture movement during evaporation. Dense liners requiring a large compactive effort are not necessary in order to prevent ground water accumulation from direct storm effects. Unlayered, naturally developing profiles are effective in severe storm yield containment.

REFERENCES CITED

1. Adam, K. M., G. L. Bloomsburg and A. T. Corey (1969), Diffusion of Trapped Gas from Porous Media, Water Resources Research, Vol. 5, No. 4.

2. Anat, A., H. R. Duke and A. T. Corey (1965), Steady Upward Flow From Water Tables, Hydrology Paper 7, Colorado State University, Fort Collins, Colorado.

3. Bloomsburg, G. L. and A. T. Corey (1964), Diffusion of Entrapped Air from Porous Media, Hydrology Paper No. 5, Colorado State University, Fort Collins, Colorado.

4. Brooks, R. H. and A. T. Corey (1964), Hydraulic Properties of Porous Media, Hydrology Paper No. 3, Colorado State University, Fort Collins, Colorado.

5. Climatic Atlas of the United States (1968), U.S. Department of Commerce, National Oceanic and Atmospheric Administration.

6. Coffin, D. L., F. A. Welder and R. K. Glanzman (1971), Geohydrology of the Piceance Creek Structural Basin between the White and Colorado Rivers, Northwestern Colorado, U. S. Geological Survey Hydrologic Investigations Atlas HA-370.

7. Corey, G. L., A. T. Corey and R. H. Brooks (1965), Similitude for Non-Steady Drainage of Partially Saturated Soils, Hydrology Paper 9, Colorado State University, Fort Collins, Colorado.

8. Corp, E. L. (1974), A Finite-Element Model for Stability Analysis of Mine-Waste Embankments Subjected to Seepage, Unpublished Ph.D. Dissertation, University of Idaho, Moscow, Idaho.

9. Golder Associates (1977), Water Management in Oil Shale Mining, Final Report on Contract No. J0265019, Kirkland, Washington.

10. Hedstrom, W. E., A. T. Corey and H. R. Duke (1971), Models for Subsurface Drainage, Hydrology Paper 48, Colorado State University, Fort Collins, Colorado.

11. Kealy, C. D. and R. E. Williams, Flow through a Tailings Pond Embankment, Water Resources Research, Vol. 7, No. 1, 1971.

12. Kealy, C. D. (1970), Seepage Patterns in Mill Tailings Dams as Determined by Finite-Element Models, Unpublished M.S. Thesis, University of Idaho, Moscow, Idaho.

13. Laliberte, G. E., R. H. Brooks and A. T. Corey (1968), Permeability Calculated from Desaturation Data, Journal of Irr. and Drain. Div. ASCE, Vol. 94, No. IRI.

14. Linsley, R. K., M. A. Kohler, and J. L. H. Paulhus, Hydrology for Engineers, 2nd Ed., McGraw Hill Book Co., New York, 1975.

15. McWhorter, D. B. (1971), Infiltration Affected by Flow of Air, Hydrology Paper 49, Colorado State University, Fort Collins, Colorado.

16. Newman, S. P., R. A. Feddes, and E. Bresler (1974), Finite Element Simulation of Flow in Saturated - Unsaturated Soils Considering Water Uptake by Plants, Third Annual Report Project No. AIO-SWC-77, Israel Institute of Technology, Haifa, Israel.

17. Richards, L. A. (1931), Capillary Conduction of Liquids through Porous Mediums, Physics, 1:318-333.

18. Schleusener, R. A. and A. T. Corey (1959), The Role of Hysteresis in Reducing Evaporation from Soils in Contact with a Water Table, Jour. of Geo. Res. 64(4).

19. Sinclair, L. R., D. W. Fitzsimmons and G. L. Bloomsburg (1974), Permeability of Unsaturated Field Soils Calculated from Laboratory Desaturation Data, Transactions ASAE, Vol. 17, No. 3.

20. Sinclair, L. R. (1973), Permeability of Unsaturated Field Soils Predicted from Desaturation Data. Ph.D. Thesis, University of Idaho, Moscow, Idaho.

21. Su, C. and R. H. Brooks (1976), Hydraulic Functions of Soils from Physical Experiments and Their Applications, Report WRRI-41, Oregon State University.

22. U. S. Dept. of Commerce - Weather Bureau (National Weather Service) (1955), Technical Paper No. 25, Rain Fall Intensity - Duration - Frequency Curves for the United States. Superintendent of Documents, Washington, D.C.

23. U. S. Dept. of Commerce - Weather Bureau (National Weather Service)(1959), Evaporation Maps for the United States, 1946-55. Superintendent of Documents, Washington, D.C.

24. Weeks, J. B., G. H. Leavesley, F. A. Welder, and G. J. Saulnier (1974), Simulated Effects of Oil-Shale Development on the Hydrology of Piceance Basin, Colorado, U. S. Geol. Survey Open-File Report 74-255, U. S. Geol. Survey Prof. Paper 908.

25. White, N. F. (1968), Desaturation of Porous Materials, Ph.D. Dissertation, Colorado State University, Fort Collins, Colorado.

26. Woodward Clyde Consultants, W. G. Holz (1976), Disposal of Retorted Shale from Paraho Oil Shale Project, Final Report, NTIS PB-263 793.

Appendix A

Program Documentation

and User Instructions

UNSAT2

PROGRAM UNSAT 2*

General Description

Program UNSAT 2 is an improved and extended version of program UNSAT 1 previously developed by Neuman (1972). It was written in FORTRAN IV for the IBM 370/165 and utilizes the Galerkin method in conjunction with a finite element discretization scheme for solving problems of nonsteady seepage in saturated-unsaturated porous media. It has been run on the IBM 370/145 at the University of Idaho.

The program can be used to investigate problems involving two spatial dimensions in the horizontal or vertical plane. Three-dimensional problems can be handled provided that the flow pattern retains an axial symmetry about the vertical coordinate. The flow region may have any complex shape and it may consist of different soil materials arranged in arbitrary patterns. Each soil material may exhibit an arbitrary degree of local anisotropy, with the principal hydraulic conductivities oriented at any desired angle with respect to the coordinates.

A wide range of time-dependent boundary conditions can be treated: Prescribed pressure head; prescribed flux normal to the boundary; seepage faces; and evaporation and infiltration boundaries where the maximum rate of flux is prescribed by atmospheric or other external conditions, whereas the actual rate is initially unknown. In addition, the program can handle water uptake by plants assuming that the maximum rate of transpiration is determined by atmospheric as well as soil and plant conditions. Internal volumetric sinks or sources of prescribed strength can be included in the flow system at any stage of the computation. A special provision has also been made for the analysis of axisymmetric flow to a well of finite radius partially penetrating an unconfined aquifer system and discharging at a prescribed time-dependent rate. The well may be partially cased and its capacity for storing water is taken into account. Several layers can be tapped by the well at the same time.

The governing equations are expressed in terms of a single dependent variable, ψ, representing the pressure head. The total head is given by $h = y + \psi$ where y is the vertical distance above a horizontal datum plane passing through the origin of coordinates. In the saturated zone ψ is positive, whereas in the unsaturated zone ψ attains negative values and is a single-valued, monotonic function of the volumetric moisture content, θ. This means that in dealing with non-zero air-entry values of ψ (i.e., when θ is equal to the saturated moisture content, θ^S, over a range of negative ψ values), θ must be set equal to $\theta^S - \varepsilon(\psi)$ where $\varepsilon(\psi)$ is an arbitrary positive variable which increases as ψ becomes more negative. It is also helpful to smooth the data somewhat or trouble will be encountered in getting the program to run.

---

*The documentation for this program was taken nearly verbatim from "Finite Element Simulation of Flow in Saturated-Unsaturated Soils Considering Water Uptake by Plants," Third Annual Report Project No. AIC-SWC-77, Israel Institute of Technology, Haifa, Israel, by S.P. Neuman, R.A. Feddes, and Eshel Bresler.

The hydraulic conductivity at each point is expressed as a symmetric tensor, $K_{ij} = K^r(\theta)K^s_{ij}$, where K^s_{ij} is the conductivity at saturation and $K^r(\theta)$ is relative conductivity $(0 \leq K^r(\theta) \leq 1)$. In addition, the saturated portion of the porous material may be assigned elastic storage properties through the concept of specific storage, S_s, which is widely used by ground-water hydrologists. The term S_s represents the volume of water instantaneously released from a unit bulk volume of soil when ψ is lowered by one unit, due to elastic compression of the soil and expansion of the water itself. If the soil and the water are incompressible, S_s must be set to equal zero.

The hydraulic properties that are required separately for each porous material in the system to be simulated are saturated conductivity, K^s_{ij}, relative conductivity as a function of moisture content, $K^r(\theta)$, porosity, θ^s, pressure head as a function of moisture content, $\psi(\theta)$, and specific storage, S_s. In addition one must know the initial values of ψ or h at each point in the system as well as the conditions to be imposed at each point along the boundary. Once these are known, the next step is to superimpose a finite element mesh on the flow system.

Construction of Finite Element Mesh

The following gives the procedure for constructing the finite element mesh and the number convention that must be strictly adhered to. One should first construct to scale a map or cross-section of the flow region and locate the important features such as interfaces between materials having different hydraulic properties, boundary conditions, etc. The finite element mesh must conform to the external boundaries of the flow region and to the internal boundaries between different materials. Fig. A-1 shows a finite element network superimposed on a vertical cross-section through a system composed of two layers having different material properties.

The dimensions of the elements should be made small parallel to directions along which large hydraulic gradients are expected to occur, and large parallel to directions along which these gradients are expected to be small. Essentially any shape of quadrilateral can be used, but, for best results, the quadrilaterals should be kept more or less equidimensional and they should not be too distorted. In the program each quadrilateral is automatically divided into two triangles having identical material properties.

As indicated on Fig. A-1, triangular elements can also be used but these should always be placed so that they open to the left or to the right along the direction of the longer axis of the model. In other words, all element boundaries along the shorter axis of the model must form non-intersecting transverse lines, not necessarily straight, that are continuous from one side of the flow region to the other. In Fig. A-1 the short axis is more or less parallel to the vertical coordinate, y, and so are the transverse lines. In general, however, there is no restriction on the orientation of the model and the transverse lines with respect to the spatial coordinates.

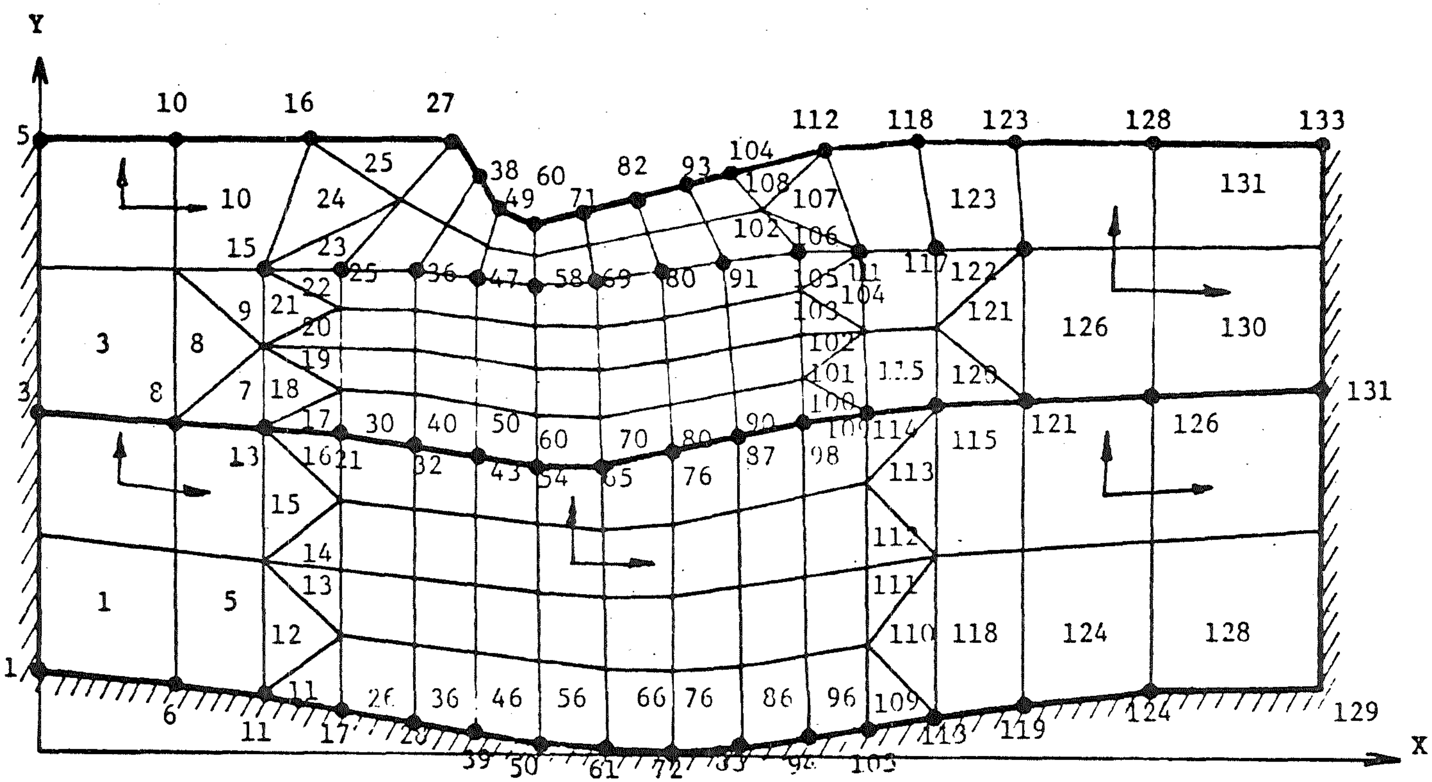

Fig. A-1 - Scheme for numbering nodes and elements in finite element mesh.

The model in Fig. A-1 has been divided into 131 elements, the shapes of which are prescribed by specifying the coordinates of the 133 nodes that form the corners. Before numbering the nodes and the elements the model is rotated into a position where the transverse lines lie along the vertical and the longer axis along the horizontal with respect to the user. Numbering of the nodes is then done along the transverse lines from bottom to top and from left to right. Elements are numbered in a similar manner. The maximum number of nodes along any transverse line, IJ, is directly related to the band-width of the finite element matrix and should therefore be always made as small as possible (IJ is 11 in Fig. A-1).

In axisymmetric three-dimensional problems the vertical axis must form the left boundary of the mesh, or lie to the left of this boundary, and all transverse lines must be more or less parallel to the vertical coordinate.

Root zones must consist only of rectangular elements with boundaries parallel to the horizontal and vertical coordinates (see Fig. A-1). Vertical boundaries between elements in the root zone are termed vertical nodal columns. Several root zones having different depths and corresponding to different plant species can be treated simultaneously in a single model. The depth of each root zone must be at least equal to the maximum depth that the roots will reach at any stage of their growth during the period simulated. The actual depth of the roots at any stage of the computation is controlled by the values assigned to the root effectiveness function.

Coding of Materials

Each material having distinct material properties is assigned an integer code number, starting with 1 and ending with NUMMAT, the total number of materials. The material properties of each element are then identified by the material code number assigned to this element. For example, the total number of materials in Fig. A-1 is NUMMAT = 2. If we decide to identify the lower layer by the code number 1 and the upper layer by 2, then each element in the lower layer will belong to material 1 and each element in the upper layer will belong to material 2.

Coding of Nodal Points

Each node in the finite element network is assigned an integer code number which identifies the type of boundary condition that must prevail at this node. The code for the N-th node is designated KODE(N). If the pressure head at node N is to have a prescribed value at the end of any time step, KODE(N) must be set equal to 1 during that time step. If the volumetric rate of water leaving or entering the system at node N is prescribed during a time step, KODE(N) must be set equal to 0 for that time step. Internal nodes which do not act as sinks or sources must be assigned KODE(N) = 0 because it is known that the amount of water which leaves or enters the system through these nodes is zero (this does not mean that the water does not flow past these nodes, but merely that this water does not leave or enter the system).

Internal nodes acting as sinks or sources outside the root zone are also assigned KODE(N) = 0. The rate of inflow or outflow prescribed at each such node, Q(N), represents the rate of flow into or out of a weighted portion of the soil volume represented by the node.

The rate of water uptake by plants in the root zone is determined automatically by the program. Set KODE(N) = 0 for all nodes in the root zone, excluding nodes at the soil surface.

Nodes at the boundary of the system where flux normal to the boundary, Q(N), is prescribed are assigned KODE(N) = 0. Along impermeable boundaries the prescribed flux is zero. Otherwise, every node represents the flux across half the boundary surface of each neighboring element.

For nodes at the soil surface where the maximum admissible rate of evaporation or infiltration is determined by atmospheric or other external conditions, whereas the actual rate is to be determined automatically be the program, KODE(N) must be set equal to -4 for the entire period simulated.

All nodes that are expected to lie on a seepage face, during any stage of the computation, must be assigned KODE(N) = ±2. Nodes that initially lie on a seepage face are assigned KODE(N) = 2 (and $\psi = 0$). Nodes that initially lie on an unsaturated segment of the boundary which is expected to become part of a seepage face during a later stage of the computation are assigned KODE(N) = -2. A node which is shared commonly by a seepage face and a prescribed pressure head boundary is not considered to be part of the seepage face. At such a node KODE(N) = 1 and the pressure head is set equal to zero.

In axisymmetric systems with a well discharging at a prescribed rate, all nodes along the cased portion of the well are assigned KODE(N) = 0 as the flux there is known to remain zero. All other nodes along the well, including those at the edges of the casing, are assigned KODE(N) = 2.

Variable Boundary Conditions

The boundary conditions at all nodes initially assigned KODE(N) = 1, or KODE(N) = 0 can be changed at any stage of the computation by means of the RESTART feature. This feature allows changing KODE(N) from 0 to 1 and vice versa, but it does not allow modifying the type of boundary condition at nodes initially assigned KODE(N) = ±2 or KODE(N) = -4. The atmospheric conditions controlling maximum soil evaporation and plant transpiration can also be changed at any time by RESTART. Similar changes can be introduced in the discharge rate from a well.

Choice of Integration Scheme

Program UNSAT 2 provides the user with an option to choose between a time-centered scheme or a backward difference scheme for time integration of the finite element equations. When the flow region remains unsaturated at all times, or when part of the system is saturated but $S_s \neq 0$ in all elements, either of these two schemes can be used. When part of the system is expected to be saturated during any stage of the computation and S_s in the saturated zone is zero, the backward difference scheme must be employed. In the latter case, the initial values of ψ at all saturated nodes that do not lie on a prescribed ψ boundary must be initially set equal to zero.

Compilation of Subroutines

Program UNSAT 2 consists of a short main program and several subroutines. The use of dynamic storage allocation makes it possible to compile all the subroutines once and then keep the object code on permanent file. Only the main program needs to be recompiled with each change in the dimensions of the problem.

Control of Problem Size

The size of each problem is limited by the dimensions assigned to the arrays BD and BS that appear in the main program. BD is assigned double precision and its length must be at least (IJ + 3) * NUMNP, where NUMNP is the number of nodal points. The length of BS must be at least 10 * NUMNP + 7 * NUMEL + NUMMAT * (2 * MK + 4 * MP) + NDIM * (2 + MAXSP) + 2 * NUMDP + NDIMP * (4 + 4 * MXCOL + 2 * MXNOD) + 2 * MXNOD where NUMEL is the number of elements, NUMMAT is the number of materials having different hydraulic properties, MK = $\max_M$[NUMK(M)] where M = 1,..., NUMMAT and NUMK(M) is the number of paired entries in the table of K^r versus θ for the M-th material, MP = $\max_M$[NUMP(M)] where NUMP(M) is the number of paired entries in table of ψ versus θ for the M-th material, NDIM = max[1,NSEEP] where NSEEP is the number of seepage faces, MAXSP = $\max_I$[1,NSP(I)] where I = 1,..., NSEEP and NSP(I) is the number of nodes having KODE(N) = ±2 on the I-th seepage face, NUMDP = max[1,NUMEP] where NUMEP is the number of evaporation or infiltration boundary nodes having KODE(N) = -4, NDIMP - max[1,NPLNT] where NPLNT is the number of different plant species, MXCOL = $\max_J$[1,NCOL(J)] where J = 1,..., NPLNT and NCOL(J) is the number of vertical nodal columns corresponding to the J-th plant species, and MXNOD = $\max_J$[1,NSOUR(J)] where NSOUR(J) is the number of nodes in each such column.

The number of materials having different hydraulic properties that can be used in a given problem is determined by the dimensions assigned to the arrays C1, C2, SS, POR, NUMK, NUMP, NUMC in COMMON / MAT / . The length of each of these arrays must be at least equal to NUMMAT. Modifications in COMMON / MAT / must be introduced in all the subroutines where this statement appears. As currently written, the maximum value of NUMMAT is 5.

Storage Files

The program requires one permanent file for restart purposes labeled TAPE 1, and two scratch files labeled TAPE 2 and TAPE 3.

TAPE 1 requires a storage area of at least 8*[100 + 6 * NUMNP + 7 * NUMEL + NUMMAT * (2 * MK + 4 * MP) + NDIM * (2 + MAXSP) + 2 * NUMDP + NDIMP * (4 + 4 * MXCOL + 2 * NXNOD)] bytes. The symbols have been defined in the previous section.

TAPE 2 requires a storage area of at least 8 * (IJ + 3) * NUMNP bytes, where IJ is the maximum number of nodes along any transverse line.

TAPE 3 requires a storage area of at least 4 * NUMNP bytes.

Data Input to Program UNSAT 2

The data input has been arranged in nineteen groups and must be punched on cards according to the following instructions.

GROUP	COLUMNS	FORMAT	SYMBOL	DESCRIPTION
A	1-80	20 A4	HED	Desired heading to be printed with each time step.
	The words END and RESTART should not appear in columns 1-7 of this group. Use only one card for this group.			
B	1-5	I 5	NUMNP	Number of nodal points.
	6-10	I 5	IJ	Maximum number of nodes in any transverse line.
	11-15	I 5	NUMEL	Number of elements.
	16-20	I 5	KAT	0 if horizontal plane flow (x_1, x_2); 1 if axisymmetric flow (x_1, x_3); 2 if vertical plane flow (x_1, x_3).
	21-25	I 5	NUMMAT	Number of materials.
	26-30	I 5	INIT	0 if initial data (see group Q) are in terms of pressure head (ψ); 1 if these are in terms of total head (h).

GROUP	COLUMNS	FORMAT	SYMBOL	DESCRIPTION
	31-35	I 5	MAXIT	Maximum number of iterations per time step. If exceeded, everything is dumped on TAPE 1 and execution terminates. May be changed at later times by RESTART. Fifteen is usually sufficient.
	36-40	I 5	INTEG	1 for backward difference scheme; 2 for time-centered scheme.
	41-45	I 5	NSEEP	Number of seepage faces expected to develop; leave blank if there are no seepage faces.
	46-50	I 5	MAXS	Maximum value of NSP(I) in Group E. Leave blank if there are no seepage faces.
C	1-5	I 5	NBW	Number of nodes at bottom of well. Leave blank if not applicable.
	6-10	I 5	NPB	Highest sequential number (N) of any node at bottom of well. Leave blank if not applicable.
	11-15	I 5	NPT	Sequential number (N) of node at top of well. Leave blank if not applicable.
	16-20	I 5	NEP	Number of seepage faces expected to develop along well bore. Leave blank if not applicable.
	21-25	I 5	LW	Sequential number (N) of node at or immediately below initial water level in well. Leave blank if not applicable.
	26-30	I 5	NUMEP	Number of evaporation and infiltration boundary nodes at which maximum allowable rate of flow is prescribed but actual rate is unknown (i.e. at which KODE(N) = -4).
	31-35	I 5	NPLNT	Number of different plant species.

GROUP	COLUMNS	FORMAT	SYMBOL	DESCRIPTION
	36-40	I 5	MXCOL	Maximum number of vertical nodal columns in root zone for any plant species. Leave blank if not applicable.
	41-45	I 5	MXNOD	Maximum number of nodes in any vertical nodal column in root zone, at any stage of plant growth, including node at soil surface. Leave blank if not applicable.

The variables NBW, NPB, NPT, NEB and LW must be specified only in dealing with axisymmetric problems where a single well discharges at a prescribed rate. If the elevation of the water level in the well is prescribed instead of the discharge, the well is treated in the same manner as other boundaries. See also Group K.

GROUP	COLUMNS	FORMAT	SYMBOL	DESCRIPTION
D	1-5	I 5	NUMK(1)	Number of paired entries $\{\theta_I^M, K_I^{rM}\}$ in table of K^r versus θ for material number 1 (see Group P). Should not be less than 2.
	6-10	I 5	NUMP(1)	Number of paired entries $\{\theta_J^M, \lvert\psi_J^M\rvert\}$ in table of ψ versus θ for material number 1 (see Group P). Should not be less than 2.
	11-15	I 5	NUMK(2)	Same for material number 2.
	16-20	I 5	NUMP(2)	
	.	.	.	
	.	.	.	
	.	.	.	
	-80			

Materials having different hydraulic properties are numbered sequentially in an arbitrary order for the purpose of identification. Specify NUMMAT pairs of NUMK(J), NUMP(J) in a sequential order. Use as many cards for this group as needed.

GROUP	COLUMNS	FORMAT	SYMBOL	DESCRIPTION
E	Omit Group E if NSEEP = 0 in Group B.			
	1-5	I 5	NSP(I)	Number of nodes having KODE = ±2 on I-th seepage face (see Section 4).
	6-10	I 5	KODES(I)	Set this variable equal to -1.
	For each value of I, this card must be immediately followed by a complete list of NP(I,J) values as shown below.			
	I-5	I 5	NP(I,1)	Sequential number (N) of first node on I-th seepage face.
	6-10	I 5	NP(I,2)	Sequential number (N) of second node on I-th seepage face.
	. . .	. . .	. . .	
	76-80			
	Use as many cards as are needed to specify all values of NP(I,J) for J = 1, 2,..., NSP(I).			
	Seepage faces are numbered in sequential order from I = 1 to I = NSEEP. On each seepage face, the nodes with KODE = ±2 are numbered sequentially from J = 1 to J = NSP(I), starting from the saturated side of the seepage face. Thus, each node on a seepage face is identified by two numbers, a local number, J, and a global number, NP(I,J).			
	Group E is repeated for each seepage face in sequential order, starting with I = 1 and ending with I = NSEEP.			
F	Omit Group F if NUMEP = 0 in Group C.			
	1-10	E10.3	EI	Maximum allowed rate of evaporation (negative sign) or infiltration (positive sign) normal to soil surface. May be changed at later times by RESTART.
	11-20	E10.3	PL	Minimum allowed pressure head, ψ, at soil surface.
	21-30	E10.3	BTPI	Fraction of EI to be imposed during first iteration (usually 0.1).

GROUP	COLUMNS	FORMAT	SYMBOL	DESCRIPTION
G	Omit Group G if NUMEP = 0 in Group C.			
	1-10 71-80	E10.3	WIDTH(I)	Soil surface width represented by I-th node at which maximum rate of evaporation or infiltration is prescribed, but actual rate is unknown. (i.e., at which KODE(N) = -4).

Nodes at the soil surface at which the maximum rate of evaporation or infiltration is prescribed by EI in Group F, whereas the actual rate is unknown, are numbered locally in sequential order from left to right starting with I = 1, and ending with I = NUMEP. Thus, each node having KODE(N) = -4 in Group Q is identified by two numbers, a local number, I, and a global number, N.

The soil surface width represented by the node, WIDTH(I), includes half the surface length of each element in the immediate vicinity of the node.

Use as many cards as are needed to specify all the values of WIDTH(I), for I = 1,...,NUMEP.

GROUP	COLUMNS	FORMAT	SYMBOL	DESCRIPTION
H	Omit Group H if NPLNT = 0 in Group C.			
	1-5	I 5	NCOL(1)	Number of vertical nodal columns in root zone of 1st plant species.
	6-10	I 5	NSOUR(1)	Number of nodes in each vertical nodal column corresponding to root zone of 1st plant species, excluding node at soil surface.
	11-15	I 5	NCOL(2)	
	16-20 76-80	I 5	NSOUR(2)	

Use as many cards as are needed to specify NCOL(J) and NSOUR(J) for J = 1,...., NPLNT.

GROUP	COLUMNS	FORMAT	SYMBOL	DESCRIPTION
I	Omit Group I if NPLNT = 0 in Group C.			
	1-10	E10.3	PW(1)	Wilting pressure head of 1st plant species. Must have negative value.

GROUP	COLUMNS	FORMAT	SYMBOL	DESCRIPTION
	11-20	E10.3	TPOT(1)	Maximum allowed rate of transpiration from 1st plant species (initial value). May be changed at later times by RESTART.
	21-30	E10.3	PW(2)	
	31-40	E10.13	TPOT(2)	
	.	.	.	
	.	.	.	
	.	.	.	
	.	.	.	
	71-80			

Use as many cards as are needed to specify PW(J) and TPOT(J) for J = 1,...,NPLNT.

J Omit Group J if NPLNT = 0 in Group C.

The variables below have a free index, J. First J = 1 and then repeat all cards in Group J for J=2,...,NPLNT, in sequential order.

	I-10	E10.3	W(1,J)	Horizontal width represented by 1st vertical nodal column in root zone of J-th plant species.
	11-20	E10.3	W(2,J)	
	.	.	.	
	.	.	.	
	.	.	.	
	.	.	.	
	71-80			

The vertical nodal columns within the root zone of each plant species are numbered locally from left to right, starting with I=1 and ending with I=NCOL(J) (see Group H).

W(I,J) is half the horizontal distance between nodal columns I and I-1, plus half the horizonal distance between nodal columns I + 1 and I.

Use as many cards as are needed to specify W(I,J) for I = 1,...,NCOL(J) (see Group H). These cards must be immediately followed by an additional set of cards:

	1-5	I 5	NRB(1,J)	Sequential number (N) of bottom node in 1st vertical nodal column within root zone of J-th plant species.

GROUP	COLUMNS	FORMAT	SYMBOL	DESCRIPTION
	6-10	I 5	NRT(1,J)	Sequential number (N) of node immediately below soil surface in 1st vertical nodal column within root zone of J-th plant species.
	11-15	I 5	NRB(2,J)	
	16-20	I 5	NRT(2,J)	
	.	.	.	
	.	.	.	
	.	.	.	
	.	.	.	
	76-80			

Use as many cards as are needed to specify NRB(I,J) and NRT(I,J) for I = 1,...,NCOL(J) (see Group H). These cards must be immediately followed by an additional set of cards:

	1-10	E10.3	RDF(1,J)	Root effectiveness function at bottom nodes within root zone of J-th plant species (initial value). May be changed at later times by RESTART.
	11-20	E10.3	RDF(2,J)	Root effectiveness function at second nodes from bottom within root zone of J-th plant species (initial value). May be changed at later times by RESTART.
	.	.	.	
	.	.	.	
	.	.	.	
	.	.	.	
	.	.	.	
	71-80			

All the nodes within a given root zone are numbered locally from bottom to top, starting with K=1 and ending with K = NSOUR(J) + 1 (see Group H). Thus, each node within the root zone is characterized by two numbers, a local number, K, and a global number, N (see Group Q).

Plant growth is treated by setting the initial values of RDF(K,J) at the bottom of the root zone equal to zero, and by gradually increasing their values via RESTART as time progresses.

Use as many cards as are needed to specify RDF(K,J) for K=1,..., NSOUR(J) + 1. The value corresponding to K=NSOUR(J) is ignored by the program and may be left blank. These cards must be immediately followed by an additional set of cards:

GROUP	COLUMNS	FORMAT	SYMBOL	DESCRIPTION
	1-5	I 5	MTR(1,J)	Sequential number of material corresponding to horizontal layer between K=1 and K=2 (see definition of K above).
	6-10	I 5	MTR(2,J)	Sequential number of material corresponding to horizontal layer between K=2 and K=3 (see definition of K above).
	.	.	.	
	.	.	.	
	.	.	.	
	76-80			

The root zone may be homogenous or it may consist of different soil layers. MTR(K,J) makes it possible to assign arbitrary properties to the soil material within the root zone. Caution must be exercised to insure that the values of MTR(K,J) be consistent with the values of KX(NUM,5) assigned to each element in Group R.

Use as many cards as are needed to specify MTR(K,J) for K=1,... NSOUR(J) (see Group H).

Repeat Group J for all J=1,...NPLNT in sequential order.

K Omit Group K if NBW = 0 in Group C.

K	1-5	I 5	NB(1)	Sequential number (N) of 1st node at bottom of well.
	6-10	I 5	NB(2)	Sequential number (N) of 2nd node at bottom of well
	.	.	.	
	.	.	.	
	.	I 5	NB(NBW)	Sequential number of last node at bottom of well.
	.	I 5	NE(1)	Set this variable equal to NB(NBW).
	.	I 5	NE(2)	Sequential number of saturated node immediately above 1st expected seepage face along well-bore.
	.	.	.	
	.	.	.	
	76-80			

GROUP	COLUMNS	FORMAT	SYMBOL	DESCRIPTION

All nodes at the bottom of the well are numbered locally in sequential order from left to right (the well must be on the left hand side of the finite element mesh) starting with L=1 and ending with L=NBW (see Group C). Thus, each node at the bottom of the well is identified by two numbers, a local number, L, and a global number, N (see Group Q).

In layered soils it is sometimes possible to obtain more than just one seepage face along the well-bore. For example, a highly permeable layer may become partially dewatered before the less permeable overlying layer does. Whenever such a situation is expected to develop, one must specify the values of NE(I) accordingly.

If the well is fully penetrating, NBW in Group C must be equal to 1. The well may be partially cased.

Use as many cards as are needed to specify NB(L) for L=1,...,NBW and NE(I) for I=1,...,NEP (see Group C).

L — Omit Group L if NBW = 0 in Group C.

GROUP	COLUMNS	FORMAT	SYMBOL	DESCRIPTION
L	1-10	E10.3	RW	Effective radius of well
	11-20	E10.3	RT	Radius of production tubing (may be zero).
	21-30	E10.3	QP	Volumetric rate of discharge from well (positive; initial value). May be changed at later times by RESTART.
	31-40	E10.3	AL	Initial elevation of water level in well.
	41-50	E10.3	ALFA	Under-relaxation factor for iterative treatment of well (default = 0.8).

The production tubing is assumed to reach the bottom of the well. Variable rates of discharge can be handled via RESTART.

GROUP	COLUMNS	FORMAT	SYMBOL	DESCRIPTION
M	1-10	E10.3	DT	Initial time interval Δt.
	11-20	E10.3	DTMAX	Maximum allowable size of Δt.
	21-30	E10.3	DMUL	At each time step, Δt is multiplied by DMUL until it becomes equal to DTMAX.

GROUP	COLUMNS	FORMAT	SYMBOL	DESCRIPTION
	31-40	E10.3	TMAX	Maximum time to be reached before the results are dumped on TAPE 1 for restart purposes. The final time corresponds exactly to TMAX.
	41-50	E10.3	TOL	Maximum absolute change in the values of ψ between any two successive iterations in a given time step allowed by user. If MAXIT>0 in Group B, iterations continue until all changes are less than or equal to TOL, or until MAXIT is exceeded. If MAXIT=0, TOL is ignored. If TOL is exceeded when MAXIT has been reached, results are dumped on TAPE 1 and execution terminates.

All of these variables can be changed at later times via RESTART. The values of this card largely determine whether the program will run. That is, the initial time DT must be small enough that a solution will begin. DT = 1 sec. or the corresponding time in other units usually works well even when water is moving into dry soil. In other problems where moisture content is not changing rapidly DT up to 2 minutes will work. DMUL determines how fast DT will increase and usually is 1.5 to 1.8 although sometimes DMUL = 2.0 will work. If time steps are too large the solution will diverge and the execution ceases in iteration "n" when the change of pressure head is larger than in iteration "n-2".

GROUP	COLUMNS	FORMAT	SYMBOL	DESCRIPTION
N	1-10	E10.3	CONS 1	Constants depending on units used
	11-20	E10.3	CONS 2	in problem.

For any consistent set of units (e.g., cgs) CONS1=CONS2=1.0 for two-dimensional planar regions. For axisymmetric regions, CONS1=1.0 and CONS2=1/ (2π).

When non-consistent units are used, both constants must be determined so that all units are converted to some consistent system for the internal calculations. In the program, the dimensional relationship for two-dimensional flow in a vertical plane is simply

$$\underbrace{K_c\, L_c^2}_{A_{nm}\psi_m+B_n} \;+\; \underbrace{L_c^{3} T^{-1}}_{D_{nm}\frac{\partial \psi_m}{\partial t}} \;=\; \underbrace{Q_c}_{Q_n}$$

GROUP	COLUMNS	FORMAT	SYMBOL	DESCRIPTION

provided the units used for h, ψ, S_S, and length are identical. Here, Q is the flow rate (L^3T^{-1}) through a cross-section of unit thickness perpendicular to the two-dimensional flow region, K is the hydraulic conductivity (LT^{-1}), and the subscript c indicates consistent units. One must first choose the units for L_c (e.g., feet) and T_c (e.g., minutes). If one then plans to use inconsistent units for Q (e.g., gpd) and K (e.g., cm/sec), then two constants need to be calculated, C_q and C_k, to convert Q and K into a consistent set of units according to

$$(\text{Units of } Q_c) = C_q \, (\text{Units of } Q)$$

$$(\text{Units of } K_c) = C_k \, (\text{Units of } K)$$

from which CONS1 and CONS2 are

$$\text{CONS1} = 1/C_k$$

$$\text{CONS2} = C_q/C_k$$

For example, if one uses gpd (gallons per day) for Q and Q_c should be in ft^3/min to be consistent, then $C_q = 9.238 \times 10^{-5}$, and if one also uses cm/sec for K and K_c should be in ft/min, then $C_k = 1.968$. Thus, CONS1 = 1/1.968 = 0.508 and CONS2 = $9.283 \times 10^{-5}/1.968 = 4.716 \times 10^{-5}$, and by using these values, units of output flow rates from the program will also be in gpd.

If the problem is axisymmetric then, in the above example, CONS2 = $4.716 \times 10^{-5}/2\pi$.

To prevent difficulties it is recommended that consistent units be used whenever possible.

GROUP	COLUMNS	FORMAT	SYMBOL	DESCRIPTION
0	1-10	E10.3	C1(M)	First principal conductivity (K^S_{11}) of M-th material.
	11-20	E10.3	C2(M)	Second principal conductivity (K^S_{22}) of m-th material.

GROUP	COLUMNS	FORMAT	SYMBOL	DESCRIPTION
	21-30	E10.3	POR(M)	Effective porosity (θ_s) of M-th material.
	31-40	E10.3	SS(M)	Specific storage (S_s, units of L_c^{-1}) of M-th material.

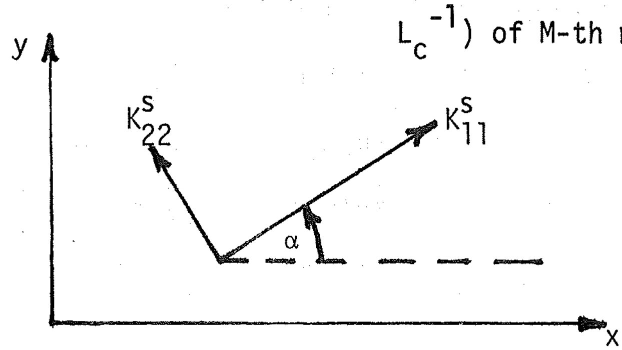

Fig. A-2 <u>Definition of principal conductivities</u>

Use one card for each material. The first card must correspond to Material 1, the second card to Material 2, etc.

The angle α between K_{11}^s and the x coordinate in Fig. A-2 may change from element to element even if all of these elements consist of the same material (for example, in folded layers). Therefore, α will be specified for each element separately in Group R.

GROUP	COLUMNS	FORMAT	SYMBOL	DESCRIPTION
P	1-10	E10.3	XK(1,M)	θ_1^M from table of $K^r(\theta)$.
	11-20	E10.3	YK(1,M)	K_1^{rM} from table of $K^r(\theta)$.
	21-30	E10.3	XK(2,M)	θ_2^M from table of $K^r(\theta)$.
	31-40	E10.3	YK(2,M)	K_2^{rM} from table of $K^r(\theta)$.
	.	.	.	
	.	.	.	
	.	.	.	
	71-80			

The function $K^r(\theta)$ is input into the program as a table of values, $\{\theta_I^M, K_I^{rM}\}$, where M denotes the material for which this table holds.

The table is punched on cards starting with I=1 and ending with I=NUMK(M), so that θ_1^M corresponds to the smallest value of θ_I^M and

GROUP	COLUMNS	FORMAT	SYMBOL	DESCRIPTION

$\theta_I^M < \theta_{I+1}^M$. A situation where $\theta_I^M = \theta_{I+1}^M$ is illegal and may cause problems. Use as many cards as are needed to complete the table. Then punch the following table:

COLUMNS	FORMAT	SYMBOL	DESCRIPTION
1-10	E10.3	XP(1,M)	θ^M from table of ψ (θ).
11-20	E10.3	YP(1,M)	$\lvert\psi_1^M\rvert$ from table of ψ (θ).
21-30	E10.3	XP(2,M)	θ_2^M from table of ψ (θ).
31-40	E10.3	YP(2,M)	$\lvert\psi_2^M\rvert$ from table of ψ (θ).
.	.	.	
.	.	.	
.	.	.	
71-80			

The function ψ (θ) is input into the program as a table of values, $\{\theta_J^M, \ \lvert\psi_J^M\rvert\}$, WHERE M denotes the material for which this table holds. The table is punched on cards starting with J=1 and ending with J=NUMP(M) so that $\theta_J^M < \theta_{J+1}^M$. A situation where $\theta_J^M = \theta_{J+1}^M$ is illegal. Use as many cards as are needed to complete the table.

After having punched both tables for Material 1(M=1), punch the tables for Material 2 on new cards, etc., until M=NUMMAT. In constructing the tables, keep in mind that, in the program, intermediate values are calculated by linear interpolation.

As mentioned previously it is usually helpful to plot the soil data and smooth any abrupt changes in the slope of the θ vs. ψ curve. Erratic data will cause the solution to diverge and the program will not run.

GROUP	COLUMNS	FORMAT	SYMBOL	DESCRIPTION
Q	1-5	I 5	N	Nodal point number.
	6-10	I 5	KODE(N)	See Section 4. If 0 or 1 it may be changed at later times by RESTART.
	11-20	E10.3	X(N)	x coordinate of node. This must be the horizontal coordinate in problems involving vertical flow.

GROUP	COLUMNS	FORMAT	SYMBOL	DESCRIPTION
	21-30	E10.3	Y(N)	y coordinate of node. This must be the vertical coordinate in problems involving vertical flow.
	31-40	E10.3	P1(N)	If INIT=0 in Group B, this is the initial value of ψ (with the appropriate sign) at node N. If INIT=1, this is the initial value of h at node N. May be changed at later times via RESTART.
	41-50	E10.3	Q(N)	Flux in (>0) or out (<0) of system at node N when KODE(N)=0, otherwise leave blank. If N is in root zone, leave blank. May be changed at later times via RESTART.

In general, one card must be provided for each node in sequential order, starting with N=1 and ending with N=NUMNP. If cards for succeeding nodes are omitted, the coordinates for the omitted points are generated by the program at equal intervals along a straight line connecting the specified points. The values of P1(N) at the omitted points are determined by linear interpolation between the specified points. KODE (N) and Q (N) are set equal to their values at the first specified point. For example, in Figure A-1, cards need only be punched for nodal points 17 and 21, and the program will generate the intervening nodes.

GROUP	COLUMNS	FORMAT	SYMBOL	DESCRIPTION
R	1-5	I 5	NUM	Sequential number of element
	6-10	I 5	KX (NUM,1)	Sequential number of i-th corner node.
	11-15	I 5	KX (NUM,2)	Sequential number of j-th corner node.
	16-20	I 5	KX (NUM,3)	Sequential number of k-th corner node.
	21-25	I 5	KX (NUM,4)	Sequential number of ℓ-th corner node.
	26-30	I 5	KX (NUM,5)	Sequential number of material whose hydraulic properties are to be assigned to element.
	31-40	E10.3	SANG (NUM)	Angle in degrees between K_{11}^{S} and the x coordinate, to be used in the element (see α in Figure A-2).

GROUP	COLUMNS	FORMAT	SYMBOL	DESCRIPTION

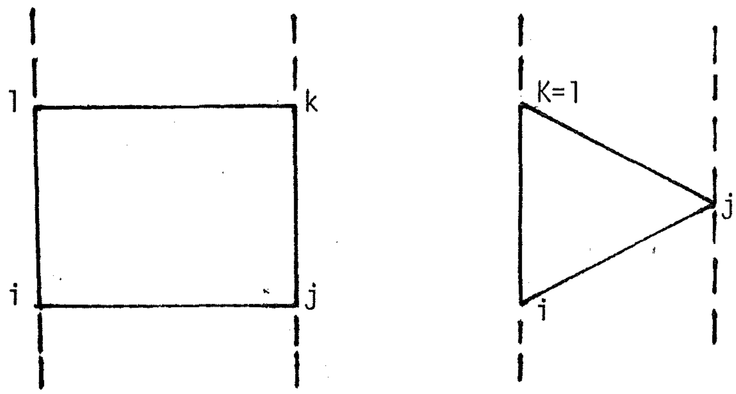

Fig. A-3. Numbering convention for element corner nodes.

Dashed lines indicate directions of transverse lines.

In general, one card must be provided for each element in sequential order, starting with NUM=1 and ending with NUM=NUMEL. However, wherever there is a sequence between two transverse lines that is composed entirely of quadrilateral elements all having the same hydraulic properties and angle α (see Figure A-23), it is only necessary to provide a card for the first element of the sequence, regardless of whether the enclosing transverse lines are straight. One card must always be provided for each triangular element, as well as for the last element in the mesh. For example, in Figure A-1 cards must be provided only for those elements whose numbers appear on the drawing.

GROUP	COLUMNS	FORMAT	SYMBOL	DESCRIPTION
S	1-3	A3	HED	If execution is to terminate when time is TMAX, punch END. If execution is to be continued beyond TMAX using the restart procedure, omit this group and punch Group RA instead.

In general, Group S is omitted when the boundary conditions are to be modified at TMAX without a pause in execution.

Restart Procedure

Whenever execution of the program terminates in a regular manner (i.e., not as a result of faulty input data or faulty operation), the results together with all necessary information are transferred to an input/output file labeled TAPE 1. If the user requests that this be a permanent tape or disc file, the problem can be restarted at a later date from the point where it stopped. When a restart is desired after a pause in execution, the original data deck (Groups A-S) must be deleted from the program and the seven groups described below introduced instead.

If Group S is omitted during the first run, the problem can be continued without a pause in execution by using the four groups of cards described below. In such a case, Groups RA - RG are placed after the cards of Group R in the data deck. If Group RG is also omitted, an additional set of Groups RA - RG can be placed at the end of the data deck, and this can be repeated as many times as desired. Thus, the data deck may have any of the following forms:

A - S

A - R, RA - RG

A - R, RA - RF, RA - RG

A - R, RA - RF, RA - RF, ..., RA - RG

RA - RF, RA - RF, ..., RA - RG

Each set of Groups RA - RF enables one to modify the boundary conditions at a selected number of nodes at prescribed values of time. In this manner, variable boundary conditions can be handled with or without a pause in the execution of the problem.

GROUP	COLUMNS	FORMAT	SYMBOL	DESCRIPTION
RA	1-7	A7	HED	Punch RESTART.
	9-80	18 A 4	HED	Desired heading to be printed with each time step.
RB	1-5	I 5	NTAPE	1 if information stored on first half of TAPE 1 is to be used upon restart; 2 if information stored on second half of TAPE 2 is to be used upon restart.
	6-10	I 5	NUMRES	Number of times Groups RC - RF are repeated without, at the same time repeating Groups RA and RB. It is recommended that NUMRES be set equal to zero.

GROUP	COLUMNS	FORMAT	SYMBOL	DESCRIPTION

The purpose of NTAPE is to enable one to restart the computation either where it last ended or where it ended during the previous run. In other words, one always has the option to repeat a complete run with modified input before continuing the computation.

Tape 1 is subdivided into two equal portions each of which is capable of storing all the information necessary for a restart. The first half of the file contains the information from the end of the previous run, whereas the second half contains the information from the end of the most recent run. To repeat a run with modified input data, NTAPE is set equal to 1. In this case the results of the computation are dumped on the second half of the file (erasing all previous information stored on the second half), whereas the information on the first half remains intact (for a possible additional repeat).

To continue the computation from the place where it ended last, NTAPE is set equal to 2. In this case all the information stored on the second half of the file is transferred to the first half (erasing all previous information from the first half). If the computation ends normally, the results are dumped on the second half of the file for future restart.

The purpose of NUMRES is to enable one to introduce variations in the boundary conditions at prescribed stages of the computation without changing the information on TAPE 1 during each such variation. It is usually safest to set NUMRES = 0 and in this manner update the file during each change in the boundary conditions.

GROUP	COLUMNS	FORMAT	SYMBOL	DESCRIPTION
RC	1-5	I 5	MAXIT	New value of MAXIT (see Groups B).
	6-15	E10.3	DD	New value of DT (see Group M). Leave blank if DT is to remain unchanged.
	16-25	E10.3	DTMAX	New value of DTMAX (see Group M).
	26-35	E10.3	DMUL	New value of DMUL (see Group M).
	36-45	E10.3	TMAX	New value of TMAX (see Group M).
	46-55	E10.3	TOL	New value of TOL (see Group M).
	56-65	E10.3	QP	New value of QP (see Group L).
	66-75	E10.3	ALFA	New value of ALFA (see Group L). (default = 0.8).

GROUP	COLUMNS	FORMAT	SYMBOL	DESCRIPTION
RD	Omit Group RD if NUMEP = 0 in Group C.			
	1-10	E10.3	EI	New value of EI (see Group F).
	11-20	E10.3	PL	New value of PL (see Group F).
	21-30	E10.3	BTPI	Factor by which the previous value of BTPI is to be multiplied (see Group F). Since BTPI changes during computation, it is recommended to set BTPI = 1.0.
RE	Omit Group RE if NPLNT = 0 in Group C.			
	The variables below have a free index, J. First set J=1 and then repeat all cards in Group RE for J=2,...,NPLNT, in sequential order.			
	1-5	I 5	NCJ	0 if RDF (K,J) (see Group J) remain unchanged; 1 if new values of RDF (K,J) are to be given below.
	6-15	E10.3	TPOT(J)	New value of TPOT(J) (see Group I).
	If NCJ = 1, punch the following cards:			
	1-10	E10.3	RDF(1,J)	New value of RDF(1,J) (see Group J).
	11-20	E10.3	RDF(2,J)	New value of RDF(2,J).
	.	.	.	
	.	.	.	
	.	.	.	
	71-80			
	Use as many cards as are needed to specify RDF(K,J) for K=1, NSOUR(J) + 1 (see Group J).			
	Group RE is repeated for each plant species in sequential order starting with J=1 and ending with J=NPLNT.			
RF	1-5	I 5	N	Node at which a change in boundary condition is to be introduced.
	6-10	I 5	NEWKOD	New value of KODE(N) (see Group Q).
	11-20	E10.3	VALUE	If KODE(N) = 0, VALUE is the new value of Q(N) at N. If KODE(N)=1, VALUE is the new value of ψ at N (see Group Q).

GROUP	COLUMNS	FORMAT	SYMBOL	DESCRIPTION

This card applies only to nodes having KODE(N) equal to 0 or 1 (not ±2 or -4). In general, one card must be provided for each node where a change in boundary condition is desired. The order of these cards can be arbitrary, but the last card in this group must always be blank. If all the boundary conditions are to remain unchanged, this group must include one blank card.

GROUP	COLUMNS	FORMAT	SYMBOL	DESCRIPTION
RG	1-3	A 3	HED	Punch END to indicate end of data deck.

The program can be restarted as often as is desired.

Output Data

The printed output of the program consists of a listing of all input information, a complete description of the finite element network, the boundary codes of all nodes, and the properties of each material. During each time step, the program prints a listing of total head values, pressure head values, moisture content values, and discharge into or out of the system (not flow through the system) at all nodes. The rate of convergence of the iterative procedure is printed during each time step together with additional information pertaining to the particular problem at hand.

Appendix B

Hydraulic Properties

of

Retorted Shale

LABORATORY METHODS AND PROCEDURES

Material Description

Capillary pressure-saturation and capillary pressure-permeability data were obtained for both disturbed and undisturbed specimens of processed oil shale.

Initially, loose oil shale retorted by the TOSCO II process was available but later material supplied by the U.S. Bureau of Mines from the Paraho process at Anvil Points near Rifle, Colorado was used in the disturbed sample testing. The undisturbed samples came from the filtration ponds at the Anvil Points site.

Disturbed retorted oil shale arrived at the laboratory presieved to 9.5 mm and finer. The unsieved sample contained sizes up to 89.0 mm but this fraction was not used. Because of the size of the test equipment, the 9.5 mm and finer was sieved to 2.0 mm and finer. The result was a black, sooty looking material that was fine enough to pack in the test apparatus. The sieving and packing procedure produced a fine black dust.

Undisturbed material in four core samples 66 cm long and 15.2 cm in diameter arrived at the laboratory in metal sleeves. They were plugged and sealed with plaster of Paris. The core material contained particles up to 38.0 mm but fines were compressed around the larger particles and did not seem to be cracked or fractured nor were there signs of cavities, fallout or excessive drying after the coring operation.

The specific gravity of all material was determined to be 2.68 after several tests on initially oven dry samples. The disturbed loose fines less than 2.0 mm averaged between 4 and 5 percent moisture by weight and freshly opened core samples varied around 18 percent. Standard dryness was taken to be after 60 minutes under a 150 watt lamp in an Ohaus Moisture Determination Balance.

Apparatus and Sample Preparation

Capillary Pressure-Saturation Equipment.

Laboratory apparatus used in this investigation was similar to that described by Sinclair (1973) and White (1968). A photograph of the capillary pressure cell used is at the right side of Figure B-1 and a schematic diagram of the apparatus is shown in Figure B-2. The apparatus provided a continuous column of water under a negative gage pressure from the permeameter membrane through a small brass fitting and flexible plastic tube to a meniscus in a glass indicator tube. This indicator tube was supported in the same horizontal plane as the center of the test specimen so that the capillary pressure applied to the specimen was the same as that measured in a mercury manometer connected to the air side of the tube. Since the sample size and porosity was known, it was only necessary to measure the specimen weight changes with pressure changes to obtain capillary pressure-saturation data.

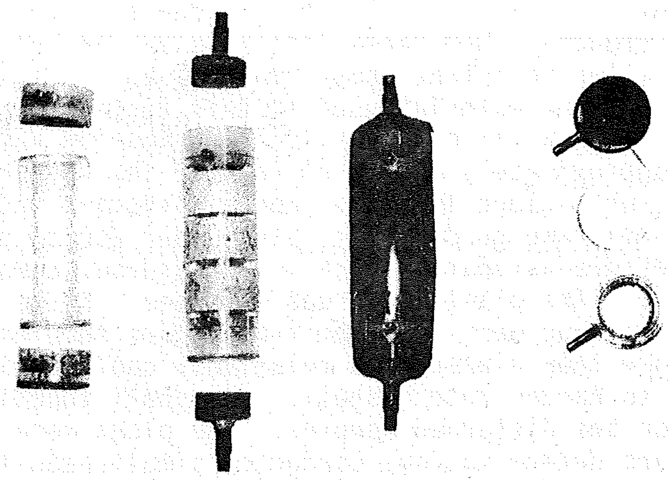

Figure B-1 Permeameters used in Disturbed Sample Tests

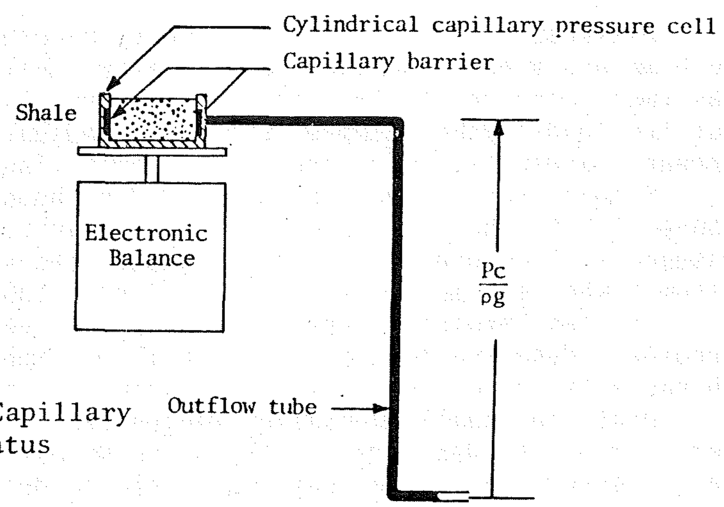

Figure B-2 Schematic of Capillary Pressure-Saturation Apparatus

Disturbed shale samples were packed into plastic cups made of 4.45 cm O.D. rigid plastic tubing with 0.65 cm walls and cut in 2.0 cm lengths. A milled 8 mm porvic membrane guide along with a deeper 4 mm channel allowed water to move through the membrane and brass fitting through the plastic tube into the glass indicator tube. Flat plastic end caps contained the sample but air vent holes were drilled in the cup to allow air to enter during saturation changes. Membranes, fittings and one end cap were secured and sealed with a water resistant epoxy resin glue.

Most of the membrane material used in this testing was "porvic paper", a plastic material with a narrow pore size distribution and an air entry pressure head of approximately 200 cm of water. The "paper" could be cut with scissors and, when glued in place, could withstand unsupported spans over channels and membrane guides up to 5 mm under 200 cm pressure head.

Capillary pressure-saturation data on undisturbed cores were obtained in a similar manner. The plastic cup was not used. Plugs 2.54 cm in diameter and about 5 cm long were cut from frozen core samples with a circular hole saw. They were then dipped into relatively cool liquid bee's wax which was allowed to harden into a shell. The shell functioned as the plastic cup did for the disturbed samples. The plugs were weighed before dipping and moisture determinations conducted simultaneously on alternate material so that the true dry density and volume could be fixed. The wax weight and density allowed for the determination of the wax volume.

The porous membrane for the "undisturbed" sample was in the form of a "porvic tip" secured in a groove cut into the wax shell. The tip was in contact with the shale sample. It was made of porvic paper wrapped around a small perforated tube approximately the size of a ball point pen refill and sealed with epoxy and wax.

Capillary Pressure-Saturation Sample Preparation and Testing.

Disturbed samples were prepared by packing dry retorted oil shale sieved to 2 mm and finer into capillary pressure cells. Undisturbed sample size was small compared to the size of the largest aggregate in the sample. Plugs cut from undisturbed samples which had unusually high density or which did not appear representative of the sample under visual examination were not used.

Samples were vacuum saturated in the apparatus shown in Figure B-3 before connection to the testing apparatus. An initial saturation condition was assumed at 1 cm pressure head. A stabilized saturation condition could be assumed when the meniscus in the indicator tube stopped after a pressure change.

The test procedure involved an initial desaturation, imbibition and secondary desaturation to produce a three limbed curve exhibiting hysteresis characteristics of the material as shown in Figure B-4.

Disturbed sample densities ranged from 65 to 100 pcf but reliable data were limited to densities in the 75 to 95 pcf. The undisturbed sample capillary pressure-saturation data were used to determine the core density and confirm the capillary pressure-saturation curve. Figure B-5 shows a comparison of capillary pressure-saturation data from undisturbed cores and from laboratory packed samples. The data plotted here for laboratory packed samples were arrived at by interpolating between the data for 85 pcf and 95 pcf to agree with the field density of 91.5 pcf. There is no significant difference between the two sets of data - probably because the large particles in the cores are permeable to water and under compaction there are few large voids.

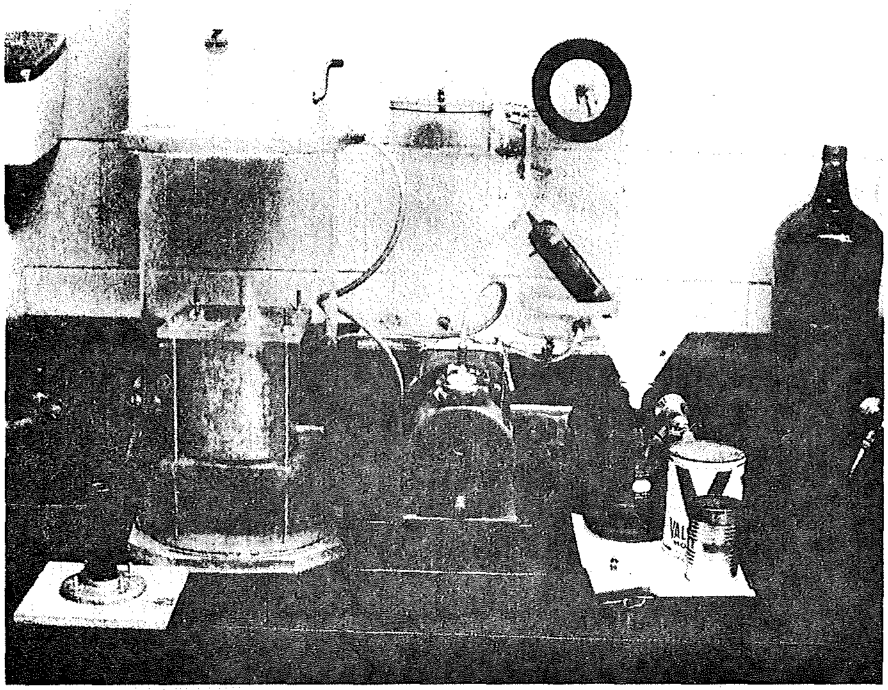

Figure B-3 Two Sets of Vacuum Saturation Apparatus

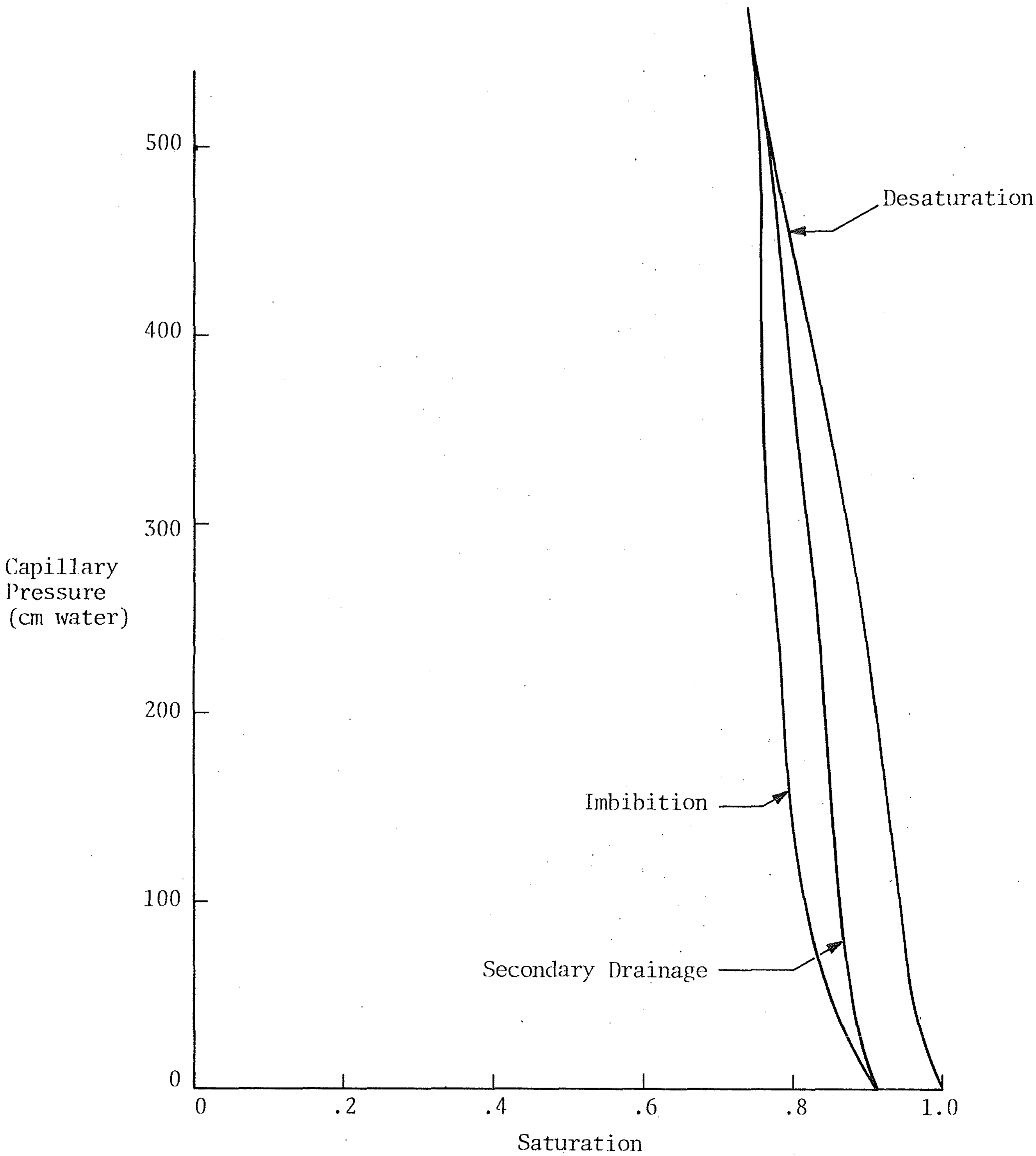

Figure B-4 Capillary Pressure Saturation Curve for 85 pcf Density

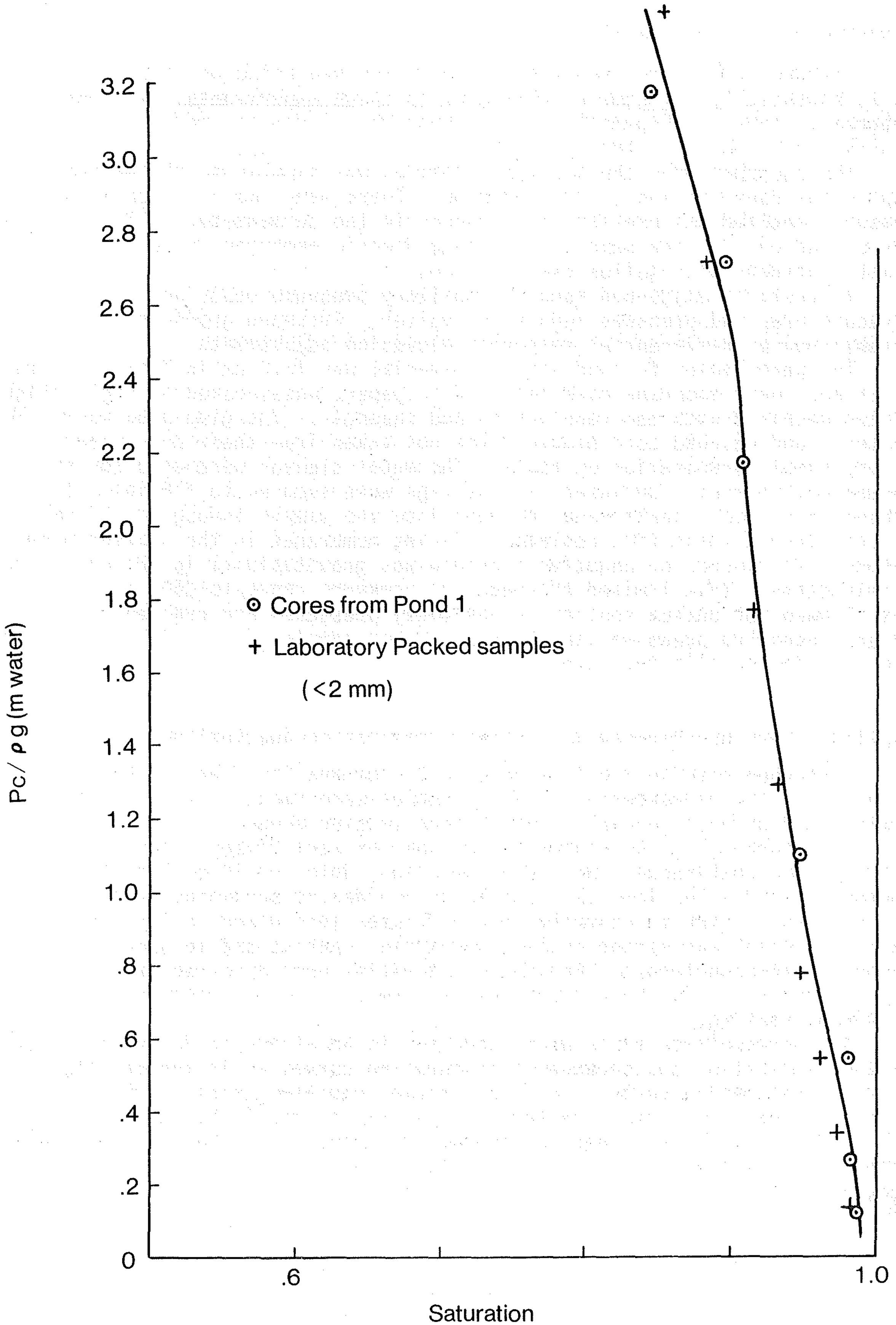

FIGURE B-5 Capillary Pressure-Saturation Data.

Capillary Pressure-Permeability Equipment.

Richards (1931) devised a permeameter for measuring unsaturated flow. It is essentially the same as that used in these experiments. A schematic diagram is shown in Figure B-6 and photographs of various parts are shown in Figures B-1 and B-7 through B-9.

The equipment for the disturbed samples was similar to the desaturation cup in the construction of the membrane. There were two ring membranes to measure longitudinal pressure differences in the permeameter. Flow into and out of the ends of the sample was through porvic membranes secured to machined plastic holders with hollow plastic stems.

In tests of disturbed samples capillary pressure heads were set using a vacuum pump and pressure regulating valves. Pressure gradients were established by differential reservoir elevation adjustments.

The permeameter for undisturbed material was 15.2 cm in diameter. The upper and lower membrane material, porvic paper, was secured to rigid plastic plates machined with membrane guides and channels. The glue used was silicone sealer. Undisturbed core samples were not taken from their core sleeves during sample preparation or tests. The metal sleeves were used for the permeameter barrel. Unglazed ceramic tips were secured to flexible plastic tubing by silicone sealer and inserted into the sample through drill holes in the sleeve; these tips replaced the ring membranes in the smaller permeameters. The source of negative pressure was gravitational in the undisturbed sample tests. This limited the negative pressure range to 250 cm of water but allowed for better control of capillary pressures and gradients. At greater negative pressures in the undisturbed samples, up to 2-1/2 days were required for equilibrium to be reached.

Capillary Pressure-Permeability Sample Preparation and Testing.

Disturbed retorted shale sieved to 2.0 mm and finer was packed dry in layers into the permeameters. These samples were vacuum saturated with a minimum four hour soaking period before testing began.

Undisturbed 15.2 cm diameter core samples were frozen, then sectioned with a slow, continuous band power hack saw. Holes on 10 cm longitudinal centers were drilled into the cylinders in order to accomodate the ceramic tip inserts. Prior to clamping the end plates into place, a layer of fine retort material was spread to improve barrier contact and to protect the membrane from punctures. The vacuum saturation procedure required three days including a four hour period of air removal with no water added and a 48 hour soaking.

The permeability tests were conducted in an effort to determine desaturation, imbibition and secondary desaturation curves as in the capillary pressure-saturation tests. To have constant capillary pressure over the length of the core it is necessary to maintain hydraulic head gradients of $h/L = 1.0$. Flux measurements were made by timing an air bubble as it moved through a calibrated glass tube. The last of a set of multiple readings provided a measurement of steady state conditions.

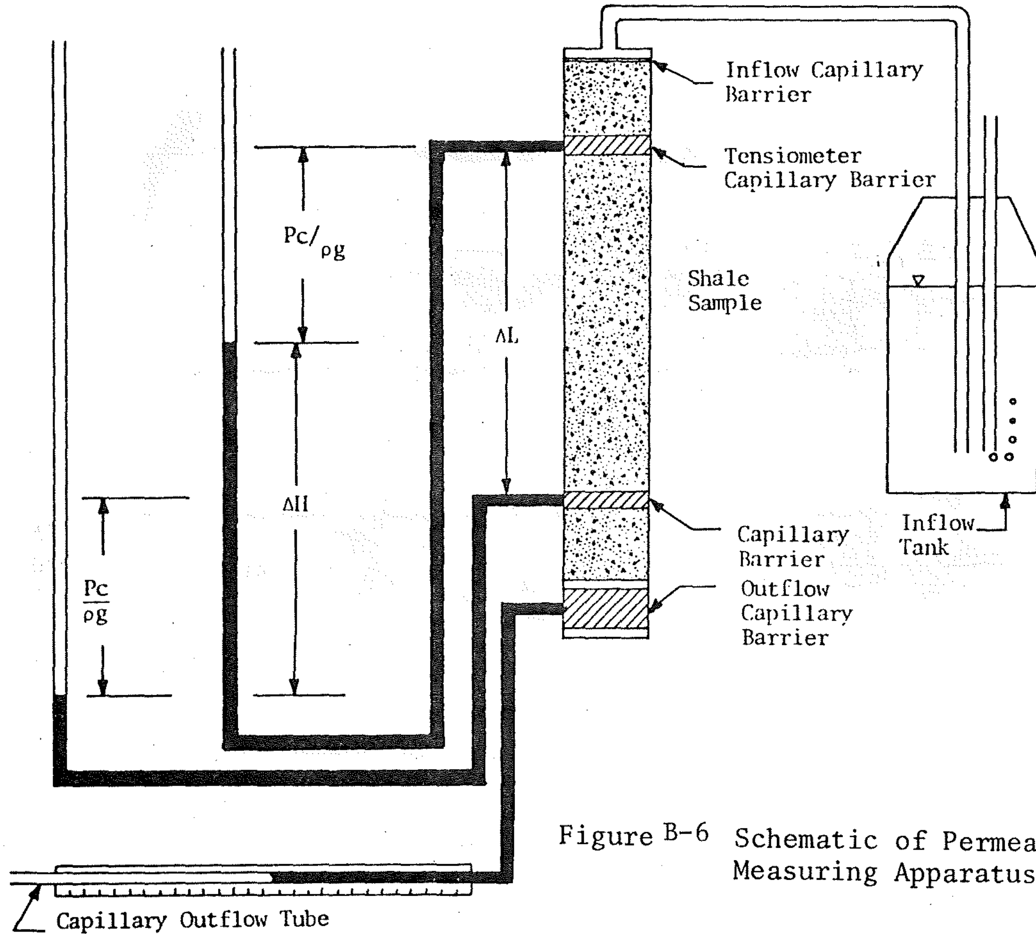

Figure B-6 Schematic of Permeability Measuring Apparatus

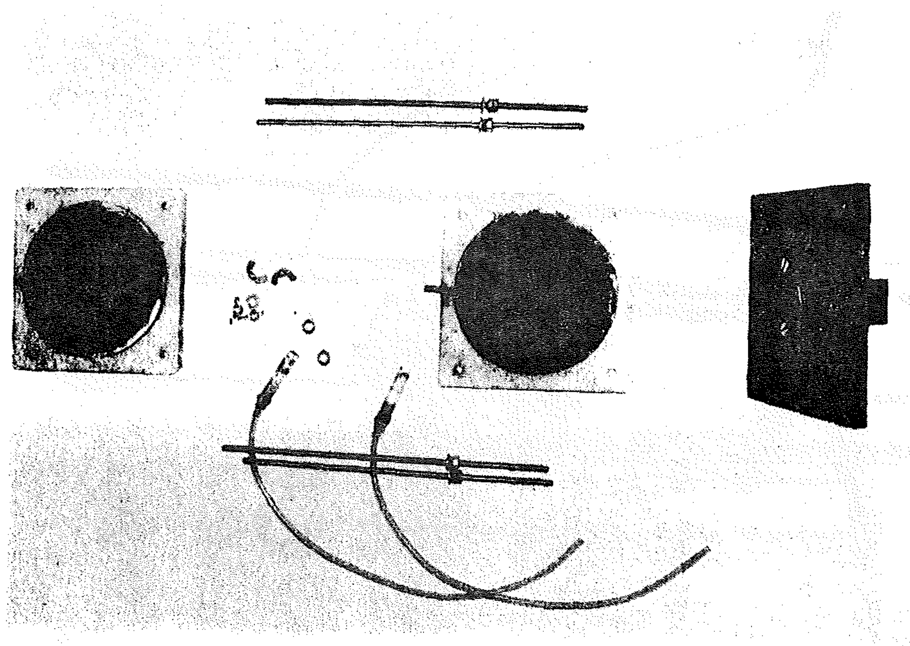

Figure B-7 Components of Undisturbed Permeameter Apparatus

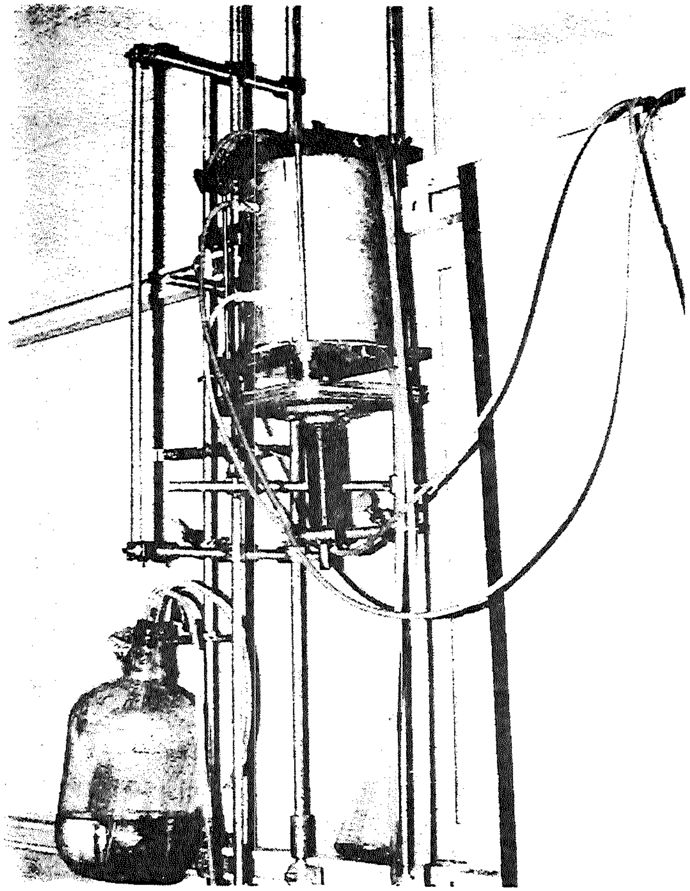

Figure B-8 Undisturbed Permeameter mounted on the Wall

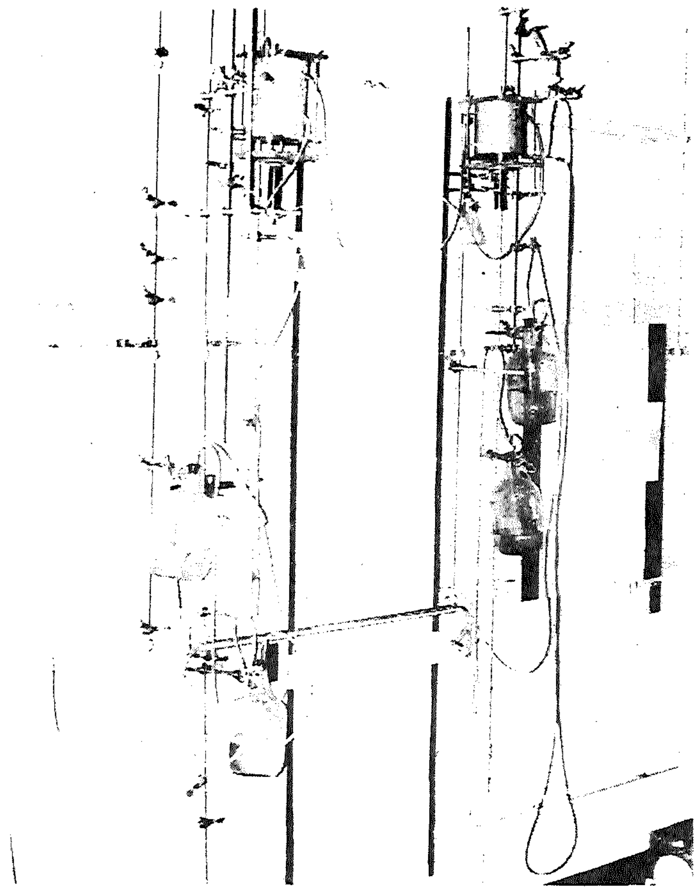

Figure B-9 Two Sets of Gravity Type Permeability Test Apparatus

Discussion of Laboratory Procedures

Porvic paper was convenient to use for capillary barriers but was subject to pin hole punctures and crushing. End barriers, unlike ring barriers, must provide a uniform flow path and must offer a minimum of flow resistance in the working range of pressures. An alternative to the paper was ceramic plate but this material is brittle, difficult to form and not readily available in diameters up to 15.2 cm.

Disturbed capillary pressure-saturation data were taken on material sieved to 2.0 mm and finer. This was a compromise to accomodate the shale in the small test apparatus, avoid damage to the membrane and to allow for uniform packing. As previously mentioned and shown in Figure B-5, data obtained from the laboratory packed samples compares well with data from undisturbed cores.

Permeability tests could be completed on disturbed material in four to five days but undisturbed specimens were larger and required longer stabilization periods. Over long periods, leaks in the system and air coming out of solution caused blockage of the small tubes and loss of head. The solution was to install larger tubing and gas traps at critical points. Bacteria began to grow in the specimen and apparatus but phenol added to the water stopped this tendency. The addition of phenol did change surface tension values from 60.2 to 58 dynes per cm. This difference was assumed to be insignificant.

Water was the saturating fluid for all of these experiments. Sinclair (1973) reported that hydrocarbon based fluid caused significant changes in the structure of undisturbed agricultural soils. This may not have occurred in processed oil shale but some of the samples already contained up to 18 percent moisture. A less dense fluid would have narrowed the range of pressures available in the gravity apparatus.

Long stabilization periods would have been reduced with smaller samples but trimming the diameter seemed questionable and shortening the sample seemed inadvisable because of the size of the capillary pressure membrane. An alternative to the radial membrane was a 2.0 mm porous ceramic chip mounted on the end of a small tube. It could be inserted through an access hole to the center of the specimen. This may have caused non-uniform pressure gradients, provided poor specimen contact, and in the end, not significantly shortened the stabilization period.

One must preface the term "undisturbed" by the term "relatively". Coring and casing compromise the "undisturbed" status of the natural profile. Freshly opened, undisturbed shale core samples contained about 18 percent moisture and were relatively strong. Drying caused the samples to weaken and disintegrate. Freezing the cores before cutting and with little lateral support, undoubtedly caused some macro- and micro-changes in the structure. Freezing did reduce mechanical damage in the sectioning process. The vacuum saturation procedure could cause damage by producing internal pressure gradients if the evacuation from a vacuum saturation chamber occurred too fast. The chambers were slowly evacuated in a dry chamber over a 30 minute period, flooded after four hours and allowed to return to atmospheric pressure over night.

The concept of conducting unsaturated permeability tests with atmospheric air pressure surrounding the sample is not representative of conditions in the profile. The method does shorten the reaction time. The alternatives involve using more complex equipment or an attempt at insitu tests with some of the methods described in the literature.

Discussion of Laboratory Results

The results of laboratory determination of hydraulic properties for retorted shale are presented in the following pages.

Saturated Conductivity.

Saturated conductivity values are given in Table B-1 and Figure B-10. The values used in the simulation of the seepage ponds for Phase II were basically field values. The values used in all Phase III work were those from the regression line given in Figure B-10 for laboratory samples. The correlation coefficients for both the regression lines were 0.98. However, certain individual measurements differ from the line by as much as 100%, and in fact one core from Pond 1 tested by Woodward-Clyde Consultants (1977) had a hydraulic conductivity corresponding more to the field values than to the laboratory measurements. This particular value was not used in either regression analysis but does give an indication of why field measured values were considerably greater than the majority of laboratory values.

It is somewhat surprising that laboratory packed samples compare as well as they do with cores taken in the field when the difference in packing technique is considered. The laboratory packed samples were prepared dry and tamped in five to ten layers to achieve the desired density. The undisturbed material was spread, moistened, vibrated and rolled when the profiles were constructed. Laboratory sieving of the disturbed material separated a large portion of plate-like particles. Similarly shaped particles were in the fraction passing the sieve. The method of deposition undoubtedly affects the particle orientation which could have a large effect on saturated conductivity.

Capillary Pressure Saturation.

Previously, in Figure B-4 the capillary pressure-saturation curves (drainage, imbibition and secondary drainage) were given for a density of 85 pcf. In applying these relationships to a field situation it must be recognized that vacuum saturated conditions do not occur in the field. There will always be trapped air unless water pressures greater than atmospheric have existed for several months. This would certainly not be the case in problems such as considered in Phase III for flow due to rainfall and evaporation. Therefore the secondary desaturation data were used in all the analysis in Phase III. The data for the various densities of shale and sand used in Phase III are given in Tables B-2 through B-5 and in Figure B-11. The data in these tables were all obtained from laboratory packed samples.

Table B-1. Saturated Hydraulic Conductivity for Waste Shale

(Water at 10°C)

		Laboratory Data		Field Data	
Porosity	Density (pcf)	K(m/yr)	Source	K(m/yr)	Source
.453	91.5			200.	Field
.453	91.5			170.	measure-
.453	91.5			68.9	ments
.453	91.5			41.1	Pond 2.
.398	100.6			5.51	Field
.398	100.6			2.70	measure-
.398	100.6			2.40	ments
.398	100.6			1.91	Pond 1.
.398	100.6			6.49	
.552	75	31.38	Laboratory Packed Samples - U of I		
.492	85	8.06			
.453	91.5	.914			
.425	96.2	.241			
.398	100.6	.0914	Cores from Pond 1 - Tested by Woodward-Clyde		
.398	100.6	.0320			
.376	104.3	.0122			
.342	110.0	1.46	Not used in Figure 4 nor in linear regression.		
.493	84.8	1.81	Core from Pond 1 - Tested at U of I		

Regression equations

Laboratory Samples: $\text{Log } K = 19.07\phi - 8.99$

Field Values: $\text{Log } K = 28.15\phi - 10.76$

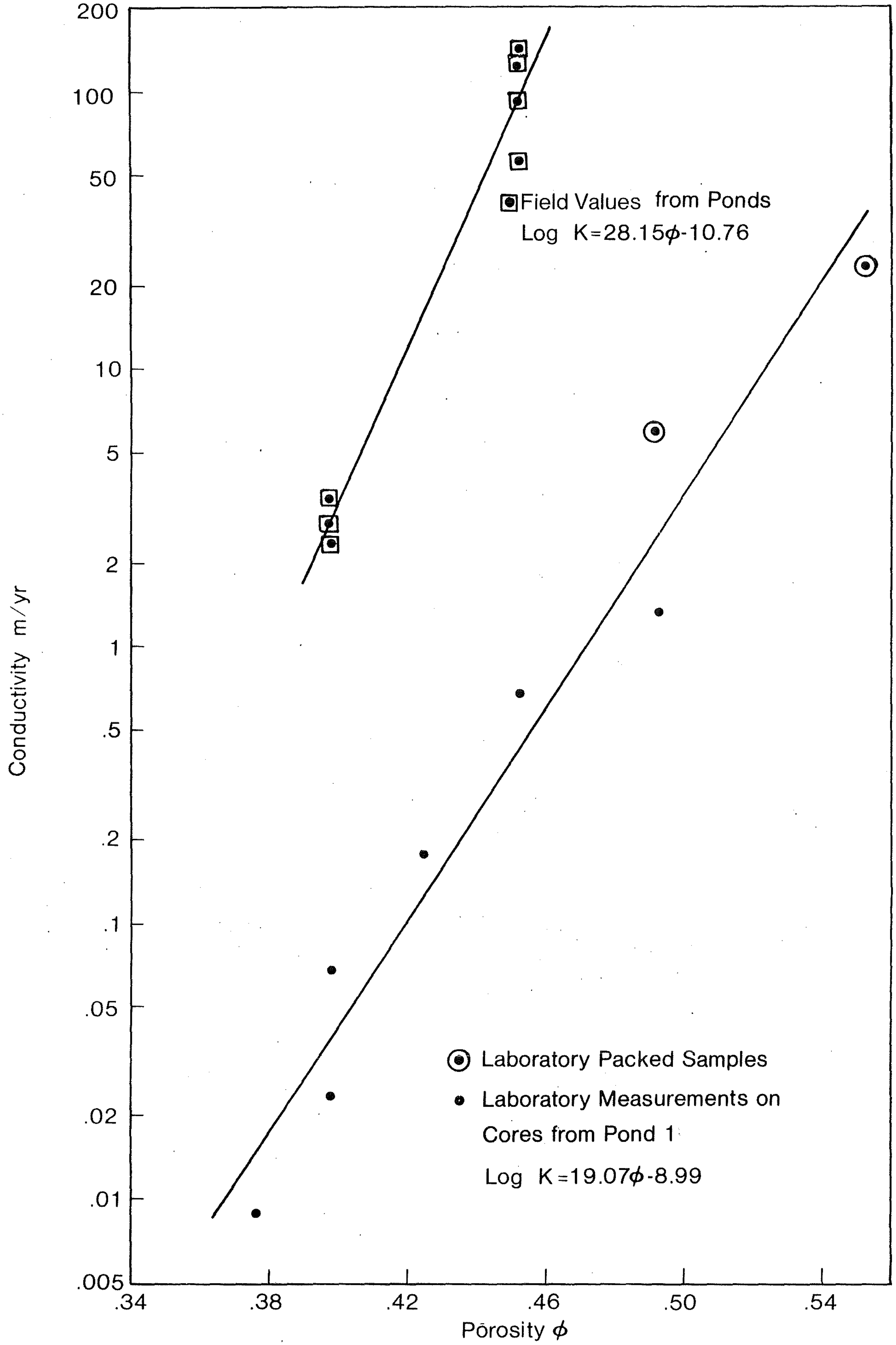

FIGURE B-10 Conductivity vs Porosity for Retorted Shale (with water at 10°C)

Table B-2. Processed Oil Shale

Permeability-Capillary Pressure-Saturation Data,

75 PCF Density

Capillary Pressure (meters)	Secondary Desaturation	Moisture Content	Relative Permeability
0.000	0.850	0.468	1.000
0.136	0.836	0.460	0.987
0.570*	0.785*	0.431	0.841*
1.084	0.742	0.408	0.450
1.354	0.725	0.399	0.353
1.762	0.700	0.385	0.265
2.033	0.687	0.378	0.226
2.507	0.667	0.367	0.180
2.710	0.660	0.363	0.165
3.252	0.640	0.352	0.136
3.726	0.627	0.345	0.117
4.336	0.598	0.329	0.099
4.810	0.582	0.320	0.089
150.000**	0.050	0.028	0.002

$K_o = 6.716 \times 10^{-3}$ m/hr

$\phi = .550, \ \phi_e = .468$

* Smoothed Value

** Dummy Value

Table B-3. Processed Oil Shale

Permeability-Capillary Pressure-Saturation Data

85 PCF Density

Capillary Pressure (meters)	Secondary Desaturation	Moisture Content	Relative Permeability
0.000	0.910	0.447	1.000
0.136	0.900	0.442	0.987
0.338	0.888	0.436	0.951
0.570*	0.875*	0.430	0.841
0.779	0.867	0.426	0.645
1.287	0.855	0.420	0.373
1.761	0.847*	0.416	0.265
2.710	0.828	0.407	0.165
3.388	0.808	0.397	0.130
4.066	0.785*	0.385	0.106
4.743	0.770	0.378	0.089
5.081	0.763*	0.375	0.083
5.419	0.752	0.369	0.077
5.758	0.737	0.362	0.073
150.000	0.050	0.025	0.002

$K_o = 4.224 \times 10^{-4}$ m/hr

$\phi = .491$, $\phi_e = .447$

* Smoothed values

Table B-4. Processed Oil Shale

Permeability-Capillary Pressure-Saturation Data

95 PCF Density

Capillary Pressure (meters)	Secondary Desaturation	Moisture Content	Relative Permeability
0.000	0.925	0.399	1.000
0.250	0.924	0.391	0.963
0.580*	0.922*	0.398	0.841*
1.000	0.918	0.365	0.491
2.000	0.910	0.393	0.231
3.000	0.903	0.390	0.148
3.370	0.900	0.389	0.131
4.500	0.883	0.381	0.095
5.750	0.865	0.374	0.073
150.000**	0.050	0.022	0.002

$K_o = 2.657 \times 10^{-5}$ m/hr

$\phi = 0.4319$, $\phi = 0.399$

* Smoothed value

** Dummy value

Table B-5. Poudre Sand

Permeability-Capillary Pressure-Saturation Data[1]

Capillary Pressure (meters)	Saturation	Moisture Content	Relative Permeability
0.230	1.000	0.396	1.000
0.350	0.990	0.392	0.950
0.368	0.980	0.388	0.904
0.391	0.970	0.384	0.750
0.408	0.900	0.356	0.578
0.429	0.870	0.345	0.422
0.508	0.610	0.242	0.094
0.663	0.420	0.166	0.010
0.759	0.350	0.139	0.003
0.849	0.290	0.115	0.001
150.000**	0.050	0.050	1.650 E-15

$K_o = 9.498 \times 10^{-2}$ m/hr

$\phi = \phi_e = 0.396$

[1]From McWhorter, D.B., 1971. Infiltration affected by flow of air. Hydrology Paper #49, Colorado State University, Fort Collins, Colorado.

** Smoothed value

FIGURE B-11

CAPILLARY PRESSURE —SATURATION DATA

DATA FROM DISTURBED SHALE SAMPLES

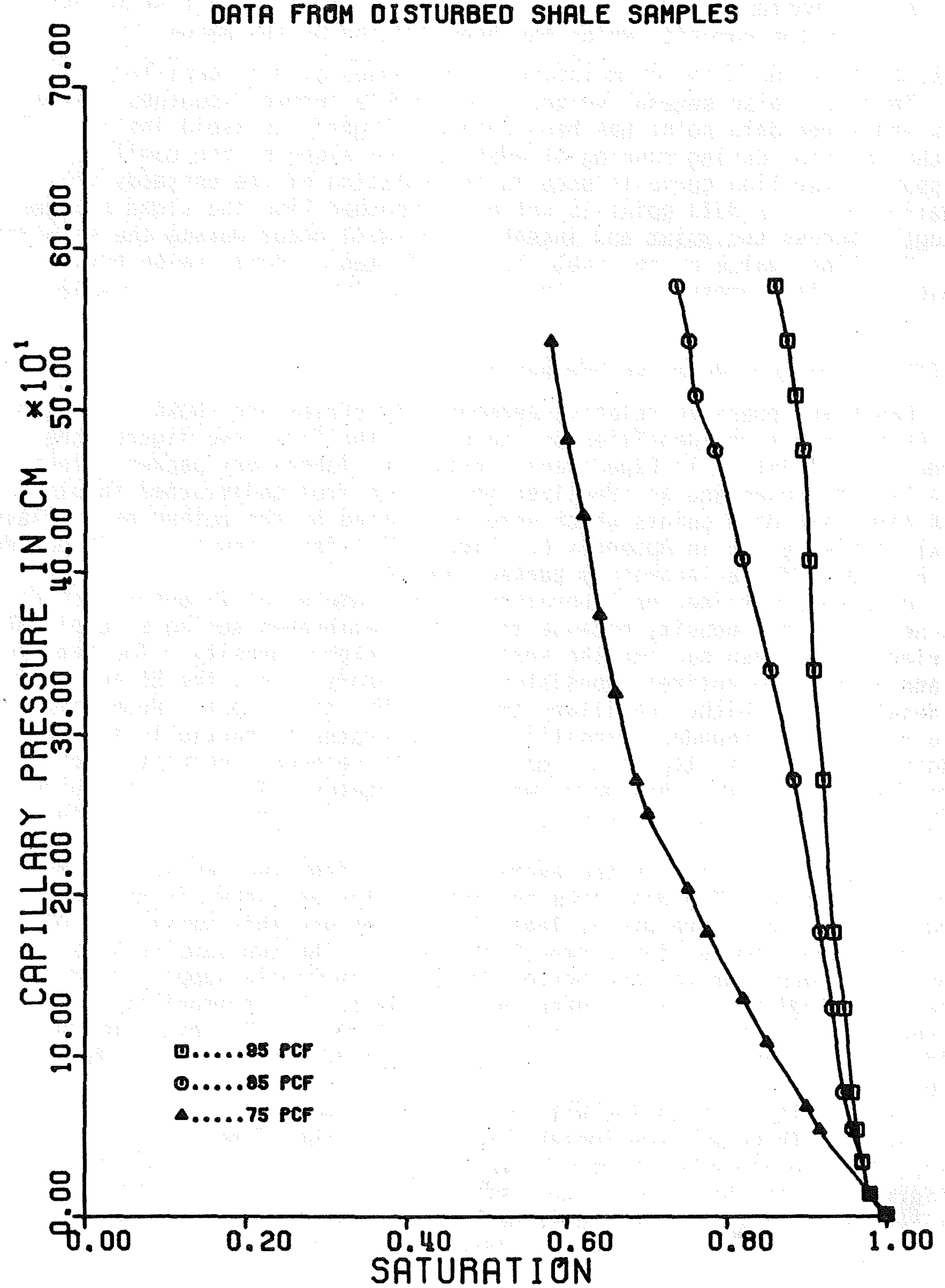

Concerning the accuracy of the data, each of the curves in Figure B-11 are the average of at least 3 independent samples of which the maximum variation of data from the line given is about ±5 percent.

At the bottom of each table a value is given for effective porosity, ϕ_e. This is the porosity which has been reduced by the amount of trapped air. Thus, this is the value of moisture content used at zero capillary pressure.

There are also several values in the table termed "smoothed" values. This means the data point has been changed slightly to avoid instabilities in the solution during running of UNSAT2. The slope of the capillary pressure-saturation curve is used in the solution of the unsteady flow equation and if a data point is not on a smoothed line the slope changes abruptly across the point and instabilities will occur during the solution.

The final value of the table is a predicted or dummy value put in at a high capillary pressure such that there is always a value with which to interpolate.

Capillary Pressure Relative Permeability.

Capillary pressure relative permeability curves are shown in Figures B-12, 13, 14 for the three densities of shale. In the first two figures there are three sets of data: 1) Experimental data from laboratory packed columns, 2) A line representing an idealized mean value from undisturbed samples and 3) A line with data points which were calculated by the method of Sinclair et al. (1974) given in Appendix C. Figure B-14 for a density of 95 pcf does not have data for a laboratory packed sample.

Data were obtained on laboratory packed samples at 75 and 85 pcf densities but not at 95 pcf density because the porous membranes acting as capillary barriers broke when packing the shale to the higher density. The data for 75 and 85 pcf are entirely consistent with theory, i.e., the 85 pcf begins to desaturate at higher capillary pressure than the 75 pcf. Both sets of data show a very rounded transition from saturated to partially saturated conditions. This is typical of material with secondary porosity such as agricultural soil that has pores within aggregates. The shale has pores within particles. The accuracy of these data is estimated to be within ±10%.

The idealized mean is the average of data from two samples of the same core from Pond 1. The data from the two samples are shown in the inserts in Figure B-15. Each core was at least 66 cm long and this particular one was cut into three samples for permeability tests. The two samples shown in Figure B-15 were the top and bottom samples; the middle sample was discarded because biological growth occurred which reduced the permeability. As can be seen the data for the two samples are different. This could be due to a difference in density as samples from the various cores did vary from 87 to 98 pcf.

The density also varied with the amount of water which had flowed through the sample. There was considerable material leached from the cores and when the effluent evaporated there was considerable residue. Because of the difference in the handling of the shale between the cores and the laboratory samples it was felt that the data were not sufficiently representative of shale packed into waste piles to differentiate between various densities for

FIGURE B-12

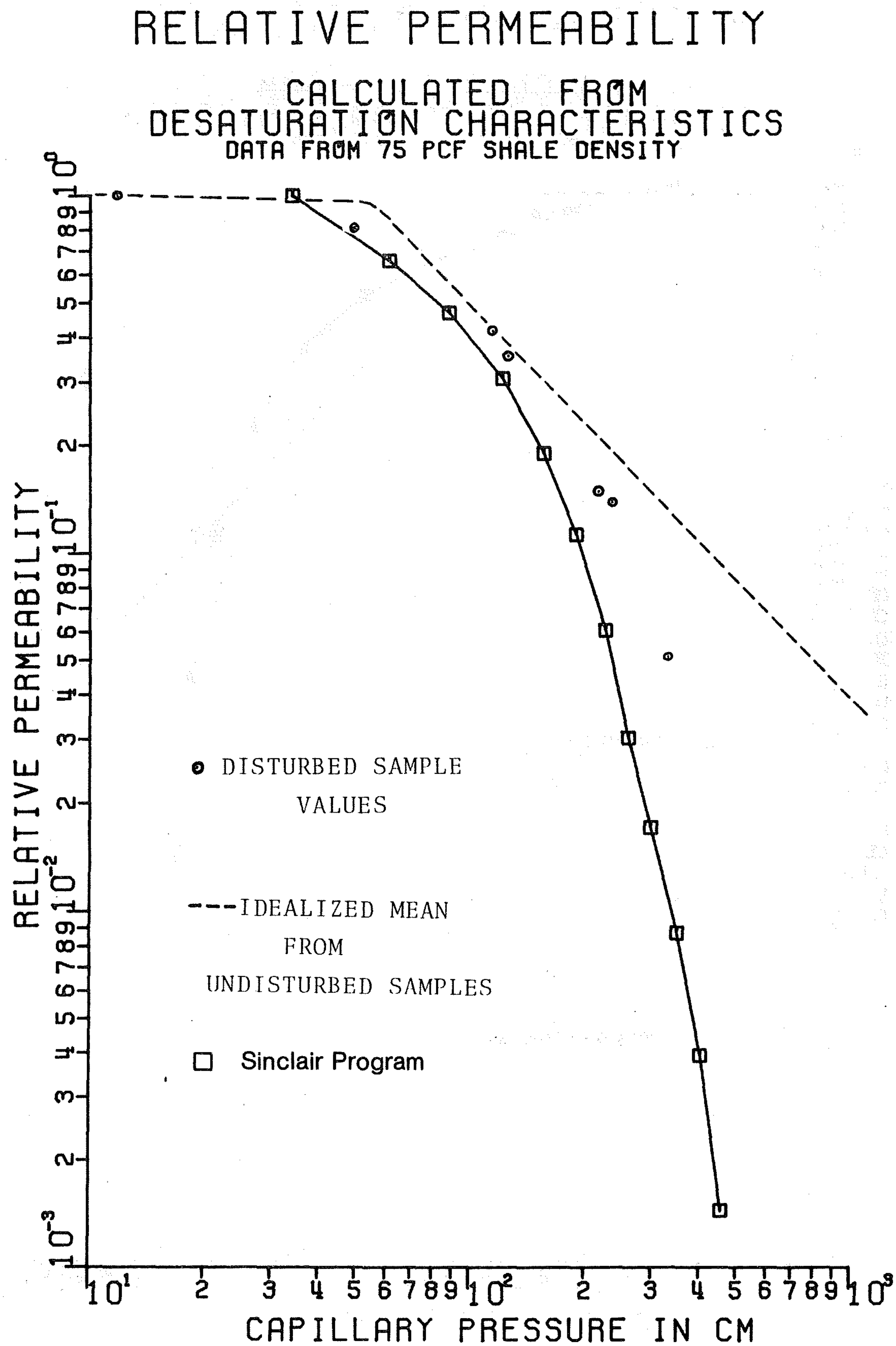
RELATIVE PERMEABILITY
CALCULATED FROM
DESATURATION CHARACTERISTICS
DATA FROM 75 PCF SHALE DENSITY
RELATIVE PERMEABILITY
CAPILLARY PRESSURE IN CM
DISTURBED SAMPLE VALUES
---IDEALIZED MEAN FROM UNDISTURBED SAMPLES
Sinclair Program

FIGURE B-13

RELATIVE PERMEABILITY

CALCULATED FROM DESATURATION CHARACTERISTICS

DATA FROM 85 PCF SHALE DENSITY

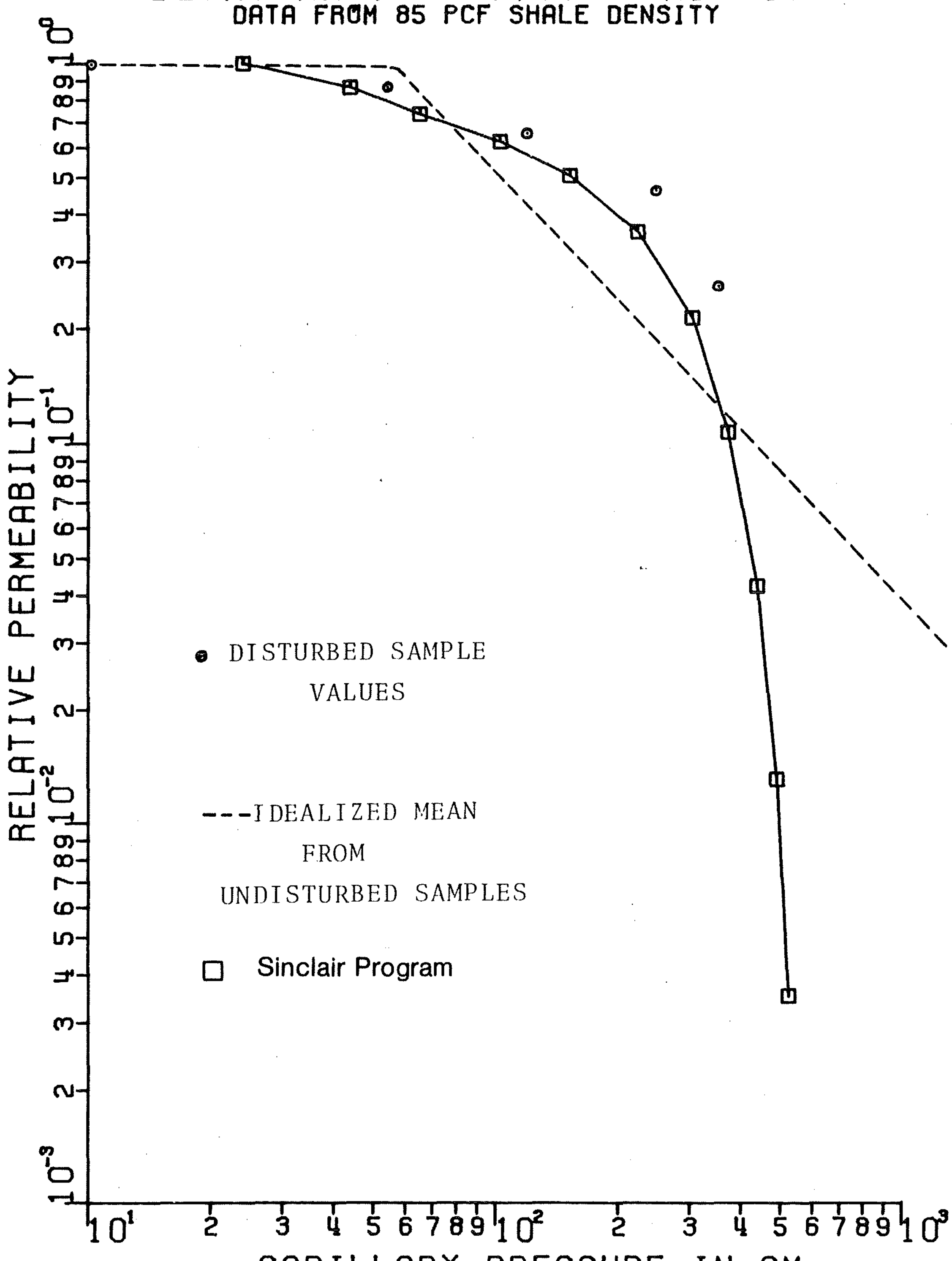

FIGURE B-14

RELATIVE PERMEABILITY

CALCULATED FROM DESATURATION CHARACTERISTICS

DATA FROM 95 PCF SHALE DENSITY

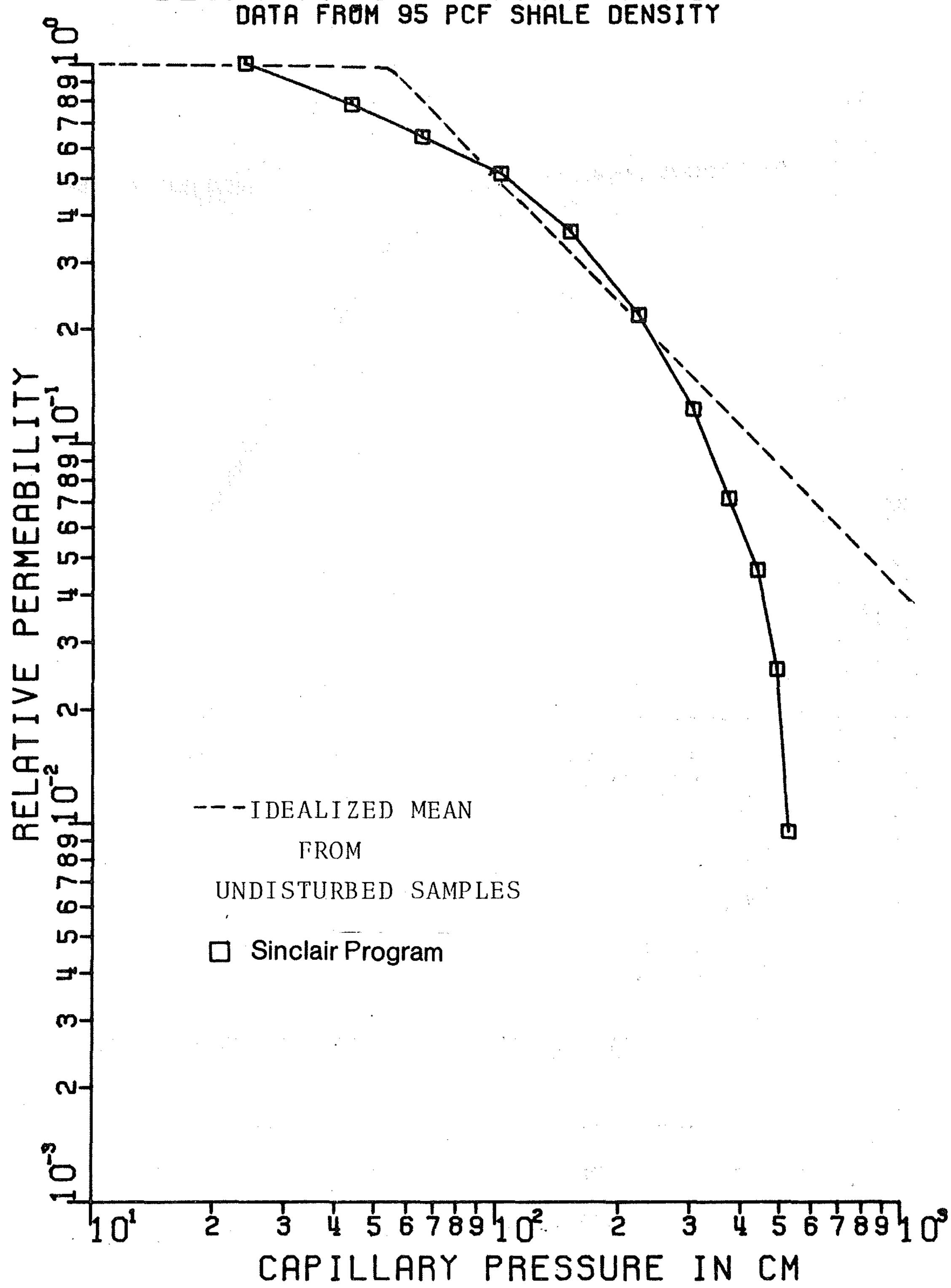

FIGURE B-15

UNDISTURBED SAMPLE PERMEABILITY VALUES

EXPERIMENTAL RESULTS

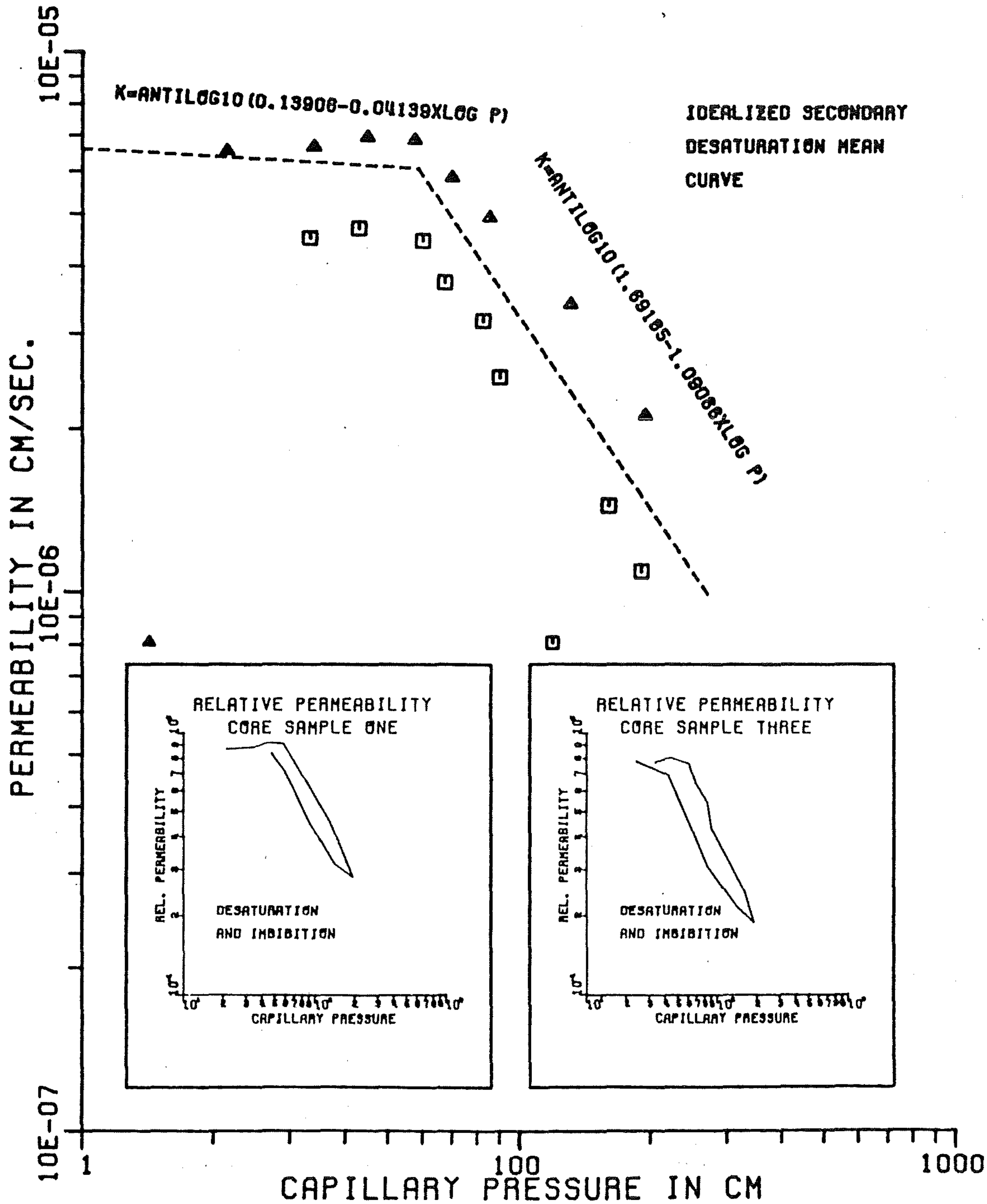

the relative permeability curves. Thus the mean of the two curves was used in all work in Phase III. The relative permeabilities given previously in Tables B-2 through B-4 are also from this average curve of the two undisturbed core samples.

The calculated curve on Figures B-12 through 14 is that calculated from capillary pressure-saturation data by use of the Sinclair program. Because of the difficulty in measuring the relative permeability it is desireable to simply calculate the relative permeability from capillary pressure-saturation data. This line compares very well with the experimental data for 75 and 85 pcf densities. For 95 pcf density there are no data to compare with; however, the line for 95 pcf is to the left of the line for 85 pcf up to about 400 cm capillary pressure head. This is contrary to theory and the reason is not known. Some of the assumptions in the Sinclair development are not well satisfied by shale and this could be part of the problem. The method of calculating relative conductivities of Su and Brooks (1976) was also tried here but it did not work as well as the Sinclair program.

For purposes of design of shale piles we feel the Sinclair program is sufficiently accurate if only the relative conductivity is calculated. The value of saturated conductivity calculated by the program is not accurate, but if the saturated conductivity is measured and the relative conductivity is calculated the data will be at least within engineering accuracy.

In summary, the data for hydraulic properties of retorted shale given in this document is the best currently available and the accuracy is comparable and in many cases better than that usually used in groundwater studies.

Appendix C

Sinclair Program

Documentation and User Instructions

Sinclair Program for Calculating Relative Conductivity

This program is based on theory of Brooks and Corey (1964) relating capillary pressure to size of pores in which interface between air and water are occurring. This equation is

$$Pc = \frac{2\sigma \cos \alpha}{r} ,$$

where σ is surface tension of water in contact with air, α is the contact angle between the air-water interface and the surface of soil particles, and r is the radius of curvature of the interface. If the contact angle is zero, the radius of curvature is essentially the radius of the pore. Using this and the Kozeny-Carmen hydraulic radius theory of permeability, the following equation can be developed for effective permeability:

$$k_e = \frac{\phi r^2 \cos^2\alpha}{k_s T_s} \int_o^S \frac{dS}{P_c^{\,2}}$$

where k_e is permeability at saturation, S, ϕ is porosity, k_s is a pore shape factor (assumed to be 2.5), T_s is tortuosity at saturation, S, and P_c, σ, and α were previously defined. Since there are some rather arbitrary factors in the above equation, the calculation of k_e can be somewhat in error. However, if the relative permeability is considered

$$k_r = \frac{k_e}{k_{sat}} = \frac{\dfrac{\phi\sigma^2\cos^2\alpha}{k_s T_s} \displaystyle\int_o^S \frac{dS}{Pc^2}}{\dfrac{\phi\sigma^2\cos^2\alpha}{k_s T_s} \displaystyle\int_o^1 \frac{dS}{Pc^2}}$$

several of the more arbitrary factors cancel out and we are left with the Burdine equation:

$$k_r = \frac{S-Sr}{1-Sr} \; \frac{\displaystyle\int_o^S \frac{dS}{P_{c^2}}}{\displaystyle\int_o^1 \frac{dS}{P_{c^2}}}$$

These equations are then integrated numerically in the computer program. Relative permeability and relative conductivity as used in UNSAT2 are identical since saturated conductivity and saturated permeability differ by the same constants as effective conductivity and effective permeability.

Data cards for the program are as follows:

GROUP	COLUMNS	FORMAT	SYMBOL	DESCRIPTION
A	1-5	I 5	ND	Number of pairs of saturation-capillary pressure data points.
	6-10	F10.3	POR	Porosity of the soil.
	11-20	F10.3	SR	Residual saturation--the value of saturation that is approached asymtotically at high capillary pressures.
B	1-10	F10.3	T_i	The saturation values are first entered starting with the smallest values. There are ND values. The corresponding capillary pressure values are then entered in the same order.
		.	.	
	11-20	.	.	
	.	.	.	
	.	.	T_{ND}	
	.	.		
	.	.	.	
	.	.	P_j	There are 8 values on each card and it is not necessary to start P_j on a new card.
	.	.	.	
	71-80	F10.3	P_{ND}	

The largest value of saturation is at zero capillary pressure, however, zero will cause difficulty in running the program and a value of $P_c = .01$ should be used to correspond to a saturation of 1. It is usually best to have two data values at small capillary pressures because the program attaches a relative permeability value to the average of the two points.

The data output consists of a table of values of moisture content, capillary pressure, average capillary pressure, average pore radius, and number of pores and another table of average capillary pressure, permeability, and relative permeability or relative conductivity.

The program is as follows:

```
//RDW  EXEC FORTGCLG
//FORT.SYSIN DD *
C
C  PROGRAM FOR CALCULATION OF RELATIVE PERMEABILITY FROM SATURATION DATA
C
C  PROGRAM WILL TAKE UP TO 50 VALUES EACH FOR SATURATION AND PRESSURE HEA
C
C  T=SATURATION EXPRESSED AS A DECIMAL, LATER AS A MOISTURE CONTENT
C  P = PRESSURE HEAD IN CENTIMETERS OF WATER
C  F = NUMBER OF PORES BETWEEN TWO CLASSES OF SATURATION
C  PA = AVERAGE PRESSURE HEAD FOR SATURATION CLASS
C  R = PORE RADIUS CORRESPONDING TO A GIVEN PRESSURE HEAD
C  RA = AVERAGE PORE RADIUS, IN CENTIMETERS, OF SATURATION CLASS
C  ND = NUMBER OF POINTS USED TO REPRESENT SATURATION CURVE
C  SR RESIDUAL SATURATION
C
      DIMENSION T(52),P(52),F(50),PA(52),RA(50),R(50),TA(52) ,
     1RPERM(52),PERM(52),WS(52)
   42 FORMAT (I2)
      IL=-1
  490 READ (5,100) ND,POR,SR
      LL=ND+2
      M=ND
      NN=ND+1
      READ (5,203) (T(I),I=1,ND),(P(J),J=1,ND)
       WRITE (6,203) (T(I),I=1,ND),(P(J),J=1,ND)
      DO 40 I=1,ND
      WS(I)=T(I)
      T(I)=T(I)*POR
   40 CONTINUE
      ND=ND-1
      WRITE (6,300)
  300 FORMAT(1X,'MOISTURE',T15,'PRESSURE',T27,'AVERAGE',T39,'AVERAGE RA
     1IUS',T60,'NUMBER OF PORES')
      DO 10 N=1,ND
C CALCULATE AVERAGE PRESSURE AND RADIUS FOR EACH CLASS OF SATURATION
       PA(N) = (P(N)+P(N+1))/2
      RA(N) =  .1228/PA(N)
      TA(N) =  (T(N)+T(N+1))/2
C CALCULATE MOISURE CONTENT AND PRESSURE CHANGE FOR EACH SATURATION CLA
      DT = T(N+1)-T(N)
      DP = (1./P(N+1))-(1./P(N))
C CALCULATE THE NUMBER OF PORES IN EACH SATURATION CLASS
      F(N)= .648*DT/(DP*RA(N)**2)
   10 WRITE (6,200)T(N),P(N),PA(N),RA(N),F(N)
  200 FORMAT(1X,3F10.3,5X,E15.8,5X,E15.8)
      ND=ND-1
      FNORM=0
C CALCULATE THE AREA UNDER THE FREQUENCY CURVE TO NORMALIZE THE CURVE
      DO 11 N=1,ND
      SUM =((RA(N+1)-RA(N))/2)*(F(N)+F(N+1))
   11 FNORM =FNORM+SUM
      WRITE (6,301)
  301 FORMAT (///4X,'AVERAGE P',2X,'PERMEABILITY',2X,'RELATIVE PERM')
      K=1
   12 AREA =0
C CALCULATE THE SECOND MOMENT
      DO 14 N=1,ND
      Y1=RA(N)**2*F(N)
      Y2=RA(N+1)**2*F(N+1)
      SUM =((RA(N+1)-RA(N))/2)*(Y1+Y2)
   14 AREA = AREA + SUM
      RSQ =AREA/FNORM
      SE=(TA(N)-POR*SR)/(POR-POR*SR)
C CALCULATE THE PERMEABILITY = PERM
       PERM(ND)=RSQ*TA(N)*SE*SE/5.
      IF (K.EQ.1) PERM1=PERM(ND)
      K=K+1
C CALCUALTE THE RELATIVE PERMEABILITY = RPERM
      RPERM(ND)=PERM(ND)/PERM1
      WRITE (6,202) PA(ND),PERM(ND),RPERM(ND)
      ND=ND-1
      IF(ND.GT.1) GO TO 12
  100 FORMAT (I5,3F10.3)
  202 FORMAT(1X,F10.3,1X,E15.8,1X,E15.8)
  203 FORMAT (8F10.3)
```

Appendix D

Input Data - Test Programs Phase I

	COLUMN NO.							
Card	10	20	30	40	50	60	70	80
A	ONE DIMENSIONAL DRAINAGE - BEGINNING OF NEXT TIME STEP							
B	18 9	8 2	1 0	10 1	1 2			
C			0	0				
D	11 11							
E	2 -1							
	1 10							
M	.5	20000.	1.8	400000.	1.			
N	1.	1.						
O	.00191	.00191	.464	.0				
P	.0718	.000003	.0824	.00002	.0986	.0002	.133	.002
θ vs K_r	.176	.01	.245	.060	.293	.130	.436	.480
	.453	.910	.459	.980	.464	1.		
	.0718	140.8	.0824	117.3	.0986	93.8	.133	74.3
θ vs ψ	.176	62.3	.245	52.3	.293	48.0	.436	40.2
	.453	31.6	.459	21.6	.464	0.		
Q	1 2	0.	0.	0.				
	2 0	0.	20.	0.	0.			
	8 0	0.	140.	0.	0.			
	9 0	0.	146.5	0.	0.			
	10 2	20.	0.	0.				
	11 0	20.	20.	0.	0.			
	17 0	20.	140.	0.	0.			
	18 0	20.	146.5	0.	0.			
R	1 1	10 11	2 1	0.				
	8 8	17 18	9 1	0.				
	END							
A	INFILTRATION SURFACE-DOWNWARD FLOW - BEGINNING OF NEXT TIME STEP							
C			2	0				
F	.0002778	-46.76	.1					
G	10.	10.						
M	.5	8000.	2.	200000.	1.			
Q	9 -4	0.	146.5	0.				
	18 -4	20.	146.5	0.				
Cards B, D, E, N, O, P, R and 6 Q cards same as above								
	END							

Card	COLUMN NO.							
	10	20	30	40	50	60	70	80
A	INFLT. SURF. - INITIALLY HYDROSTATIC DIST. - BEGINNING OF NEXT TIME STEP							
B	18 9	8 2	1 0	10 2	1 2			
C			2	0				
D	11 11							
E	2 -1							
	1 10							
F	.0002778	-146.5	.1					
G	10	10						
M	1.	4000.	1.5	80000.	1.			
Cards N, O and P same as previous problem								
Q	1 2	0.	0.	0.				
	2 0	0.	20.	-20.	0.			
	8 0	0.	140.	-140.	0.			
	9 -4	0.	146.5	-146.5				
	10 2	20.	0.	0.				
	11 0	20.	20.	-20.	0.			
	17 0	20.	140.	-140.	0.			
	18 -4	20.	146.5	-146.5				
R	same as previous problem							
	END							
A	EVAPORATION FROM A WATER TABLE - BEGINNING OF NEXT TIME STEP							
B	18 9	8 2	1 0	10 1				
C			2	0				
D	11 11							
F	-.0005	-140.	.1					
G	5.	5.						
M	1.	16384.	2.	131071.	1.			
Cards N, O, P same as previous problem								
Q	1 1	0.	0.	0.				
	2 0	0.	10.	0.	0.			
	3 0	0.	20.	0.	0.			
	9 -4	0.	50.	0.				
	10 1	10.	0.	0.				
	11 0	10.	10.	0.	0.			
	12 0	10.	20.	0.	0.			
	18 -4	10.	50.	0.				

This problem uses INTEG = 2

Card	10	20	30	40	50	60	70	80
R	1 1	10 11	2 1	0.				
	8 8	17 18	9 1	0.				
	END							
A	INFILTRATION, SEMI-INFINITE COLUMN - BEGINNING OF NEXT TIME STEP							
B	14 7	6 2	1 0	12 2				
C			0	0				
D	13 13							
M	.5	25.	1.1	1500.	1.			
N	1.	1.						
O	.001203	.001203	.396	.0				
P (θ vs K_r)	.127	.001	.150	.004	.158	.006	.174	.013
	.186	.036	.246	.096	.253	.118	.285	.204
	.321	.362	.352	.690	.356	.800	.360	.816
	.364	.820						
θ vs ψ	.127	73.6	.150	56.8	.158	50.7	.174	45.0
	.186	38.9	.246	34.6	.253	32.0	.285	28.9
	.321	25.6	.352	19.0	.356	12.7	.360	7.2
	.364	.0						
Q	1 0	.0	.0	-70.	.0			
	6 0	.0	25.0	-70.	.0			
	7 1	.0	25.4	1.6				
	8 0	5.0	.0	-70.	.0			
	13 0	5.0	25.0	-70.	.0			
	14 1	5.0	25.4	1.6				
	1 1	8 9	2 1	.0				
	6 6	13 14	7 1	.0				
	END							
A	TWO-DIMENSIONAL DRAINAGE - BEGINNING OF NEXT TIME STEP							
B	75 7	60 2	1 1	10 1	1 2			
C			0	0				
D	19 19							
E	2 -1							
	4 5							
M	1.	50000.	2.	1000000.	1.0			
N	1.	1.						
O	.0063	.0063	.485	.0				

Card	COLUMN NO. 10	20	30	40	50	60	70	80
P	.152	.0000021	.154	.0000036	.157	.0000065	.160	.000012
	.164	.000026	.169	.000057	.175	.000141	.185	.000402
θ vs K_r	.198	.001387	.218	.006292	.250	.04286	.273	.134
	.304	.4137	.319	.5909	.335	.7629	.353	.8886
	.393	.9874	.415	.9998	.440	1.		
	.152	130.	.154	120.	.157	110.	.160	100.
	.164	90.	.169	80.	.175	70.	.185	60.
θ vs ψ	.198	50.	.218	40.	.250	30.	.273	25.
	.304	20.	.319	18.	.335	16.	.353	14.
	.393	10.	.415	5.	.440	0.		
Q	1 1	0.	0.	40.67				
	2 1	0.	20.33	40.67				
	3 1	0.	40.67	40.67				
	4 2	0.	61.00	61.00				
	5 2	0.	81.33	81.33				
	6 0	0.	101.67	81.33	0.			
	7 0	0.	122.	81.33	0.			
	8 0	25.	0.	81.33	0.			
	14 0	25.	122.	81.33	0.			
	15 0	50.	0.	81.33	0.			
	21 0	50.	122.	81.33	0.			
	22 0	75.	0.	81.33	0.			
	28 0	75.	122.	81.33	0.			
	29 0	100.	0.	81.33	0.			
	35 0	100.	122.	81.33	0.			
	36 0	150.	0.	81.33	0.			
	39 0	150.	122.	81.33	0.			
	40 0	200.	0.	81.33	0.			
	43 0	200.	122.	81.33	0.			
	44 0	250.	0.	81.33	0.			
	47 0	250.	122.	81.33	0.			
	48 0	300.	0.	81.33	0.			
	51 0	300.	122.	81.33	0.			
	52 0	350.	0.	81.33	0.			

Card	COLUMN NO.										
		10		20		30	40	50	60	70	80
Q cont	55	0		350.		122.	81.33	0.			
	56	0		400.		0.	81.33	0.			
	59	0		400.		122.	81.33	0.			
	60	0		450.		0.	81.33	0.			
	63	0		450.		122.	81.33	0.			
	64	0		500.		0.	81.33	0.			
	67	0		500.		122.	81.33	0.			
	68	0		550.		0.	81.33	0.			
	71	0		550.		122.	81.33	0.			
	72	0		610.		0.	81.33				
	75	0		610.		122.	81.33				
R	1	1	8	9	2	1	0.				
	7	8	15	16	9	1	0.				
	13	15	22	23	16	1	0.				
	19	22	29	30	23	1	0.				
	25	29	36	30	30	1	0.				
	26	30	36	37	37	1	0.				
	27	30	37	31	31	1	0.				
	28	31	37	32	32	1	0.				
	29	32	37	38	38	1	0.				
	30	32	38	33	33	1	0.				
	31	33	38	34	34	1	0.				
	32	34	38	39	39	1	0.				
	33	34	39	35	35	1	0.				
	34	36	40	41	37	1	0.				
	37	40	44	45	41	1	0.				
	40	44	48	49	45	1	0.				
	43	48	52	53	49	1	0.				
	46	52	56	57	53	1	0.				
	49	56	60	61	57	1	0.				
	52	60	64	65	61	1	0.				
	55	64	68	69	65	1	0.				
	58	68	72	73	69	1	0.				
	60	70	74	75	71	1	0.				
	END										